

AD-A234 440

GL-TR-90-0248

Meteor Scatter Communication Between
Thule and Station Nord, Greenland

Jens Ostergaard

University of Lowell
Center for Atmospheric Research
450 Aiken Street
Lowell, MA 01854

September 1990

Scientific Report No. 3

Approved for public release; distribution unlimited.


GEOPHYSICS LABORATORY
AIR FORCE SYSTEMS COMMAND
UNITED STATES AIR FORCE
HANSCOM AIR FORCE BASE, MA 01731-5000

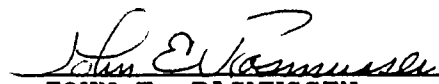
DTIC FILE COPY

DTIC
ELECTE
APR 16 1991
C D

91 4 15 135

"This technical report has been reviewed and is approved for publication"


ALAN D. BAILEY
Contract Manager


JOHN E. RASMUSSEN
Branch Chief

FOR THE COMMANDER


ROBERT A. SKRIVANEK
Division Director

This report has been reviewed by the ESD Public Affairs Office (PA) and is releasable to the National Technical Information Service (NTIS).

Qualified requestors may obtain additional copies from the Defense Technical Information Center. All others should apply to the National Technical Information Service.

If your address has changed, or if you wish to be removed from the mailing list, or if the addressee is no longer employed by your organization, please notify GL/IMA, Hanscom AFB, MA 01731. This will assist us in maintaining a current mailing list.

Do not return copies of this report unless contractual obligations or notices on a specific document requires that it be returned.

UNCLASSIFIED

SECURITY CLASSIFICATION OF THIS PAGE

REPORT DOCUMENTATION PAGE

Form Approved
OMB No. 0704-0188

1a. REPORT SECURITY CLASSIFICATION Unclassified			1b. RESTRICTIVE MARKINGS		
2a. SECURITY CLASSIFICATION AUTHORITY			3. DISTRIBUTION/AVAILABILITY OF REPORT		
2b. DECLASSIFICATION/DOWNGRADING SCHEDULE			Approved for public release; distribution unlimited.		
4. PERFORMING ORGANIZATION REPORT NUMBER(S) ULRF-462/CAR			5. MONITORING ORGANIZATION REPORT NUMBER(S) GL-TR-90-0248		
6a. NAME OF PERFORMING ORGANIZATION University of Lowell		6b. OFFICE SYMBOL (If applicable)	7a. NAME OF MONITORING ORGANIZATION Geophysics Laboratory		
6c. ADDRESS (City, State, and ZIP Code) Center for Atmospheric Research 450 Aiken Street Lowell, Massachusetts 01854			7b. ADDRESS (City, State, and ZIP Code) Hanscom Air Force Base Massachusetts 01731-5000		
8a. NAME OF FUNDING/SPONSORING ORGANIZATION Geophysics Laboratory		8b. OFFICE SYMBOL (If applicable)	9. PROCUREMENT INSTRUMENT IDENTIFICATION NUMBER F19628-88-K-0004		
8c. ADDRESS (City, State, and ZIP Code) Hanscom Air Force Base Massachusetts 01731-5000			10. SOURCE OF FUNDING NUMBERS		
			PROGRAM ELEMENT NO. 62101F	PROJECT NO. 4643	TASK NO. 10
			WORK UNIT ACCESSION NO. AI		
11. TITLE (Include Security Classification) Meteor Scatter Communication Between Thule and Station Nord, Greenland					
12. PERSONAL AUTHOR(S) Jens Ostergaard					
13a. TYPE OF REPORT Scientific No. 3		13b. TIME COVERED FROM _____ TO _____		14. DATE OF REPORT (Year, Month, Day) September 1990	
15. PAGE COUNT 162					
16. SUPPLEMENTARY NOTATION This work accomplished in collaboration with the Commission for Scientific Research in Greenland, Projects No. 24/87 and 29/88. Polar Radio Propagation.					
17. COSATI CODES			18. SUBJECT TERMS (Continue on reverse if necessary and identify by block number)		
FIELD	GROUP	SUB-GROUP	Meteor Scatter Overdense Throughput Communication		
			Meteor Trail Propagation Wait Time		
			Underdense Capacity Antenna		
19. ABSTRACT (Continue on reverse if necessary and identify by block number) Meteor scatter as a mode of communication was first examined in Canada in the late 1940's and later in Europe in 1960. It was found to provide a good, but relatively low capacity digital communication channel. In comparison with high yield satellite links, meteor scatter was too complex for widespread utilization then. However, the advent of the micro-processor has removed the most costly obstacles to its economical use in areas where no regular communication systems exist. This report examines such meteor scatter paths between selected Greenland sites and Station Nord. A 1800 km link was found to provide virtually no throughput and discussion focuses on probable causes. In contrast, a 1150 km link traversing northern Greenland produced very high throughput. Extensive analyses are presented of propagation properties and potential communication capabilities. These are discussed extensively in light of several scenarios.					
20. DISTRIBUTION/AVAILABILITY OF ABSTRACT <input checked="" type="checkbox"/> UNCLASSIFIED/UNLIMITED <input type="checkbox"/> SAME AS RPT <input type="checkbox"/> DTIC USERS			21. ABSTRACT SECURITY CLASSIFICATION Unclassified		
22a. NAME OF RESPONSIBLE INDIVIDUAL Alan D. Bailey			22b. TELEPHONE (Include Area Code) 617-377-2525		22c. OFFICE SYMBOL GL/LID



Accession For	
ETH	<input checked="" type="checkbox"/>
DEPT	<input type="checkbox"/>
Unsubscribed	<input type="checkbox"/>
Justification	
By	
Distribution/	
Availability Codes	
Dist	Availability/or Special
A-1	

TABLE OF CONTENTS

	Page
ACKNOWLEDGEMENT	xvii
BACKGROUND	xix
1.0 INTRODUCTION TO METEOR SCATTER COMMUNICATION	1
1.1 Meteor Trail Availability	4
1.2 Scatter Mechanisms	5
2.0 DESCRIPTION OF THE MEASUREMENT CAMPAIGNS	11
3.0 DESCRIPTION OF THE LINKS	14
3.1 Geographic Locations and Common Volume Considerations	14
3.2 Antennas and Their Deployment	19
3.3 Effects of the Foreground Terrain	19
3.4 Illumination of the Scattering Volume	26
3.5 Transmitter and Receiver Equipment	32
4.0 SYSTEM NOISE AND INTERFERENCE IN METEOR SCATTER SYSTEMS	34
4.1 Galactic Noise in Meteor Scatter Systems	34
4.2 Man-Made Noise and Interference in Meteor Scatter Systems	35

TABLE OF CONTENTS (Continued)

	Page
4.3 Multiplicative Noise	38
5.0 OVERALL PRESENTATION OF THE DATASAMPLE	40
6.0 THE PROPAGATION STATISTICS	62
6.1 Arrival Rate Statistics	65
6.2 Duty Cycle Statistics	73
6.3 Duration Statistics	85
6.4 Fading Statistics	97
6.5 Underdense Decay Time Constants	97
7.0 DERIVED COMMUNICATION STATISTICS	102
7.1 The Dependence on Transmitter Power	103
7.2 Communication Properties of a Thule Station Nord Link	105
7.3 Properties of a Data Collection Link	113
8.0 SUMMARY AND RECOMMENDATIONS	126
9.0 BIBLIOGRAPHY	128
9.1 Introduction to Meteor Scatter	128
9.2 Meteor Scatter in General	128
9.3 Ionospheric Absorption	132

TABLE OF CONTENTS (Continued)

	Page
9.4 Aurora and Scatter	133
9.5 System Noise	135
9.6 Communication Theory and Technology	136

LIST OF FIGURES

Figure No.		Page
1.1	Meteor Scatter Propagation Geometry	1
1.2	Positions of the Hot Spots for a 1000 km Link	6
1.3	Examples of Underdense Meteor Trail Signals With and Without Fading	9
1.4	Examples of Overdense Meteor Trail Signals With and Without Fading	9
1.5	Example of a 15 sec. Continuous Sequence of Signal Reflected from a Sporadic-E Layer	10
3.1	Geographical Location of the Sondrestrom Nord and Thule Nord Paths	16
3.2	Common volume for the Sondrestrom station Nord link with (A) and without (B) the terrain blockage present for the current transmitter location at Sondrestrom.	17
3.3	Common volume for the Thule Station Nord Link	18
3.4	Fresnel reflection coefficients for Greenland terrain for 45 MHz. The polarization is horizontal and vertical. The conductivity is 0.0001, and the permittivity is 2.5.	21

LIST OF FIGURES (Continued)

Figure No.		Page
3.5	Fresnel reflection coefficients for Greenland terrain for 104 MHz. The polarization is horizontal and vertical. The conductivity is 0.0001, and the permittivity is 2.5.	21
3.6	Radiation pattern for a six element, horizontally polarized Yagi mounted 1.5 wavelengths above the ground at Nord. The antenna is pointed at the horizon.	23
3.7	Radiation pattern for a six element, horizontally polarized Yagi mounted 1.5 wavelengths above the ground at Nord. The antenna is elevated 30 degrees.	24
3.8	Radiation pattern for a six element horizontally polarized Yagi, mounted 6 wavelengths above the ground at station Nord	25
3.9	Illumination of the Common Volume for the Thule Station Nord Link	27
3.10	Antenna Installation at Thule Used for the August 1987 Campaign	28
3.11	Antenna installation at Station Nord Used for the August 1987 Campaign	29

LIST OF FIGURES (Continued)

Figure No.		Page
3.12	Radiation Properties of a Commercially Available Five Element Yagi Antenna of Low Quality Electrically as Well as Mechanically	30
3.13	Radiation Properties of a Commercially Available Five Element Yagi Antenna of Good Quality Electrically as Well as Mechanically	31
3.14	Block Schematic of the Phase Locked Loop Receiver Used at Station Nord	33
4.1	Computed and measured noise power in a 100 Hz bandwidth at station Nord. The antenna is a six element horizontally polarized Yagi mounted 10 m above the ground and pointed towards Thule.	36
4.2	Computed noise power in a 100 Hz bandwidth at Thule. The antenna is a six element horizontally polarized Yagi mounted 10 m above the ground and pointed towards station Nord.	37
5.1	Received Underdense Trail Signal With Classification Information	41
5.2	Low Resolution Plots of Signals Received at Station Nord August 22, 1987	43
5.3	Low Resolution Plots of Signals Received at Station Nord August 24, 1987	45

LIST OF FIGURES (Continued)

Figure No.		Page
5.4	Low Resolution Plots of Signals Received at Station Nord August 27, 1987	47
5.5	Low resolution plots of signals received at station Nord August 28, 1987. The measurements ended at 08 Ut.	50
5.6	Example of a Series of Three Underdense Trail Signals Occurring Within a Five Second Time Interval	51
5.7	A Ten Second Time Interval Where a Long Lasting Underdense Meteor Trail Signal is Being Overlaid by an Overdense Trail Signal	52
5.8	Example of an Overdense Meteor Trail Shortened by Fading	53
5.9	Example of an Overdense Trail Signal With Fading	54
5.10	Example of an Overdense Meteor Trail Signal With Severe Wind Distortion	56
5.11	Example of a Weak Ionoscatter Signal Often Observed on Very Sensitive Meteor Scatter Links	57
5.12A	Sequence of Received Signals Showing the Long Enduring High Level Signal Observed on August 24 at 1147 UT	58

LIST OF FIGURES (Continued)

Figure No.		Page
5.12B	Sequence of Received Signals Showing the Long Enduring High Level Signal Observed on August 24 at 1147 UT	59
5.12C	Sequence of Received Signals Showing the Long Enduring High Level Signal Observed on August 24 at 1147 UT	60
6.1	Derivation of Arrival Rate, Duty Cycle, Duration, Fades, and Underdense Time Constants from the Classified Waveforms	66
6.1.1	Meteor Arrival Rate as a Function of RSL for August 1987 at Station Nord	67
6.1.2	Meteor Arrival Rate as a Function of SNR for August 1987 at Station Nord	68
6.1.3	Arrival Rate vs. Time of Day for Signals Exceeding -130 dBm for August 1987 at Station Nord	70
6.1.4	Arrival Rate vs. Time of Day for Signals Exceeding -110 dBm for August 1987 at Station Nord	71
6.1.5	Arrival Rate vs. Time of Day for Signals Exceeding -100 dBm for August 1987 at Station Nord	72
6.1.6	Arrival Rate of Signals Exceeding 20 dB SNR for the Period 20-28 August 1987 at Station Nord	74

LIST OF FIGURES (Continued)

Figure No.		Page
6.1.7	Arrival Rate of Signals Exceeding 30 dB SNR for the Period 20-28 August 1987 at Station Nord	75
6.1.8	Arrival Rate of Signals Exceeding -110 dB RSL for the Period 20-28 August 1987 at Station Nord	76
6.1.9	Arrival Rate of Signals Exceeding 30 dB SNR for the Period 20-28 August 1987 at Station Nord	77
6.2.1	Diurnal variation of the duty cycle exceeding -110 dBm. August 1987 at station Nord.	78
6.2.2	Diurnal variation of the duty cycle exceeding a SNR of 10 dB. August 1987 at station Nord.	79
6.2.3	Diurnal variation of the duty cycle exceeding a SNR of 20 dB. August 1987 at station Nord.	80
6.2.4	Diurnal variation of the duty cycle exceeding a SNR of 30 dB. August 1987 at station Nord.	81
6.2.5	Diurnal variation of the duty cycle exceeding a SNR of 40 dB. August 1987 at station Nord.	82
6.2.6	Duty Cycle Exceeding a RSL Threshold for August 1987 at Station Nord	84

LIST OF FIGURES (Continued)

Figure No.		Page
6.2.7	Duty Cycle Exceeding a SNR Threshold for August 1987 at Station Nord	84
6.2.8	Duty cycle exceeding a RSL threshold vs. time of day for the period August 20-29, 1987 at station Nord. Top: For all events. Bottom: For meteor trails only.	86
6.2.9	Duty cycle exceeding a RSL threshold vs. time of day for the period August 20-29, 1987 at station Nord. Top: For all events. Bottom: For meteor trails only.	87
6.3.1	Average Duration of Meteor Signals as a Function of RSL for August 1987 at Station Nord	89
6.3.2	Average Duration of Meteor Signals as a Function of SNR for August 1987 at Station Nord	89
6.3.3	Normalized Distribution of Signal Dura- tions Exceeding 10 dB for August 1987 at Station Nord	91
6.3.4	Normalized Distribution of Signal Dura- tions Exceeding 20 dB for August 1987 at Station Nord	91
6.3.5	Normalized Distribution of Signal Dura- tions Exceeding 30 dB for August 1987 at Station Nord	92

LIST OF FIGURES (Continued)

Figure No.		Page
6.3.6	Normalized Distribution of Signal Durations Exceeding 40 dB for August 1987 at Station Nord	92
6.3.7	Diurnal variation of the average duration of signals exceeding -120 dBm at station Nord. August 1987.	93
6.3.8	Diurnal variation of the average duration of signals exceeding 30 dB SNR at station Nord. August 1987.	93
6.4.1	Average Number of Fades/Trail vs. Time of Day for August 1987 at Station Nord	94
6.4.2	Average Number of Fades/Sec vs. Time of Day for August 1987 at Station Nord	96
6.4.3	Normalized Distribution of Fades/Second for August 1987 at Station Nord	96
6.4.4	Normalized Distribution of Fade Durations in Seconds for August 1987 at Station Nord	98
6.5.1	Normalized Distribution of Underdense Meteor Trail Decay Time Constants for August 1987	100
6.5.2	Average Diurnal Variation of the Underdense Decay Time Constant for August 1987	100

LIST OF FIGURES (Continued)

Figure No.		Page
6.5.3	Daily Variation of the Underdense Decay Time Constant for the Period 20-30 August 1987	101
7.2.1	Illustration of the Communication Capacity of a Underdense Meteor Trail Signal When Adaptive and Fixed Signaling Rates are Used	107
7.2.2	Derived Capacity for a Meteor Scatter Link Between Thule and Station Nord for August 1987 as a Function of Signaling Rate	108
7.2.3	Derived fully adaptive capacity for a meteor scatter link between Thule and station Nord in August 1987. Meteor trail signals only.	110
7.2.4	Derived fully adaptive capacity for a meteor scatter link between Thule and station Nord in August 1987. Meteor trail and sporadic E-signals are included.	110
7.2.5	Distribution of Signaling Rates for a Fully Adaptive Meteor Scatter Link Between Thule and Station Nord August 1987	112
7.3.1	Waiting time for a 2000 bit message as function of time of day for August 1987 at station Nord. Message piecing is not used.	117

LIST OF FIGURES (Continued)

Figure No.		Page
7.3.2	Waiting time in seconds for a 2000 bit message as function of time of day for August 1987 at station Nord. Message piecing is used.	119
7.3.3	Waiting time in seconds for messages as function of message length for August 1987 at station Nord. Message piecing is used.	120
7.3.4	Waiting time in seconds for a 2000 bit message as a function of signaling rate. Message piecing is used.	122
7.3.5	Waiting time in seconds for a 20,000 bit message as a function of signaling rate. Message piecing is used.	123
7.3.6	Waiting Time in Seconds for a 1024 bit Message as a Function of Confidence	125

LIST OF TABLES

Table No.		Page
3.1	Locations and Lengths of the Two Meteor Scatter Links Investigated	15

ACKNOWLEDGEMENT

The author wants to express gratitude and acknowledgement to the following persons and institutions:

The Danish Academy of Technical Sciences ATV and the Danish Technology Council, The Commission for Scientific Research in Greenland and Scandinavian Telecommunication Industry SKANTI in Copenhagen for the technology grant that made this analysis possible.

ElektronikCentralen ATV for granting leave of absence for the duration of the analysis work.

Geophysics Laboratory, Ionospheric Interactions Branch, USAF for invitation to be a guest scientist with the division for a year and have access to the GL meteor scatter analysis facilities in Boston.

To the Danish Scientific Liaison Officer for Greenland, Mr. J. Taagholt for support and never ending enthusiasm for cooperative research in Greenland.

To the Danish Defence Command for giving access and support for the measurements at station Nord. Especially the support from Major Clemmensen and the staff at station Nord is highly appreciated.

To Ms. M. Kjuel Nielsen of the Danish Ministry of Foreign affairs for advice and guidance during the preliminary stages of the project.

To Mr. John Rasmussen, Chief GL/LID and Dr. Paul Kossey for invitations to participate in the meteor scatter research program in Greenland and providing the transmissions from

Sondrestrom and Thule used for the measurements at Nord as well as continued encouragement and kind tutoring throughout.

To Mr. Alan Bailey, Ms. P. Bench, SMSGT T. Coriaty, Mr. D. DeHart, Sgt C. Curtis, Sgt D. Carter of GL for outstanding help and encouragement and great companionship during the field campaigns.

To Mr. Eric Li, Dr. A. L. Snyder, Jr., Dr. G. S. Sales and Dr. J. A. Weitzen of the University of Lowell Center for Atmospheric Research and Dr. P. S. Cannon of Royal Aerospace Establishment UK for helpful discussions and suggestions for the analysis.

BACKGROUND

This report describes the results of a feasibility study of meteor scatter communication between Thule AB and Station Nord, Greenland. The feasibility study was initiated by interests expressed by Danish Authorities to establish a communication link into station Nord other than the existing short wave connection.

Station Nord is situated in the extreme north east Greenland at latitude 82° North, well beyond the reach of geostationary satellites. Existing polar orbiting satellites intended for data collection are restricted for data of interest to the World Meteorological Organization, WMO network, and they have too low capacities to qualify as general communication paths into Nord. The proposed meteor scatter communication link is intended to connect station Nord with the Greenland Telecommunication network in West Greenland. This network links all West Greenland towns through a line of sight microwave chain, augmented with satellite paths to Thule in North Greenland, Scoresbysund in East Greenland and Denmark. The network offers both telephone and telex channels as well as packet digital networks based on the X-25 protocol.

The communication capacity for the link is required to be at least 100 bits/sec average year around, with a wanted capacity potential of 300 bits/sec, to cover future needs.

Short wave radio, HF, provides suitable voice communications to station Nord under most circumstances, and recent developments of digital transmission systems at HF could be used for the Nord link. However, an average capacity exceeding 100 bits/sec will be very difficult to obtain without resorting to very high power transmitters and an elaborate scheme of frequency management. Also, the link is and will be affected by the well known problems inherent with HF: Interference, polar blackouts

unsuitability for moderate speed digital transmissions due to limited coherence bandwidth and finally lack of privacy.

Ruling out HF and satellite communication, few other possibilities exist, as this part of Greenland is without communication infrastructure, and has a small traffic requirement. This eliminates ordinary telephone connections by cable or microwave radio to be established well into the future.

Meteor scatter communication, which combines privacy, a channel capacity of one to a few telex channels, low equipment complexity and a modest price can provide a communication link into Station Nord, that does not exhibit the drawbacks of short wave radio. Meteor scatter operates in the low VHF frequency band 30 - 100 MHz. Fixed frequencies, moderate power transmitters and small antennas are used, making this communication channel of interest for unattended operation at remote stations.

Meteor scatter communication systems utilize the ionized trails created by micro-meteorites burning up in the earth's atmosphere at heights of 80 - 120 km. The trails can reflect radiowaves in the lower VHF frequency band (30 - 100 MHz) providing a intermittent propagation path. Billions of such meteorites enter the earth's atmosphere each day, creating enough trails to provide a substantial communication capacity between stations separated up to 1800 km. The average lifetime of a meteor trail is approximately 0.5 sec. and the interval between trails approximately 10 - 20 sec. at 45 MHz. Thus the meteor scatter channel is very intermittent, and inherently suited for digital transmissions only.

Meteor scatter as a mode of communication was first examined in Canada in the late 1940's, and later in Europe in 1960. Meteor scatter was found to provide a good, but relatively low capacity digital communication channel. In comparison with the

yield of satellite links, meteor scatter was too complex for widespread utilization then, but the advent of the microprocessor has removed the most costly obstacles to economical use of meteor scatter communication in areas where no regular communication systems exist.

The renewed interest in meteor scatter throughout the last five years, has resulted in new and extended investigations, theoretical as well as experimental, of the properties of meteor scatter propagation and communication. The investigations aim at providing systems designers with much wanted information pertinent to the design of new meteor scatter communication systems. Such systems should exploit the medium better than previous systems.

One such experiment is undertaken by Air Force Systems Command, Geophysics Laboratory, Hanscom AFB between Thule AB and Sondrestrom AB, Greenland. The experiment is aimed at assessing the properties of meteor scatter propagation and communication in the frequency range 35 - 147 MHz at high latitudes. The experiment is coordinated with the Danish authorities through the Commission for Scientific Research in Greenland and the Scientific Liaison Officer for Greenland. The experiment and results obtained are described in Refs. 1, 2, 3, 4, 5, 6, 7, 8, 9.

The results of the experiments in Greenland are used to validate computer models that are useful for the computation of the properties of target meteor scatter communication systems for other locations than those investigated by the experiments. The accuracy of computer models is improving and they will be of great value to system planners in the near future. Such models were not available when the link to station Nord was contemplated. Thus measurements of the meteor scatter activity between selected locations and Station Nord were needed.

Two paths were of primary interest for the link into station Nord. One 1800 km long between Sondrestrom and station Nord, and one 1150 km long between Thule and Station Nord. Sondrestrom is the traffic hub of Greenland, with an international airport, and access to the microwave link. Nuuk, the capital of Greenland would be even better suited, but the distance between Nuuk and Station Nord is too long to be covered by meteor scatter. Thule is situated in the far Northwest Greenland. The distance between Thule and Station Nord is approximately 1150 km, which is well established as a near optimum distance for meteor scatter. Thule has a satellite link of good quality into the West Greenland Chain and station Nord is logistically closer connected to Thule than to other points in West Greenland.

Two measurement campaigns were conducted in April and August 1987. The first campaign attempted measurements between Sondrestrom AB and Station Nord using the existing meteor scatter transmitter operated by GL. Over a period of one week, very few signals were received at 45 MHz at station Nord, and none at all at 65 and 104 MHz. It was concluded that the distance, 1800 km, in conjunction with the terrain blockage at Sondrestrom eliminated all but a small fraction of the common scattering volume between the stations, and that this link is not feasible without relocating the transmitter at Sondrestrom to a position with less terrain blockage. Even then the obtainable communication capacity may not be sufficient to support the required 100 bits/sec average capacity.

A second campaign between Thule AB and Station Nord was conducted in August 1987. Measurements were performed at 45 MHz only, and a one week sample of data taken. The connectivity of the link was found to be very high and signals propagating via several different mechanisms, many different types of signals meteoric and from other types of propagation were recorded. The data has been analyzed, and the results are presented in this report.

The data collected at station Nord has been subjected to the analysis procedure used at GL to analyze data from the Sondrestrom to Thule meteor scatter link. The analysis procedure first classifies all the received signals into separate categories of meteoric and non-meteoric origin. Signals of meteoric origin are separated in two classes: underdense and overdense trails, and the long lasting signals of non-meteoric origin are ascribed to sporadic E-layer scatter. A fourth category, GOK, "God Only Knows," collects the remaining unidentifiable weak and short lasting signals. Then statistics of signal level and duration as well as signal to noise ratio are produced. These propagation statistics describe the channel as a time varying transfer function.

The communication properties, i.e. capacity and bit error rate of a radio channel can be derived from the signal to noise ratio in the channel, provided no dispersion exists in the bandwidth used by the proposed communication system. This is the case for the meteor scatter channel at signaling speeds up to several hundred K bits/sec. Thus, derived communication statistics can be produced for target communication systems by the analysis program. Such statistics have been produced with the data acquired at station Nord in August 1987, to examine the design of communication systems with properties covering the needs for a future link between Thule and station Nord.

In addition to investigating the feasibility of using meteor scatter for communication between West Greenland and Station Nord, the use of meteor scatter for collection of environmental data from unmanned sensors in remote areas in Greenland is discussed, as this topic has general interest for a range of users in Greenland, and is closely connected with the analysis of the Nord data.

1.0 INTRODUCTION TO METEOR SCATTER COMMUNICATION

Normally, the ionosphere is not sufficiently dense, nor are the ionization gradients large enough to efficiently reflect or scatter VHF signals back to the Earth. However, from time to time ionization produced by micro-meteorites entering and burning up in the Earth's atmosphere provide a suitable scattering mechanism. Such meteor trails are typically just one meter in diameter, but can have lengths of 25 km, and more. The meteor trails occur 85 - 120 km above the Earth and they can be used to establish communication over ranges from about 300 to 1800 km. Figure 1.1 presents the geometry of meteor scatter.

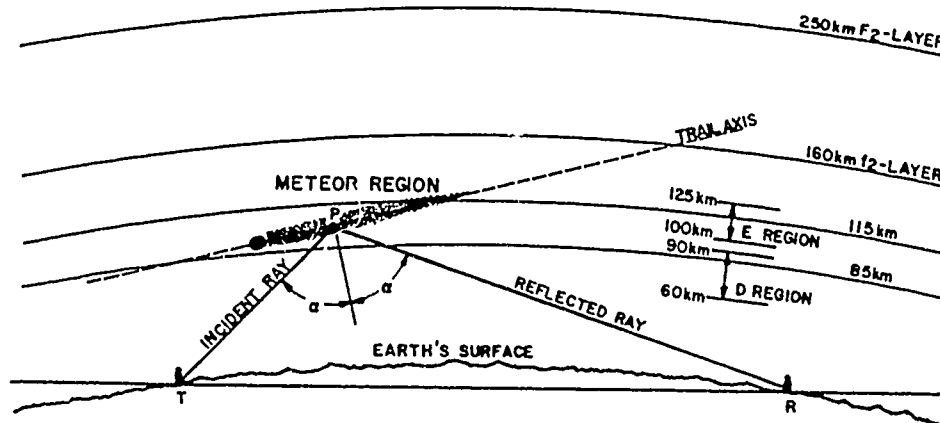


Figure 1.1 Meteor Scatter Propagation Geometry

The first truly operational meteor scatter communication system, JANET was operated in Canada in the mid-1950's at approximately 40 MHz. However, the system was severely impaired by a Solar Proton Event during testing between Yellowknife and Edmonton, and experimental interest in meteor scatter propagation essentially vanished. This was partially due to the failure to operate under disturbed conditions, and partially because the technology needed to handle the handshaking and intermittent data storage requirements was not available in the 1950's.

NATO's SHAPE Technical Centre developed and tested a new meteor scatter communication system, COMET in the mid-1960's in Central Europe and in Norway. The system worked well although it had a fairly low capacity (1-4 telegraph channels). The system was tested both at 40 MHz and at 100 MHz to explore the frequency dependent properties of meteor scatter propagation and it was found that the communication capacity decreased fast with an increase in operating frequency. The advent of satellite communication diverted interest away from meteor scatter propagation for obvious reasons of stable propagation and large bandwidth. Since then, Meteor scatter communication systems have been constructed by the U.S. Department of Agriculture and a number of private corporations in the Western U.S (SNOTEL), and in Alaska (MBCS). These systems are currently in operation using fixed data rate signaling using a half duplex handshake protocols configuration. Their success has established confidence in the operational use of meteor scatter communication for remote stations with limited traffic requirements.

Recently interest in meteor scatter communication has been revitalized as a result of rapid advances in microcomputer technology and digital communication techniques. Some suggested uses for modern meteor scatter communication systems include automatic data collection from unmanned sites, thin-line digital radio links, where privacy and exclusive ownership of the communication

terminals are essential. These could be either fixed or mobile services, possibly incorporating some form of vehicle tracking. Meteor scatter could also be a candidate mode for operation of digital HF communication systems with extended frequency range of operation into the VHF band as well as back up or replacement of conventional HF circuits.

To the communication system designer meteor scatter is a very complex communication channel. The channel availability is, dependent on the transmitter power used, only a few percent. It is not known in advance when the channel is open, the availability is a stochastic process which can be described statistically. The meteor scatter channel is therefore not suited for voice communication, but is inherently a digital communication channel.

It is necessary to have available a description of the channel in order to design communication systems with predictable performances, and to select suitable types of modulation and signaling schemes. Such a description must contain as much detail as possible on both the microscopic and macroscopic time properties of the channel if the channel capacity is to be efficiently utilized. The description of the meteor scatter channel thus contains two main groups of information.

The Macroscopic time properties of the channel, are descriptions of the astrophysical mechanisms behind the formation of ionized meteor trails and the statistics of trail availability. That is: when is the channel open? How long do the openings last? Are there any effects of season, location, path length and time of day on the availability of the channel?

The Microscopic time properties of the channel are descriptions of the properties related to the quality of the channel such as the signal strength or path loss, the available bandwidth for signaling and the channel distortion. These are needed to select or

construct the modulations and signaling schemes to be used with the channel, and to predict the performance of the communication system. The most important properties are: Path loss, system noise and interference, time and frequency dispersion of the channel, and depolarization of the radio waves by the channel.

1.1 Meteor Trail Availability

The availability of meteor trails show both a diurnal and a seasonal variation caused by the Earth's rotation and the inclination of the Earth's axis relative to the Ecliptic plane. Most meteorites orbit the sun in the same direction as the Earth, and the majority of the orbits are within $\pm 10^\circ$ of the Ecliptic plane. The escape velocity for a meteor at Earth's distance from the sun is 43 km/s. The velocity of the Earth is 29 km/s, and the gravity acceleration of a meteor moving with the earth is 11 km/s. The resulting range of meteor velocities when entering the atmosphere is then 11 - 72 km/s.

Approximately 10^{12} meteorites are swept up by the Earth everyday, and at a given location the Earth's rotation creates a diurnal variation of the number of meteor trails dense enough to scatter VHF signals. At mid-latitudes there is a maximum of meteor trails at 06 hours local time when the position of the meteor scatter link is near the Earth's apex, and a minimum at 18 hours local time when the position is near the Earth's antapex.

A seasonal variation is introduced due to the inclination of the Earth's axis with the Ecliptic plane. At northern latitudes, a seasonal maximum is encountered in July - August when the location is closest to the Earth's apex, and similarly a minimum is found in January - February when the location is farthest away from the Earth's apex. At northern mid-latitudes a seasonal variation of a factor 3-4, and a diurnal variation of a factor 5-6 is observed, and a

total variation over the year can reach 1 - 20. At higher latitudes a smaller diurnal variation is found.

The meteorite orbits are fairly uniformly distributed along the Earth's orbit, but at certain periods the Earth orbit crosses orbits of broken up comets. The density of micro-meteorites in these orbits is much higher than the average density and a substantial increase of the amount of meteor trails is observed for a few days. These are termed meteor showers, and the most well known shower is the Perseids which occur in the period 5 - 14 August. Although meteor showers can provide enhancements of the channel throughput at very specific times during the year, they are not usable for the planning of operational networks, which must rely on seasonal and yearly channel availability averages.

1.2 Scatter Mechanisms

Not all meteor trails created within the common scattering volume of a pair of communication terminals will result in a channel opening. The meteor trail axis must be tangent to one of a family of confocal spheroids with foci at the positions of the terminals to connect the terminals. This feature implies a certain privacy in meteor scatter communication systems, as the trails which link a pair of terminals are not necessarily the same trails linking other terminals. This means that a single frequency can be used with a network of many stations, and that it is difficult to disturb a meteor scatter link with ground based transmitters separated some distance from the meteor scatter terminals. However, no protection is inherent in the propagation mechanism for interference from other users of the spectrum within view of one of the terminals.

Not all parts of the common scattering volume are of equal importance for the scattering of signals by meteor trails between two terminals. Limited parts of the common scattering

volume between the terminals contribute a major part of the duty cycle on a meteor scatter link. These are termed hot spots. For a 1000 km link, two hot spots are found, one on either side of the great circle line between the terminals approximately at mid path. Figure 1.2. The importance and position of the individual hot spot varies with both the geographical positions of the terminals and with the time of day. Antennas for meteor scatter links must be chosen to properly illuminate the hot spots.

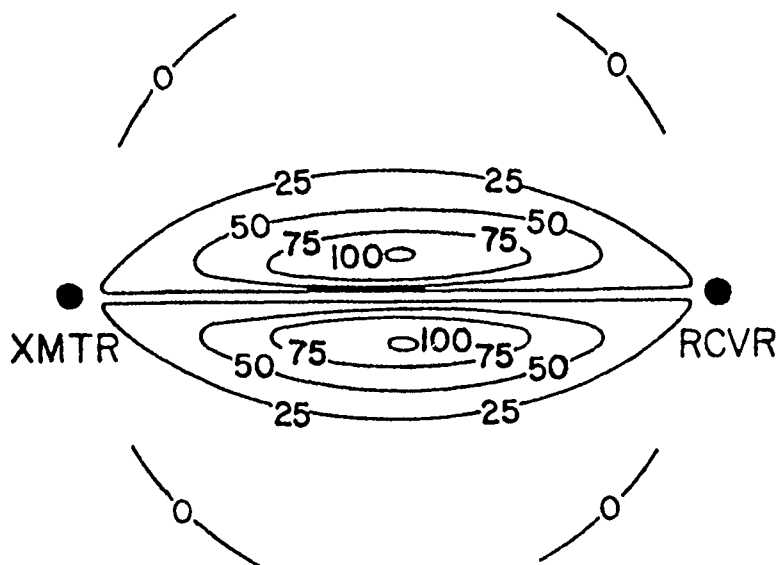


Figure 1.2 Positions of the Hot Spots for a 1000 km Link

The meteor scatter mechanism as described by Eshleman (1957) contain two different main modes of scattering dependent on the electron line density of the ionized meteor trail. One is called specular underdense scattering and is characteristic of meteor trails with electron line densities less than approximately 10^{14} electrons/cm. The trail scattering is composed from the scatter of the individual electrons of the meteor trail. The amplitude of the scattered signal rises sharply in less than 100 msec as the trail is formed, and is strongest just after the formation of the trail. In the course of time, the trail diffuses, and the amplitude of the signal decreases exponentially. The mean duration of the return from underdense trails is approximately half a second. However, the duration distribution spans values from tenths of a second to several seconds, the longer trails being the least common. Figure 1.3 shows a generic underdense meteor trail signal received at station Nord.

Some underdense trail signals exhibit fading during their exponential decay. This phenomenon is usually observed with long lasting trails, and may be attributed to high altitude winds moving portions of the trail to different positions and attitudes such that they each fulfill the geometric conditions for scattering between the terminals of the link. These fades can be deep, occasionally reaching down to the receiver noise level; i.e. a complete cancellation of the total received power by destructive interference between signals from the different scatter paths. The fades attributed to wind distortion of the trail differs from the amplitude oscillations seen on most of the waveforms near the point of maximum amplitude. These oscillations occur during the formation of the meteor trail, as the micro-meteorite moves through the Fresnel zones of the scattering geometry. This mechanism is discussed in McKinley's excellent book: Meteor Science and Engineering, McGraw-Hill, 1961. Figure 1.3 presents an example of a underdense return with fading received at station Nord.

The other main scattering mode is specular scattering from over dense meteor trails. These are modelled as cylinders of ionization for which the electron density is large enough to completely reflect the transmitted wave at the surface. The signal strength rises sharply in less than 100 msec as the trail is formed. As the trail diffuses after its formation, the reflecting surface is enlarged, and the signal strength continues to increase for a while until the electron density of the trail has decreased enough that the wave cannot be completely reflected. The signal then decreases exponentially as the trail diffuses further. The signals from overdense meteor trails tend to last longer and provide larger signal strengths than do the signals from underdense trails. The longest lasting signal so far observed at Thule lasted in excess of 40 seconds, but such signals occur very rarely. The majority of the returns which lasts longer than 1 second can be classified as overdense returns. As the overdense trails generally tend to last longer than underdense trails, they are especially prone fade due to wind distortion. Figure 1.4 presents a generic overdense meteor trail return, and a overdense return with fading received at station Nord.

Other scattering mechanisms are sometimes observed at VHF frequencies. Sporadic E-layers may attain electron densities sufficiently large to provide a long lasting channel (lasting 30 minutes to hours). This channel is presumed to have properties similar to those of an HF channel. Thus they provide a long lasting communication possibility with limited bandwidth due to multipath distortion. Sporadic E-layers may reflect TV signals without imposing much signal distortion, so the available bandwidth can be very large, in the order of several MHz. Figure 1.5 presents a sequence of signals reflected from a sporadic E-layer. The signal is characterized by a large amplitude and slow fading, as is a shortwave channel. Sporadic E layers can be a mixed blessing. They can provide a welcome channel enhancement, but can also contribute considerable interference from other users of the radio spectrum at

METEORIC 890228 220609 45MHZ

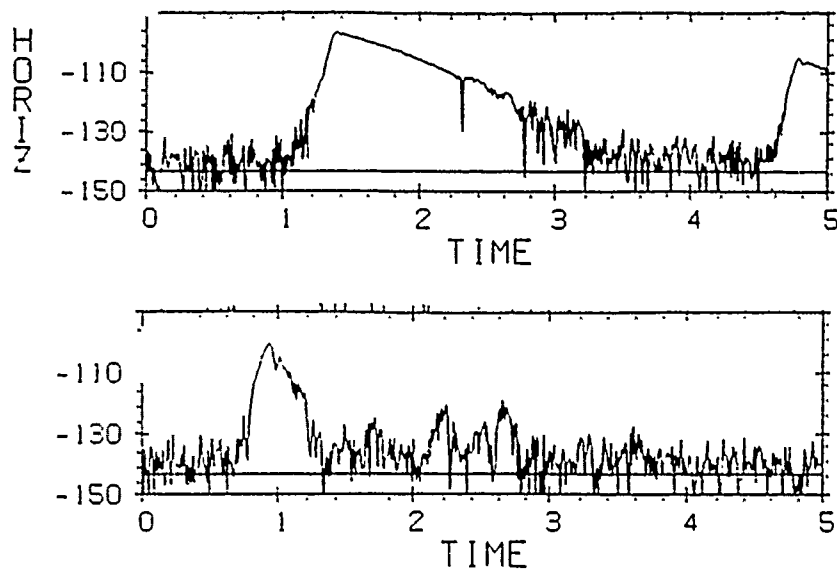


Figure 1.3 Examples of Underdense Meteor Trail Signals With and Without Fading

METEORIC 890228 200549 45MHZ

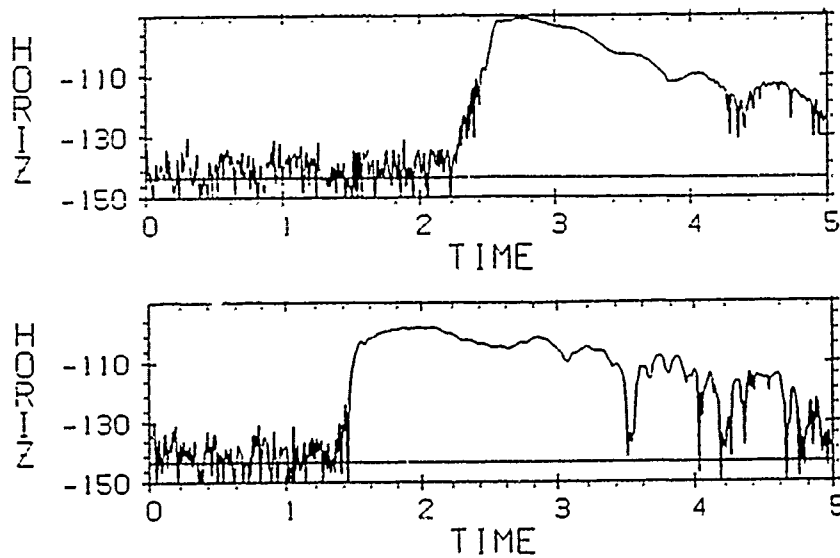


Figure 1.4 Examples of Overdense Meteor Trail Signals With and Without Fading

times, when the channel connects one end of a meteor scatter link with parts of the world where the frequency is heavily used by others. An example is interference from CB radios and other line of sight users, which can obtain world wide coverage during high sunspot years. Thus, it is advisable not to use frequencies in the range 25 to 40 MHz, if this kind of interference is to be avoided.

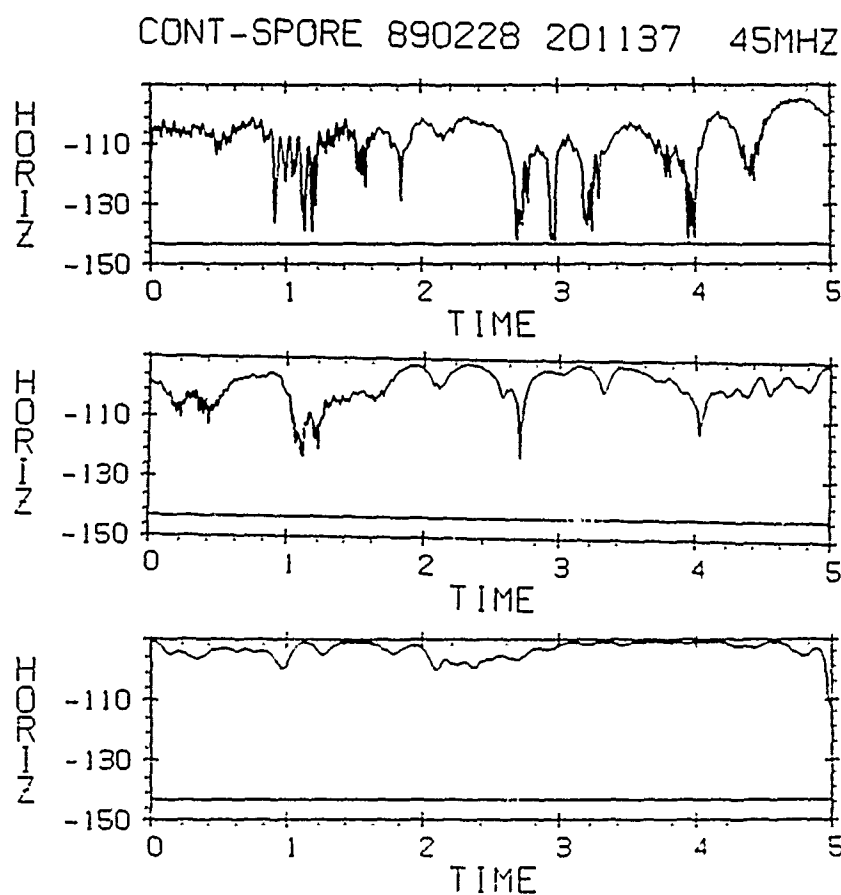


Figure 1.5 Example of a 15 sec Continuous Sequence of Signal Reflected from a Sporadic-E Layer

2.0 DESCRIPTION OF THE MEASUREMENT CAMPAIGNS

Two campaigns were conducted in April and August 1987 to assess the potential capacity of a meteor scatter link between station Nord and West Greenland. Two paths were of primary interest: Sondrestrom to station Nord; and Thule to station Nord.

The path between Sondrestrom and station Nord has some logistical advantages above the path between station Nord and Thule, as Sondrestrom has daily flights to and from Copenhagen, and data from Nord could, if necessary, be recorded at Sondrestrom and shipped to Copenhagen. Both paths connect to terminals on the West Greenland telecommunication system, which is currently being enhanced to include X-25 type digital connections. Thus data from Nord can be transferred to Copenhagen through this net.

During the April 1987 campaign measurements of received signal strength and duration of signals transmitted from the GL transmitter installation at Sondrestrom AB were attempted at station Nord. Three frequencies: 45, 65, and 104 MHz were investigated. The transmitter is primarily used for meteor scatter measurements between Sondrestrom AB and Thule AB, but the extent of the transmitter antenna beams cover the path between Sondrestrom and station Nord. The transmitter power is nominally 1000 W, fed to 5 element, horizontally polarized Yagi antennas. The antennas are mounted 1.5 wavelengths above the ground. This produces a main lobe in the radiation pattern with enhanced gain at elevation angles in the range 4 - 20 degrees, which is advantageous for a meteor scatter link of 1000 to 1200 km. The length of the link between Sondrestrom and Nord is approximately 1800 km, well below the theoretical maximum distance obtainable with meteor scatter propagation.

The receiver installation at Station Nord consisted of a phase locked loop receiver controlled by a PC computer. The receiver was mounted on the antenna tower below the receiving antennas, which consisted of a pair of 5 element crossed Yagis for each frequency. Each pair was mounted 1.5 wavelengths above the ground. The measurement period spanned one week, and throughout this time less than 10 meteor scatter signals were received at 45 MHz and no signals were received at 65 and 104 MHz. It was apparent that the link configuration could not support communication at all. Later analysis of the path geometry presented in Section 3.0 of this report has shown that very different antenna configurations are needed for such a long path, and that the expected capacity of the link will be limited by a small common scattering volume.

A new campaign was undertaken in August 1987. This time a 1000 W transmitter was kindly made available, installed and operated at Thule AB by GL. A six element horizontally polarized Yagi antenna 1.5 wavelengths above the ground was used for the transmissions. The receiver installation at station Nord was the same as the one used for the April campaign except for a new and sturdier 45 MHz antenna. Successful measurements were conducted in 25 min. periods every two hours for one week. Approximately 60 Mbytes of waveform data was collected and brought to Copenhagen for analysis.

The first impression of the data collected at Nord was that the duty cycle was much larger than anything previously seen in Thule. Often the signal was almost continuous although rather weak. An abundance of meteor scatter signals were seen, and one long lasting sequence of strong sporadic-E signal occurred at noon one of the days. Also, a seemingly too large number of very long lasting meteor scatter signals were observed. The receiver used at station Nord has a noise bandwidth of 100 Hz, as compared to the 4

kHz noise bandwidth of the receiver then used with the Sondrestrom AB to Thule AB meteor scatter link operated by GL. Thus the Thule station Nord link had 16 dB more sensitivity than the Sondrestrom Thule link receiver and this explains part of the observed difference in duty cycle. However, the abundance of long lasting signals did not immediately compare to anything seen on the Sondrestrom AB to Thule AB link. Analysis of the data has been performed by the author in 1988 - 89 during a stay with GL in Boston as a guest scientist. The results are presented in Sections 5.0 to 7.0 of this report.

The publication date of the report suggests that the analysis took awhile. After the conclusion of the August 1987 campaign, funding for the analysis could not be raised, and no analysis effort was undertaken until late 1988, when funds were made available to the author through a Technology Grant issued by the Danish Academy for Technical Sciences, a Grant from the Commission for Scientific Research in Greenland and support from Scandinavian Telecommunications Industry, SKANTI, Copenhagen. The grant was used for the one year stay with GL in Boston mentioned above.

The project has also been heavily supported throughout by GL with funds, scientific mentorship and access to the GL meteor scatter statistics analysis facility.

Access to station Nord as well as transportation to and from Station Nord was granted by the Danish Defense Command, and the arrangements needed to coordinate the combined US-Danish meteor scatter investigations in Greenland are undertaken by the Danish Liaison Officer for Greenland, Mr. J. Taagholt.

3.0 DESCRIPTION OF THE LINKS

This section of the report describes the geographical properties of the two paths between station Nord and West Greenland and the equipment used for the investigations.

It may seem obvious that the properties of the meteor trails and their availability are the main topics of interest for an investigation of meteor scatter propagation. The experience gathered during the last five years operation of the GL link between Sondrestrom and Thule, however, has confirmed that the performance of a meteor scatter link is distressingly sensitive to the properties of the antenna installation, the terrain surrounding the antennas and the local interference level. At the same time, the antenna deployment scheme is one of the link parameters that can be selected by the link designer in order to obtain the best possible communication capacity from the link. Thus a thorough treatment of station location selection and antenna deployment is warranted.

3.1 Geographic Location, and Common Volume Considerations

Station Nord is located in the extreme Northeast Greenland. Thule and Sondrestrom are located in Northwest- and Southwest Greenland respectively. The receiver was located at station Nord for both campaigns, and the transmitters were located at Sondrestrom and Thule. The location of the stations and the length of the links measured along the Earth's surface are shown in Table 3.1 and Figure 3.1.

Location	Latitude	Longitude	Distance to Nord
Nord	81.60°N	16.66°W	N/A
Sondrestrom	66.98°N	50.65°W	1780 km.
Thule	76.55°N	67.85°W	1160 km.

Table 3.1 Locations and Lengths of the Two Meteor Scatter Links Investigated

Meteor trails occur between 80 and 120 km above the earth's surface and the theoretical maximum distance covered by a meteor scatter link should be approximately 2200 km. A shortwave link, relying on reflections from the E-layer at an altitude of 100 km is certainly feasible for this distance. However, a meteor scatter link utilizes meteor trails occurring within a large volume of the lower ionosphere in view of the antennas of both stations, not just a small area around the midpoint of the path. This volume is termed the common volume, or the scattering volume. The common volume must include the hot spots for the particular link and they must be illuminated properly by the antennas of both stations. Otherwise, the communication capacity of the link will be drastically degraded. The common volume can be limited by blockage of the horizon in front of the antennas, and the illumination is dependent on the radiation patterns of the antennas and the ground in front of them. The best visibility is obtained if the foreground terrain is flat. This is the case at station Nord, where the nearest obstacles are more than 50 km away from the station in the direction towards Sondrestrom and Thule.

The foreground terrain at Sondrestrom features a mountain ridge north of the transmitter site which defines a minimum elevation angle of 4.2 deg. This mountain ridge severely limits the common volume. Figure 3.2 shows the common volume, as it would have been if an unobstructed horizon was available at both stations, and when the effects of the mountain ridge at Sondrestrom

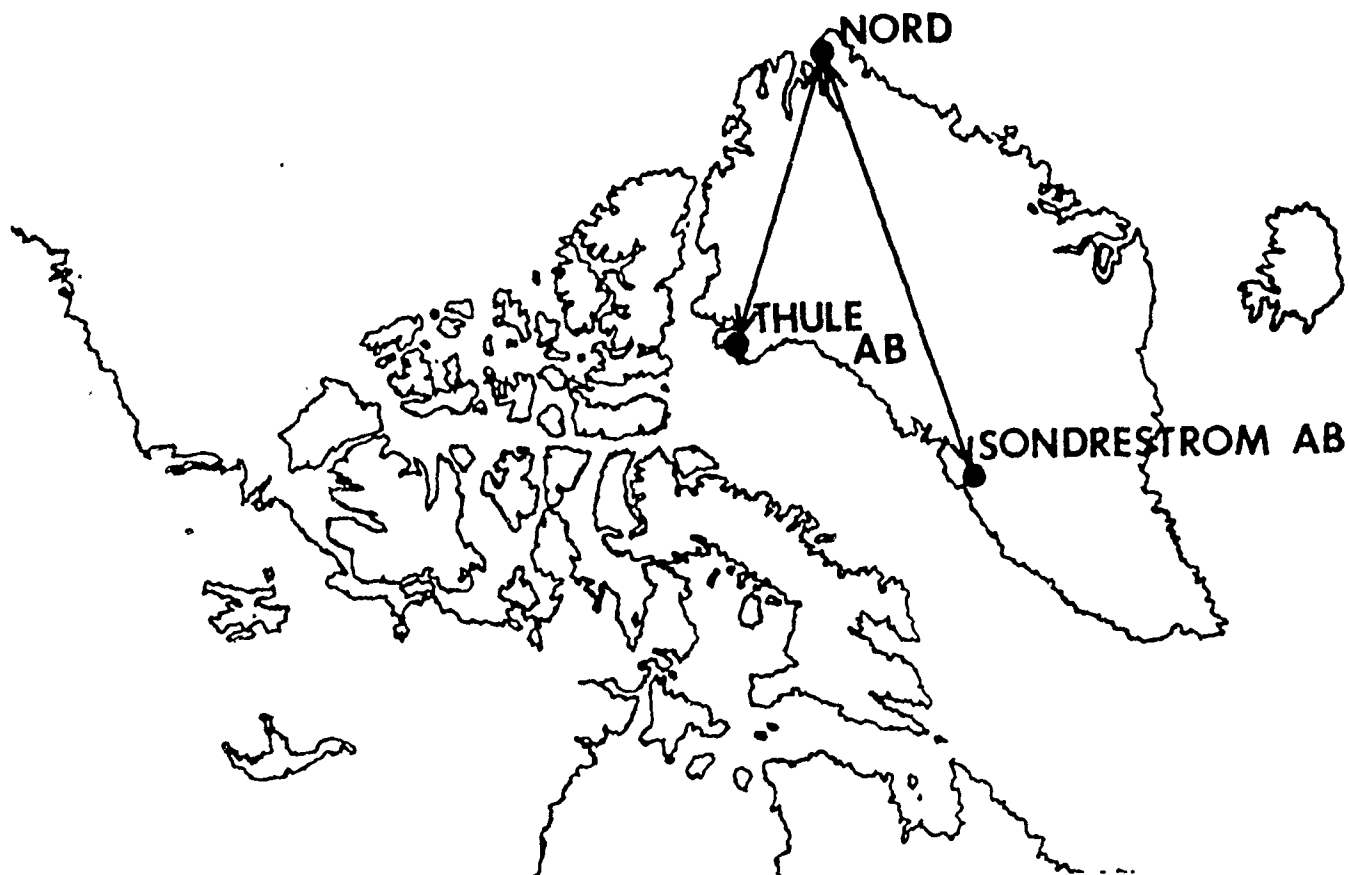
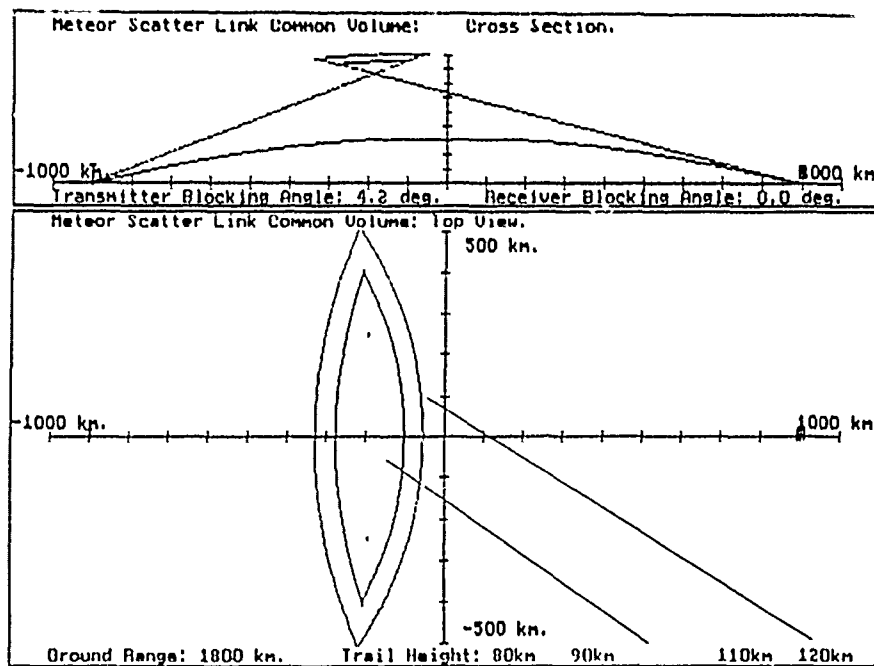
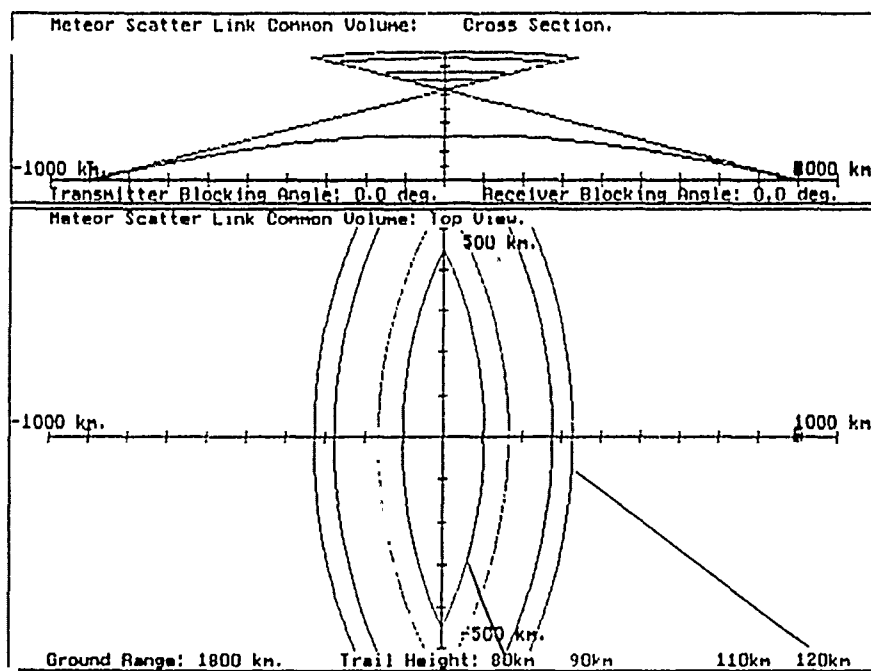


Figure 3.1 Geographical Location of the Sondrestrom Nord and Thule Nord Paths



A



B

Figure 3.2 Common volume for the Sondrestrom station Nord link with (A) and without (B) the terrain blockage present for the current transmitter location at Sondrestrom.

are included. The common volume is severely limited on this long link by the mountain ridge in front of the transmitting antenna. The mean height of occurrence of the meteor trails is approximately 95 km, and it is seen that not much common volume is available at this height.

The foreground terrain at Thule in the direction towards station Nord is unobstructed. The immediate foreground terrain is flat, and the horizon is defined by a Glacier. The minimum elevation is less than 1 deg. Figure 3.3 shows the common volume for the Thule Nord link. It is seen that the common volume is large, and no link degradation should be expected from blocking of the horizon by terrain features.

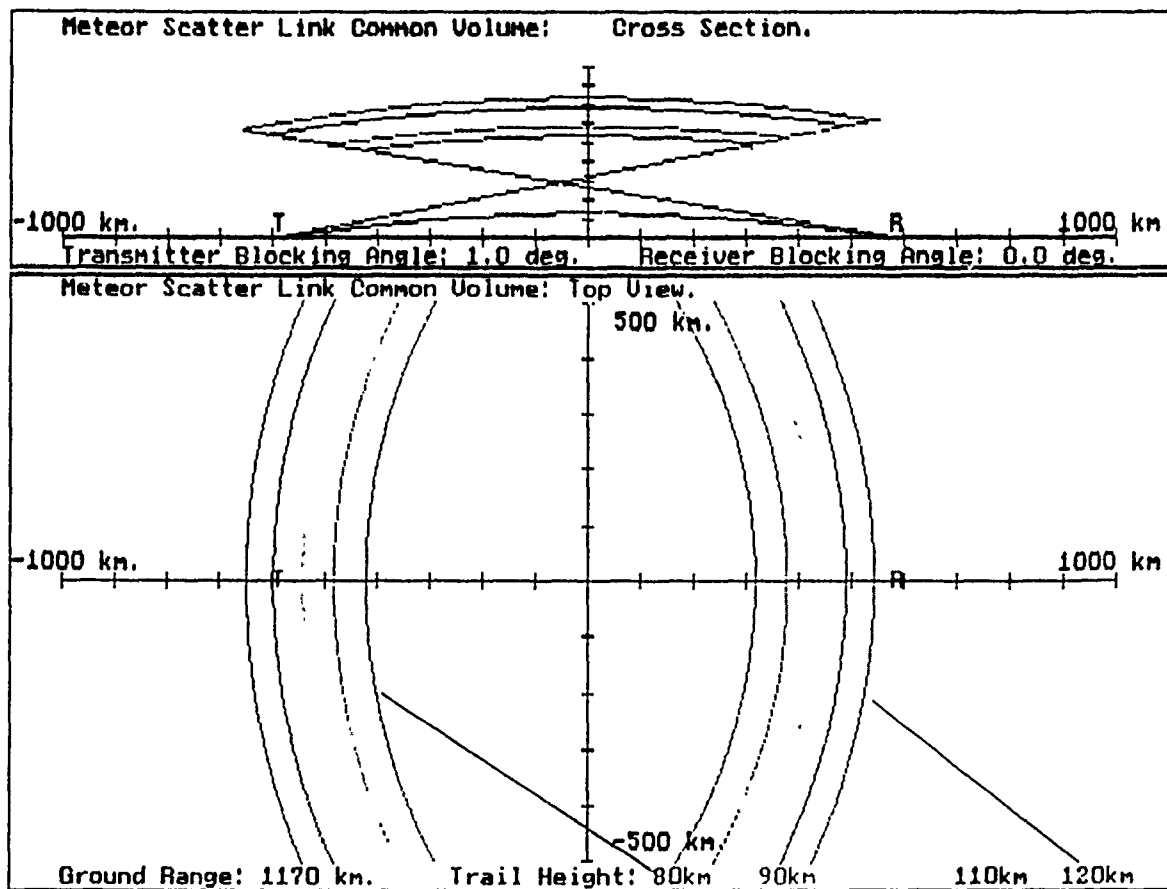


Figure 3.3 Common Volume for the Thule Station Nord Link

3.2 Antennas and Their Deployment

As mentioned previously, certain regions of the sky, termed the hot spots, are more important than others in terms of their contributions to the overall performance of a meteor scatter communication system. For a 1000 - 1800 km link the hot spots are off to the side of the great circle path between the terminals in the vicinity of the midpoint of the path. The activity of the individual hot spots has a diurnal variation as illustrated by Brown (1985), and the antennas of a meteor scatter communication system should be selected and positioned to illuminate these optimally. This calls for adaptive antennas, or at least antennas with steerable beams. However, such antennas are very large for frequencies in the lower VHF spectrum, and their use have not been reported in conjunction with meteor scatter links.

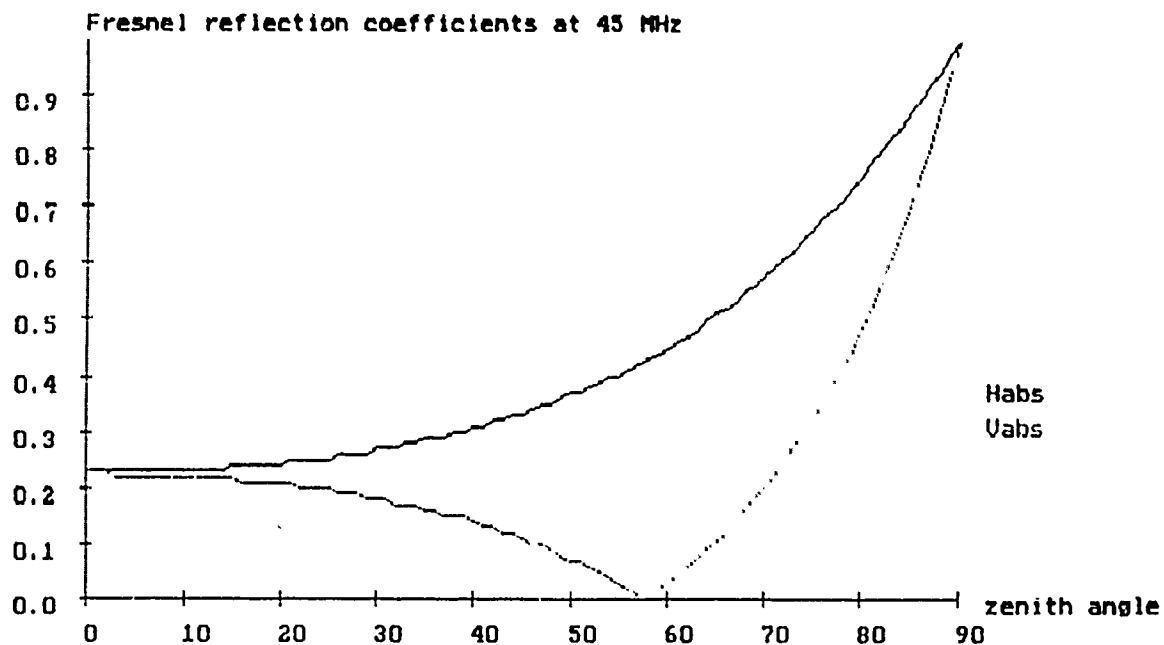
The path loss on a meteor scatter link is so large (180 dB or more), that a high level of transmitted power is necessary to obtain a satisfactory communications capacity. This can usually be obtained by a suitable combination of transmitter power and directive antennas. Most fixed meteor scatter communication systems use simple Yagi antennas with 2 to 10 elements. Long links can use higher gain antennas than short links, as the most important part of the common volume, i.e. the hot spots are found close to the midpath. In some cases arrays of four Yagi antennas have been used with long links to further increase directivity. Short links must use more moderate gain antennas, as the common volume extends over a large range of azimuth and elevation angles.

3.3 Effects of the Foreground Terrain

The height and elevation of the antennas must be chosen to illuminate the scattering volume uniformly. The effective radiation pattern of an elevated antenna is determined by the

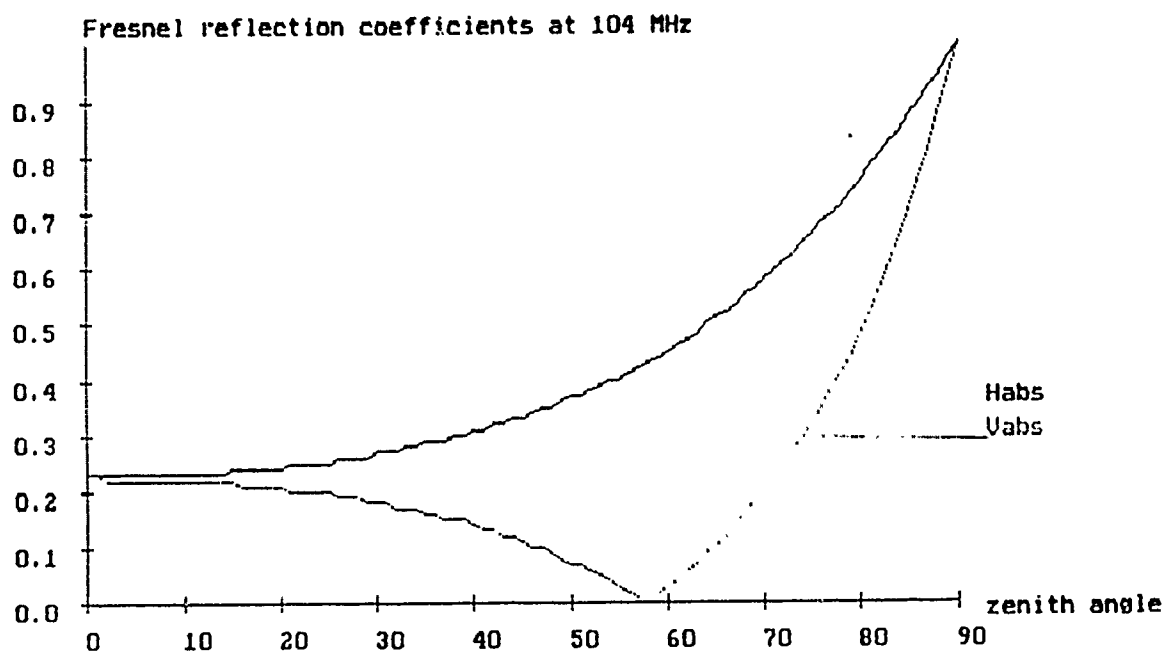
directive properties of the antenna itself, and by the influence of the foreground in front of it. A part of the antenna radiation will be reflected by the terrain in front of the antenna. The magnitude reflection coefficient which is dependent on the electrical properties of the terrain, the wave polarization and the angle of incidence ranges from 1, for perfectly conducting surfaces, to 0 for very special combinations of low conductivity and angles of incidence. The terrain in Greenland has a low conductivity of approximately 0.0001 S/m, and a relative permittivity of approximately 2.5, but the ground still reflects. Figures 3.4 - 3.5 presents the reflection coefficients, magnitude and phase, for Greenland terrain. The reflection coefficients are presented for horizontally and vertically polarized waves as a function of the angle of incidence for 45 MHz and 104 MHz. The reflections from the foreground modifies the radiation pattern of the antenna, as the direct and the reflected rays add vectorially in the far field.

Dependent on the phase difference between the direct ray and the reflected ray, enhancements and cancellations of the radiated field are produced for given elevations. A maximum enhancement of 6 dB can be obtained if the ground is perfectly reflecting. The reflections from even a very dry foreground will significantly modify the radiation pattern, although a full 6 dB enhancement will not be obtained. The importance of the influence of the foreground terrain can be illustrated by computing the antenna radiation pattern and the part of the path loss originating from the gain of the antennas and the spatial spreading of the propagating waves. Although these losses do not include those associated with the meteor scatter mechanism itself, it is instructive to investigate how they vary in accordance with the common volume that is illuminated by the transmitting and receiving antennas.



Soil conductivity 0.0001 S/m, relative permittivity 2.5

Figure 3.4 Fresnel reflection coefficients for Greenland terrain for 45 MHz. The polarization is horizontal and vertical. The conductivity is 0.0001, and the permittivity is 2.5.



Soil conductivity 0.0001 S/m, relative permittivity 2.5

Figure 3.5 Fresnel reflection coefficients for Greenland terrain for 104 MHz. The polarization is horizontal and vertical. The conductivity is 0.0001, and the permittivity is 2.5.

A computer program has been written to calculate the radiation pattern of a Yagi antenna mounted at a specified distance above a reflecting foreground. The foreground need not be flat, a linear segment approximation of the terrain features can be used to model the terrain features of the foreground.

Figure 3.6 presents the radiation pattern for a horizontally polarized 6 element Yagi, mounted 1.5 wavelengths above the ground at station Nord. It is seen that a single main lobe is produced in the elevation range 3 - 35 deg. The maximum gain exceeds the gain of the antenna itself by 5 dB. Also, a null is present at the horizon. The null will decrease the illumination of the part of the common volume, seen close to the horizon. Nulls at elevations above 35 deg. will likewise decrease the illumination of the common volume seen at the particular elevations.

The depth of the nulls can to a certain extent be controlled by tilting the antenna axis, and thus eliminating part of the ground reflections. The radiation pattern for a 6 element Yagi horizontally polarized 1.5 wavelengths above the ground and tilted 30 deg. is presented in Figure 3.7. A more uniform radiation pattern versus elevation is obtained at the expense of gain enhancement at low elevation angles. The null at the horizon is still present, however.

An antenna height of 1.5 wavelength has proven to be a good compromise for a 100 - 1200 km link, i.e. Sondrestrom-Thule or Thule-Nord. Likewise, an antenna height of 1 wavelength with a tilt of 30 degrees is a good compromise for a link of 600 km, i.e. Sondrestrom-Narsarsuaq. However, the common volume for the 1800 km link between Sondrestrom and station Nord is seen at very low elevations from both ends. Thus, the antenna radiation patterns must provide maximum gain at a few degrees elevation. That is not the case for the antenna configurations presented in Figures 3.6-3.7. Gain at low elevation angles in the presence of a reflecting

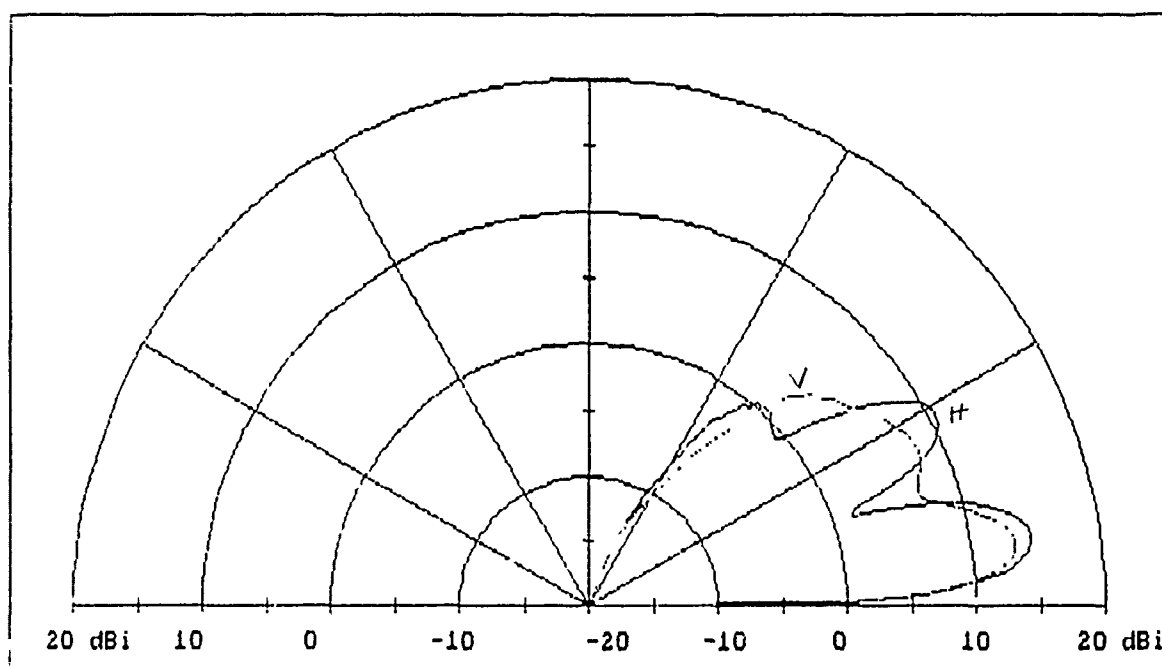


Figure 3.6 Radiation pattern for a six element, horizontally polarized Yagi mounted 1.5 wavelengths above the ground at Nord. The antenna is pointed at the horizon.

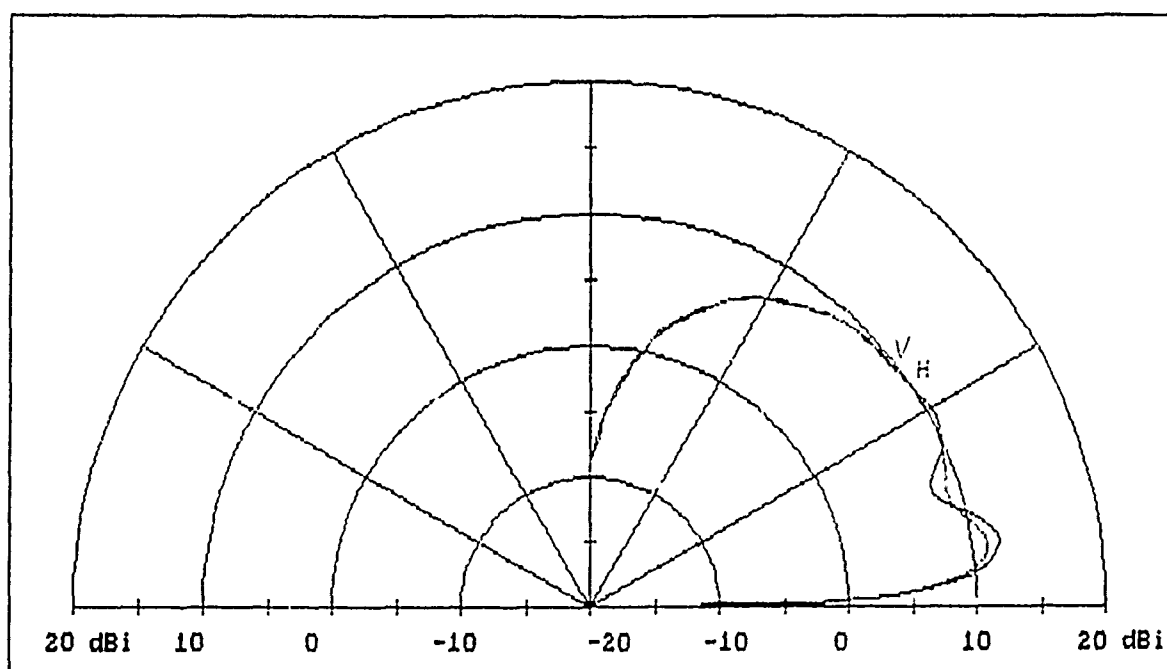


Figure 3.7 Radiation pattern for a six element, horizontally polarized Yagi mounted 1.5 wavelengths above the ground at Nord. The antenna is elevated 30 degrees.

foreground can be obtained by mounting the antennas at larger heights above the ground. Such positions will also create more nulls in the radiation pattern, but this is of no consequence as long as none of the nulls are in directions towards the common volume. Figure 3.8 presents the radiation pattern of a six element Yagi, horizontally polarized mounted 6 wavelengths (40 m at 45 MHz) above the ground at station Nord. This configuration could be suitable for a renewed investigation of the properties of a Sondrestrom-Nord link. However, the blocking of the horizon at Sondrestrom must still be eliminated, as enhanced antenna gains cannot compensate for the lack of common volume.

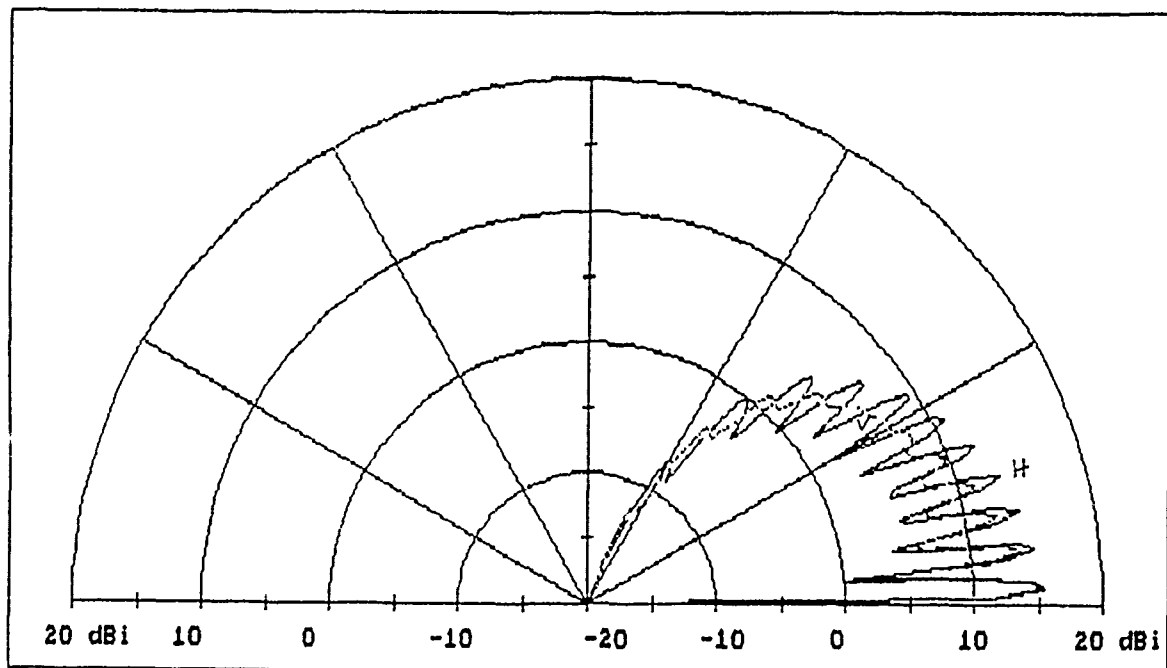


Figure 3.8 Radiation pattern for a six element horizontally polarized Yagi, mounted 6 wavelengths above the ground at station Nord.

3.4 Illumination of the Scattering Volume

The illumination of the common volume can be illustrated by calculating the path loss, excluding the scattering loss, between the two stations as a function of the position of the meteor trail. The path loss thus contains the antenna gains and the path losses between the antennas and the meteor trail.

Figure 3.9 shows the result of calculations of the path losses associated with the position of scatterers within the scattering volume for the Thule to station Nord link. Six element Yagi antennas, horizontally polarized and pointed at the horizon such as used for the investigation are depicted. It is seen that the illumination is uniform throughout the area of the hot spots at altitudes between 80 and 100 km, where the majority of the meteor trails occur.

Figures 3.10 and 3.11 show the antenna installations used for the investigation of the Thule to station Nord link in August 1987. Both antennas were mounted 10 m above the ground pointed at the horizon. The transmitter antenna is a six element Yagi, horizontally polarized. The receiving antennas are cross polarized 6 element Yagis one horizontally polarized, one vertically polarized. The array can be used to measure the depolarization of the propagation path, by measuring the amplitudes and the phase difference of the signals from the two antennas.

The transmitter antenna was mounted on a telephone pole conveniently located close to the transmitter building. The receiving antenna was mounted on an existing tower at station Nord formerly used for receiving antennas. The design of the antennas was based on an existing design at GL and were constructed at ElektronikCentralen. Experience with commercially available Yagi antennas as well as special designs has shown that the radiation properties of a Yagi antenna are not necessarily good because the

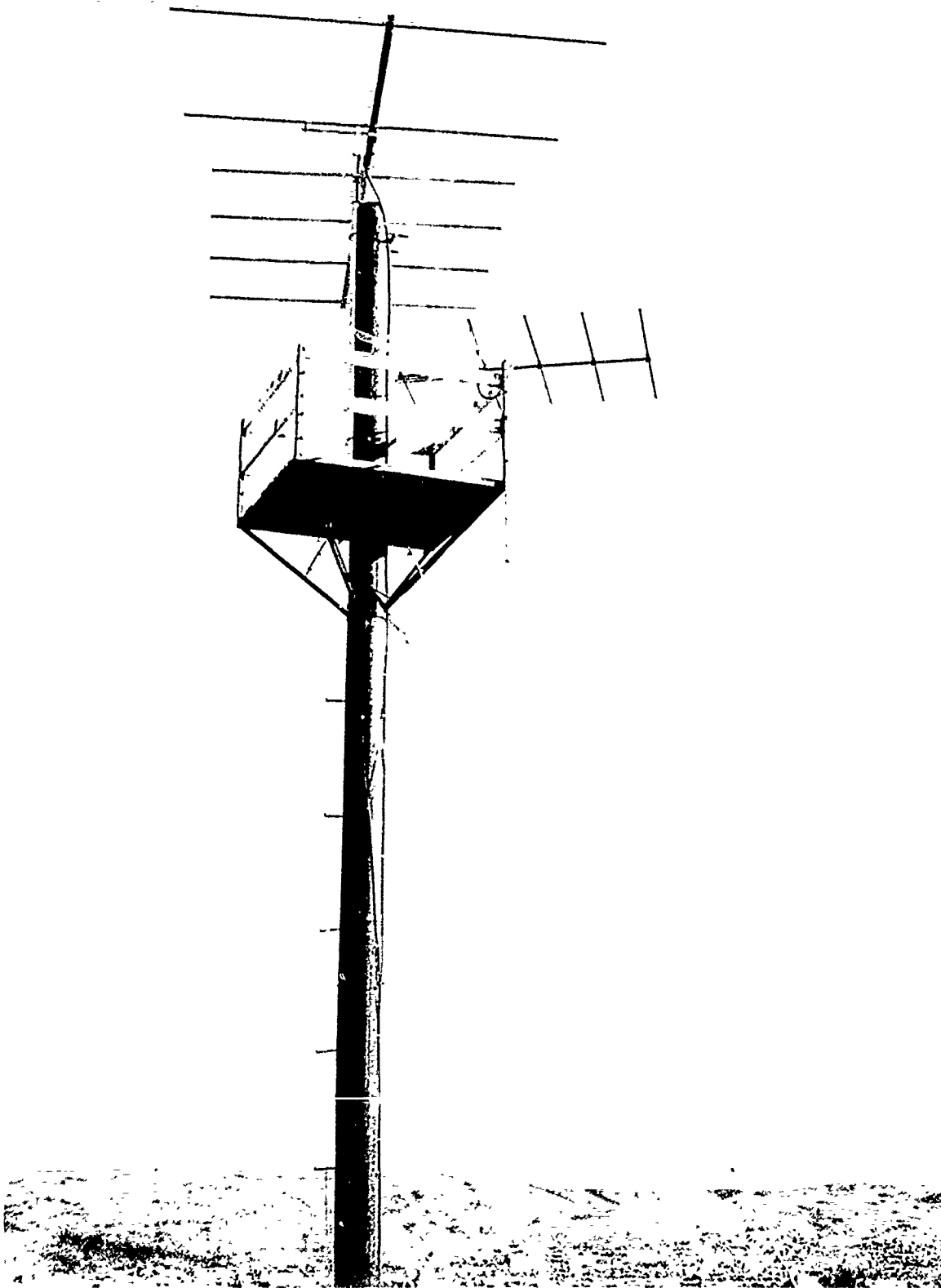


Figure 3.10 Antenna Installation at Thule Used for the August 1987 Campaign

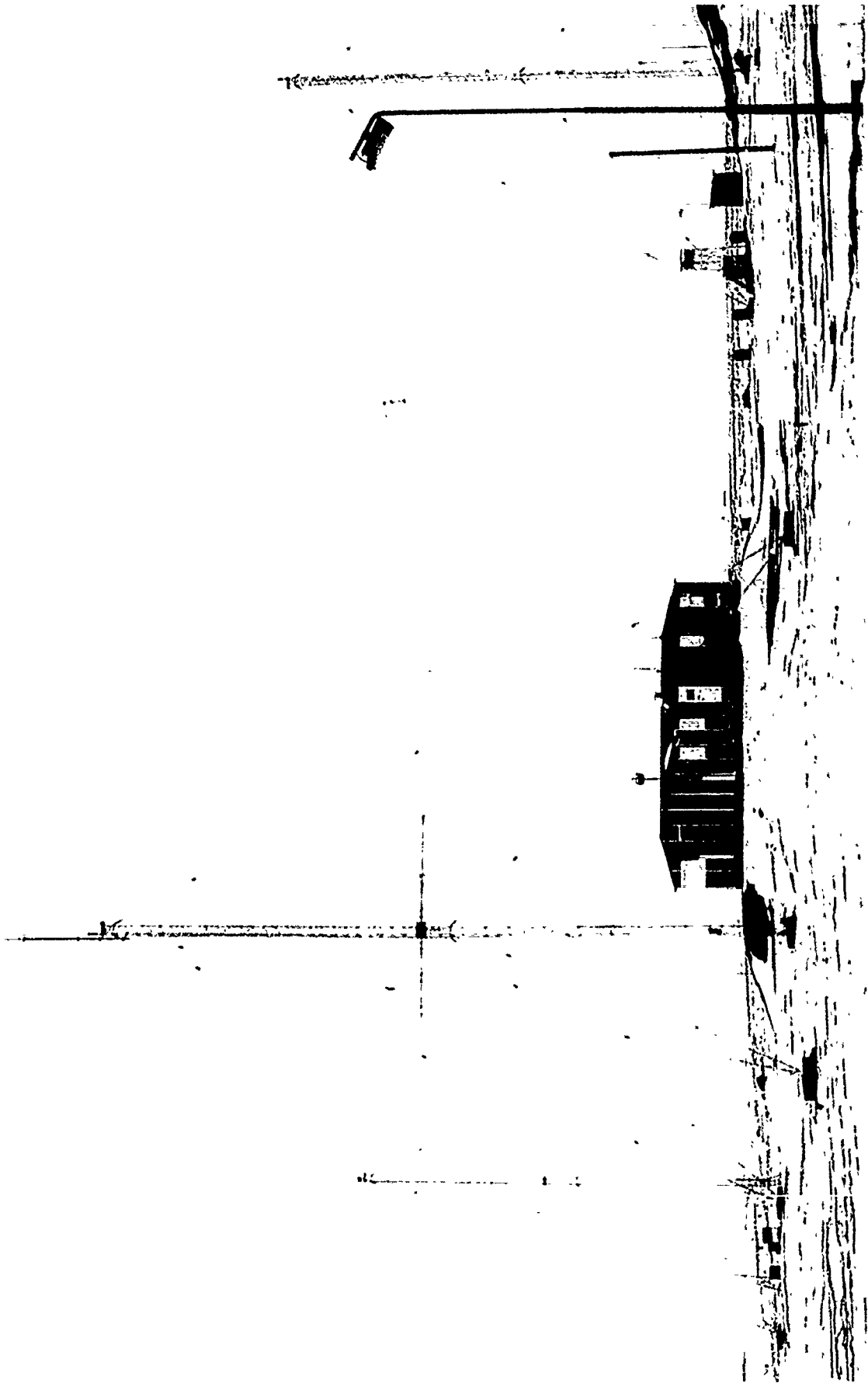


Figure 3.11 Antenna Installation at Station Nord Used for the August 1987 Campaign

antenna is a production item. It is therefore advisable to verify the radiation properties of Yagi antennas intended for meteor scatter communication systems by computation before they are deployed. Such computations have become feasible recently with the availability of computer programs such as PLASYD developed by the Electromagnetics Institute at The Technical University of Denmark or NEC, distributed by the Applied Computational Electromagnetics Society, ACES in the USA. Both programs use the method of moments for the calculations. The value of such calculations are illustrated in Figures 3.12 and 3.13. The example in Figure 3.12 shows properties of a commercially available, five element Yagi for 85 MHz. The Forward gain has a narrow maximum close to but not at the design frequency and the front to back ratio is low at this frequency. The front to back ratio becomes negative, i.e. the antenna starts to radiate

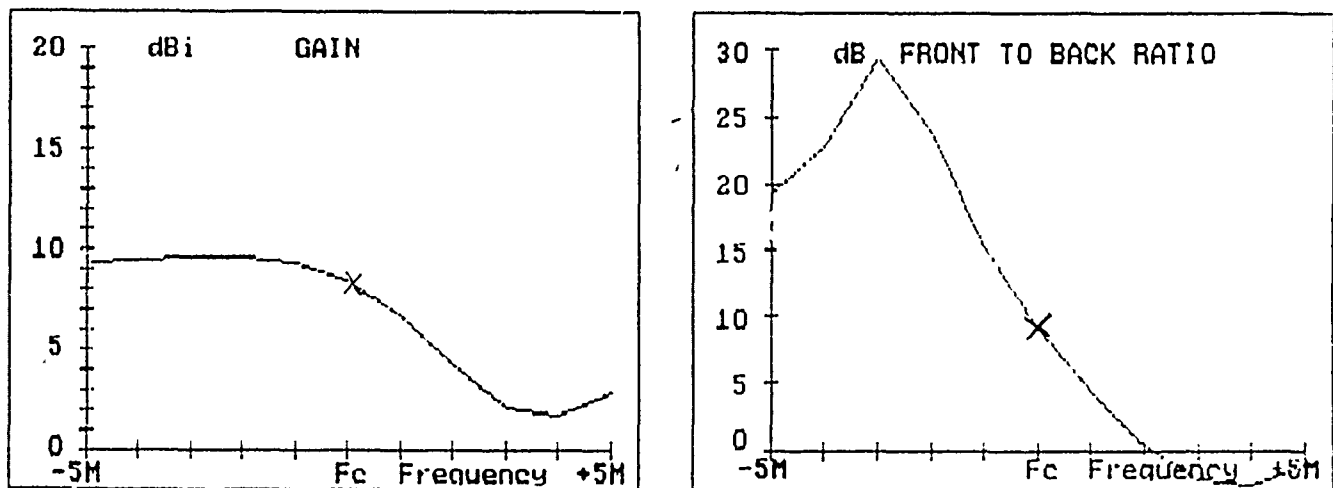


Figure 3.12 Radiation Properties of a Commercially Available Five Element Yagi Antenna of Low Quality Electrically as Well as Mechanically

backwards two MHz above the design frequency. This particular antenna was examined, when poor performance in the field was observed. The example in Figure 3.13 shows a commercially available five element antenna of a better mechanical quality and

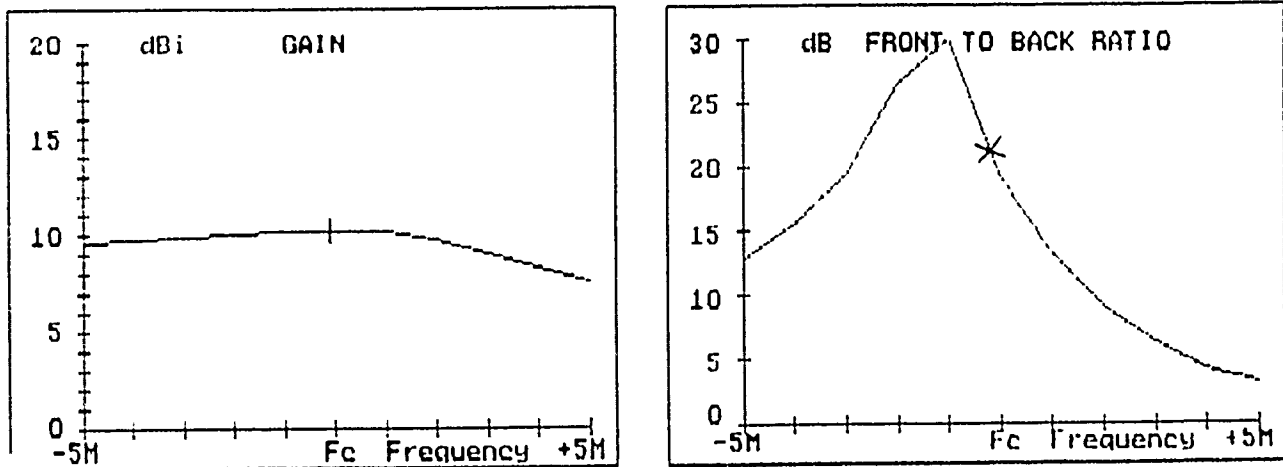


Figure 3.13 Radiation Properties of a Commercially Available Five Element Yagi Antenna of Good Quality Electrically as Well as Mechanically

also a higher price. The gain of this antenna is lower than the gain of the other antenna, but much more independent of frequency. Also, the front to back ratio is high at the design frequency. This antenna is clearly a much better choice for an operational meteor scatter link.

In conclusion, the deployment of antennas for a meteor scatter link should address three items:

- The common volume visible by the stations must be as large as possible, and must include the hot spot areas.
- The illumination of the common volume must be uniform, and a antenna with a suitable gain, i.e. width of the main lobe of the radiation pattern must be chosen.
- The antenna positioning relative to the ground, and its angular elevation with respect to the horizon must be chosen to take as much advantage of the ground reflections as possible.

3.5 Transmitter and Receiver Equipment

The transmitter used for the Thule station Nord measurements consisted of a frequency synthesizer driving a 1 kW output power amplifier. The frequency of operation was 45.113 MHz. The transmissions were modulated with a 400 Hz FM modulation, with a 0.7 kHz deviation. The purpose of the modulation was to identify the signals from the transmitter. No other information was carried. A HP 85 desktop controller was used to start and stop the transmissions according to a schedule of 25 minutes of transmission every two hour time period throughout the experiment.

The receiver used at station Nord was a dual channel phase locked loop receiver developed at ElektronikCentralen for GL. The receiver channels have a common local oscillator so that the phase difference between the two channels is preserved through the conversion and detection within the receiver. One channel is connected to the horizontally polarized antenna, the other to the vertically polarized antenna. This way the complex polarization of a signal can be measured. The received signals are converted to 10.7 MHz and amplified. The signal in the horizontal channel is then phase locked to an internal 10.7 MHz oscillator used as a reference for a set of synchronous detectors. A block schematic of the receiver is shown in Figure 3.14. The phase locked loop tracks the FM modulation, and only the carrier is present as DC levels at the output of the synchronous detectors. The post-detection filters have a bandwidth of 50 Hz. The noise bandwidth of the receiver is thus 100 Hz, but the output of the detectors can still be sampled at 100 samples/sec, as the spectrum is only 50 Hz wide.

The four outputs from the synchronous detectors were sampled every 10 msec, by a PC type computer fitted with a analog/digital converter with 12 bit resolution. Five second sequences of samples were stored on the computer's hard disk, if the phase locked

loop acquired the signal from the transmitter at any time during the sequence. The sampling was continuous, so signals lasting more than five seconds are stored in consecutive sequences. Once a day the information was transferred to floppy disks for permanent storage. The August measurements between Thule and station Nord collected approximately 60 Mbytes of propagation data. The data analysis is described in Sections 5.0, 6.0 and 7.0 of this report.

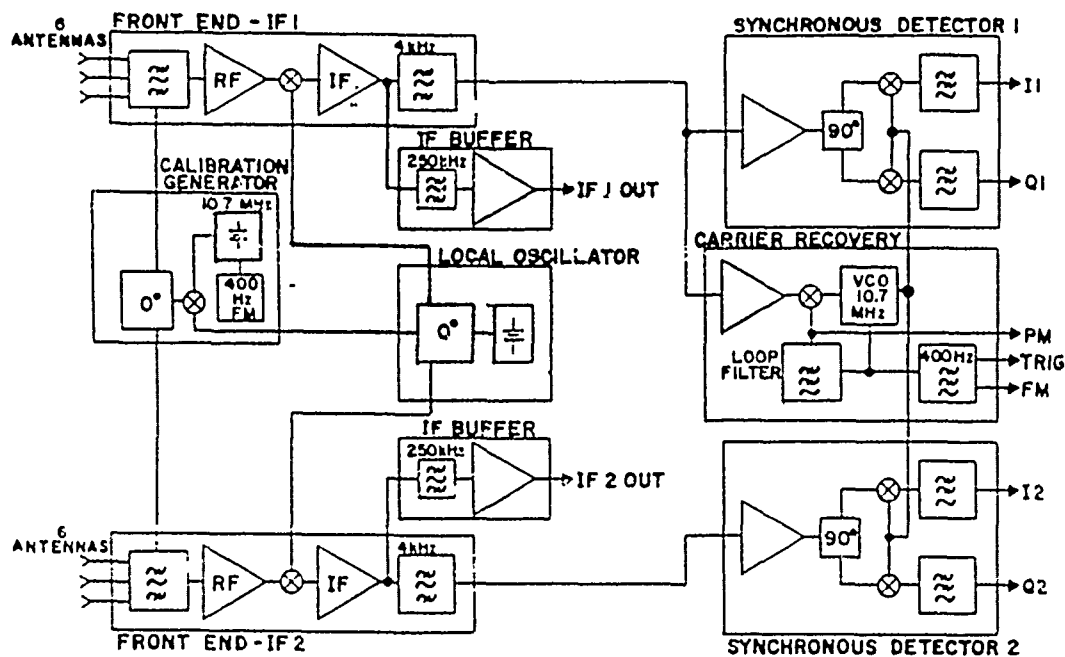


Figure 3.14 Block Schematic of the Phase Locked Loop Receiver Used at Station Nord

4.0 SYSTEM NOISE AND INTERFERENCE IN METEOR SCATTER SYSTEMS

This section of the report describes the different noise sources present in a meteor scatter system, and their impact on the operation of the system.

4.1 Galactic Noise in Meteor Scatter Systems

The noise in meteor scatter communication systems for use in Greenland is primarily galactic and man-made, as receivers with low noise figure front ends (3 dB or less) are readily available. Atmospheric noise is normally not a factor in Greenland at frequencies above the HF band because no propagation paths from the tropical source regions into the polar cap exist. The receiver noise can be much less than the galactic noise at frequencies up to 120 MHz and therefore insignificant.

The antenna temperature due to galactic noise for a receiving antenna is the average brightness of the sky within the antenna aperture. For very big apertures covering a large part of the sky and foreground terrain, little diurnal variation will be seen in the system noise, but the diurnal variation will be several dB for smaller apertures. In addition, the galactic noise at different terminals within the system will not be the same at any instant of time, as their antennas point at different parts of the sky which may have very different galactic noise temperatures. This means that the meteor scatter channel is not in a strict sense a reciprocal channel when the receiving systems are galactically noise limited. Such systems are operating optimally compared to systems which are not galactically noise limited, as any man made noise or interference will reduce the signal to noise ratio in the channel, resulting either in

decreased throughput or a higher bit error rate than otherwise obtained. The galactic noise sources are fixed with respect to sidereal time, so the diurnal variation of the antenna temperature will be offset by two hours each month when observed in solar time.

Noise maps of the galactic sphere for 136 MHz and 400 MHz exist (Taylor), and the noise temperature at other frequencies in the VHF spectrum can be calculated from these, as the noise power is a decreasing function of the frequency ratio to a -2.3 power. A computer program has been designed to compute the antenna temperature of an antenna mounted above a partially reflecting ground. Computations can be made for any time, location and antenna pointing throughout the year.

The computed and measured noise power at 45 MHz for the meteor scatter receiver at station Nord pointed towards Thule is presented in Figure 4.1 for the month of August 1987. The diurnal variation of the galactic noise which amounts to 4 dB is seen. As a comparison the computed noise for a station placed at Thule AB pointed towards Nord is presented in Figure 4.2. The maximum and minimum noise level is encountered at different times at the two stations.

4.2 Man-Made Noise and Interference in Meteor Scatter Systems

Man-made noise and interference can often exceed the galactic noise by more than 10 - 20 dB. Such levels of noise easily degrades the operation of a meteor scatter communication system, as many meteor scatter signals will be obscured by noise and interference. Several distinct sources of man-made noise are important to consider. Interference from other users of the VHF spectrum can easily degrade the throughput of a meteor scatter system, and it follows from this that frequency allocation is an important issues to be addressed. Little interference is expected at

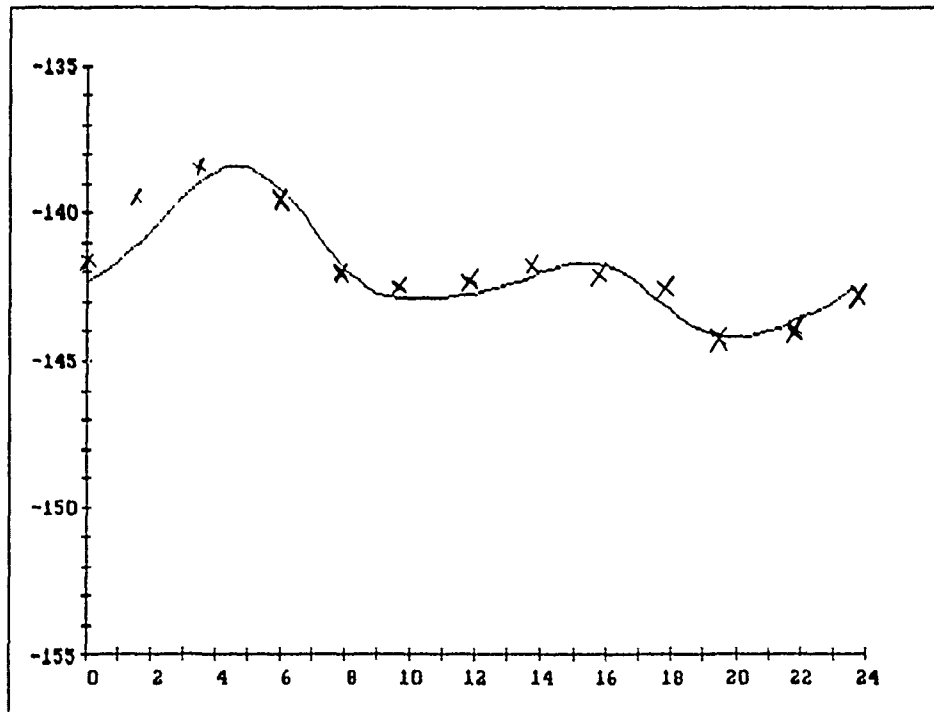


Figure 4.1 Computed and measured noise power in a 100 Hz bandwidth at station Nord. The antenna is a six element horizontally polarized Yagi mounted 10 m above the ground and pointed towards Thule.

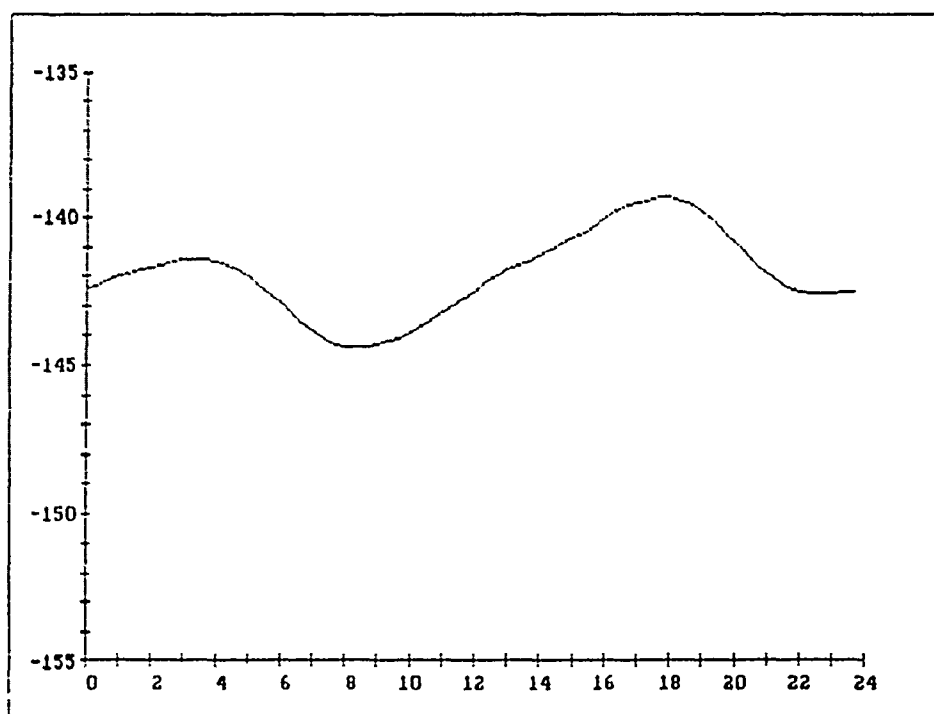


Figure 4.2 Computed noise power in a 100 Hz bandwidth at Thule. The antenna is a six element horizontally polarized Yagi mounted 10 m above the ground and pointed towards station Nord.

frequencies exceeding 40 MHz. At lower frequencies, F2 layer propagated signals from line of sight systems such as mobile telephones, CB and Military users can severely interfere with high latitude meteor scatter communication systems during years of high solar activity. Selecting the lowest possible frequency for a meteor scatter system to obtain the largest communication capacity may therefore not be a good idea.

Two noise sources within the meteor scatter communication system itself are of special importance. The transmitters in systems which operate in full duplex signaling modes must possess very low sideband noise in the spectrum used for reception. The sideband noise should ideally not exceed the galactic noise level. This demand is especially difficult to fulfill if the transmitter and the receiver share a common antenna through a duplex filter. The noise generated by the systems own switching power supply, data processor and other digital system components can exceed the galactic noise power by several tens of dB if no precautions have been taken to shield these components.

Experience shows that many standard laboratory instruments and small computers which contain microprocessors are not sufficiently well shielded to be operated near a meteor scatter receiving terminal. Recently, more and more microprocessors are being incorporated in communications equipment with success, and the required shielding procedures are thus well known.

4.3 Multiplicative Noise

For completeness of the treatment, multiplicative noise should also be mentioned. Multiplicative noise originates from the transmitter, and is propagated to the receiver through a scatter path with a high Doppler spread. The scatter distorts the coherency of the signal, so it resembles noise rather than signal when reaching the

receiver. The level is proportional to the transmitter power, and improvements in Signal to Noise ratio in order to improve communication properties cannot be obtained by raising the transmitter power. The occurrence and magnitude of multiplicative noise in meteor scatter systems has not yet been fully investigated, but it is a phenomenon associated with very high transmitter powers in conjunction with high antenna gains. Thus it will most probably be a problem of little importance for low power meteor scatter with radiated powers of 25 kW or less.

5.0 OVERALL PRESENTATION OF THE DATA SAMPLE

The measurements between Thule and station Nord were started on August 20 in the late afternoon on a continuous basis, but the measurements through the evening and night produced, unexpectedly, so much data that not enough storage would be at hand for more than one or two days of recording. Consequently the measurement schedule was limited to 25 minutes every two hours, a schedule similar to the one used for the Sondrestrom Thule link. The measurements were interrupted for 36 hours on August 25 and 26 as the supply of floppy disks for data storage was exhausted. More floppy disks arrived from Copenhagen in time to secure measurements from the late part of August 26, 27 and a part of August 28. All in all approximately 60 Mbytes of data was taken.

The data was then transferred to a nine track tape and onto the GL minicomputer at Hanscom AB in Boston. The signals were classified into four categories corresponding to underdense and overdense meteor trail signals, sporadic E-layer signals and ionosscatter, and signals propagated by unknown scattering. A large number of signals were plotted for visual inspection of the received waveforms and for control of the automatic classification.

Figure 5.1 shows an underdense trail signal with classification information. The date and time of occurrence and the frequency are printed above the graphs. The top graph shows a set of lines indicating the endurance of the signal. The upper line shows when the phase locked loop detector in the receiver had acquired lock to the signal, and the lower line shows the endurance of the signal determined by the computer as a combination of the presence of the receiver lock flag and a signal-to-noise ratio exceeding 9 dB. The amplitudes in dBm of the signals received by the vertical and horizontal antennas are shown below the flags. The signal levels are

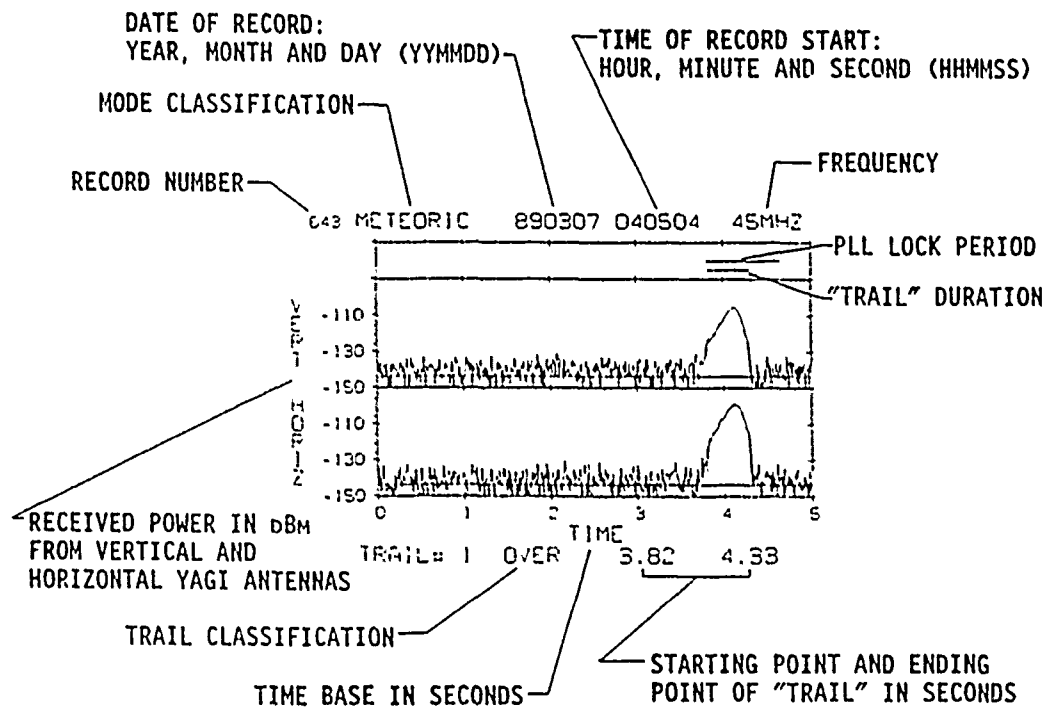


Figure 5.1 Received Underdense Trail Signal With Classification Information

referred to the antenna feedpoints. A straight line on the plots show the noise level of the channels. The vertical channel has a noise offset which is due to an instrumentation error, and the polarization of the signals cannot be evaluated for signal levels below -120 dBm. This deficiency has been corrected in later versions of the receiver. The signal classification and the start and end times are shown below the graphs.

It is difficult to get an impression of the content of the data sample by examining all received signals with a resolution of five seconds and a condensed presentation has been constructed to present a 25 minute data sample in one graph. Only the horizontal antenna signal in dBm whenever it exceeded the noise level by 9 dB is shown. Figure 5.2 presents all data sampled on August 22. Each of

the twelve graphs presents the signals received in one bi-hourly measurement period. Few signals exceed a level of -100 dBm and the activity is smaller in the night and early morning hours than during the rest of the day. In every measurement period several strong long lasting signals with endurances up to one or two minutes are seen. These are too long lasting and too often occurring to be large overdense meteor trail signals. Although meteor trail signals can be this long lasting with large signal levels, their occurrence rate is very small, i.e. one such signal could be expected a week or month. On the other hand these signals do not last long enough to immediately be classified as sporadic E-layer propagated signals. Such signals often last 10 to 30 minutes or more, and the majority of the long lasting signals observed at station Nord lasted between 30 seconds and two minutes. It is speculated if the signals were scattered by polar cap auroral arcs passing through the scattering geometry of the link. Such arcs represent ionospheric currents flowing between the day and night sides of the Auroral oval over the polar cap. Their occurrence present an enhancement of the channel capacity for a link between Thule and station Nord and must be seen as a bonus.

Figure 5.3 presents the data sample from August 24, 1987. Two sporadic E-layer events occurred on this day. One in the period 1530 - 1600 UT and one in the period 2338 - 2350 UT. The first event lasted longer than the measurement period, 25 minutes, and had a signal level between -105 and -110 dB. The second event had little fading and signal levels high enough, (-90 dBm), to saturate the receiver. These events were clearly different from the shorter enduring signals described above and they had the same characteristics as sporadic E-layer propagated signals observed between Sondrestrom and Thule. Apart from the two sporadic E-layer events a large number of the long enduring signals were present on August 24, and also on August 27 and 28, Figure 5.4, and

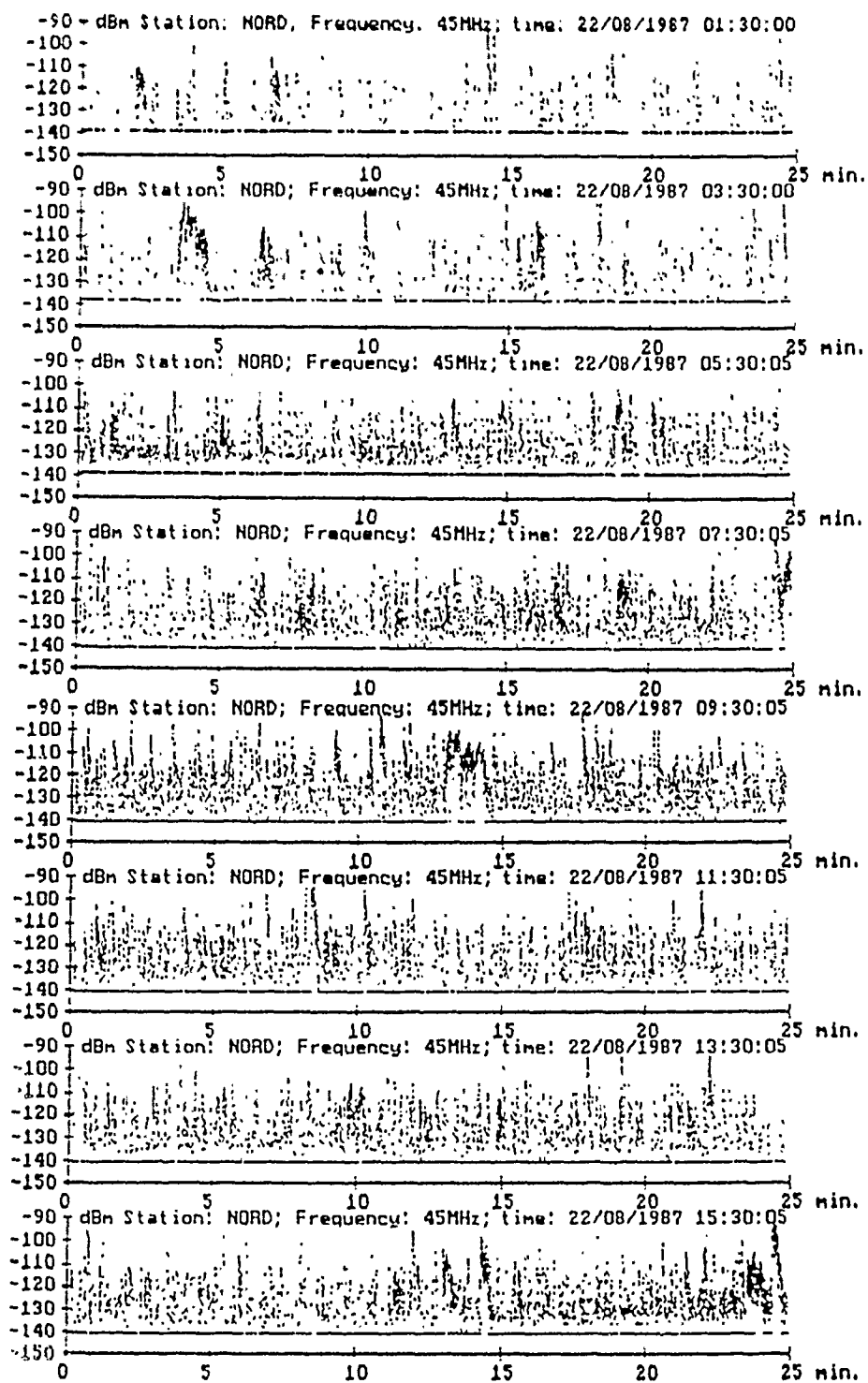


Figure 5.2 Low Resolution Plots of Signals Received at Station Nord
August 22, 1987

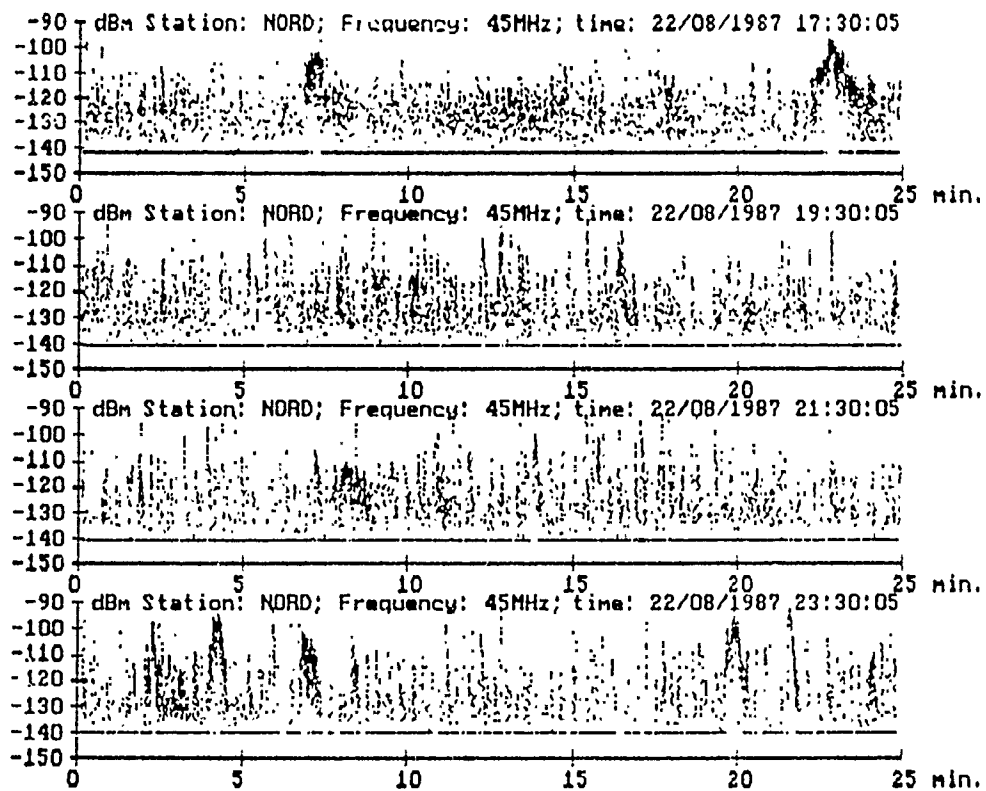


Figure 5.2 Low Resolution Plots of Signals Received at Station Nord
August 22, 1987 (Continued)

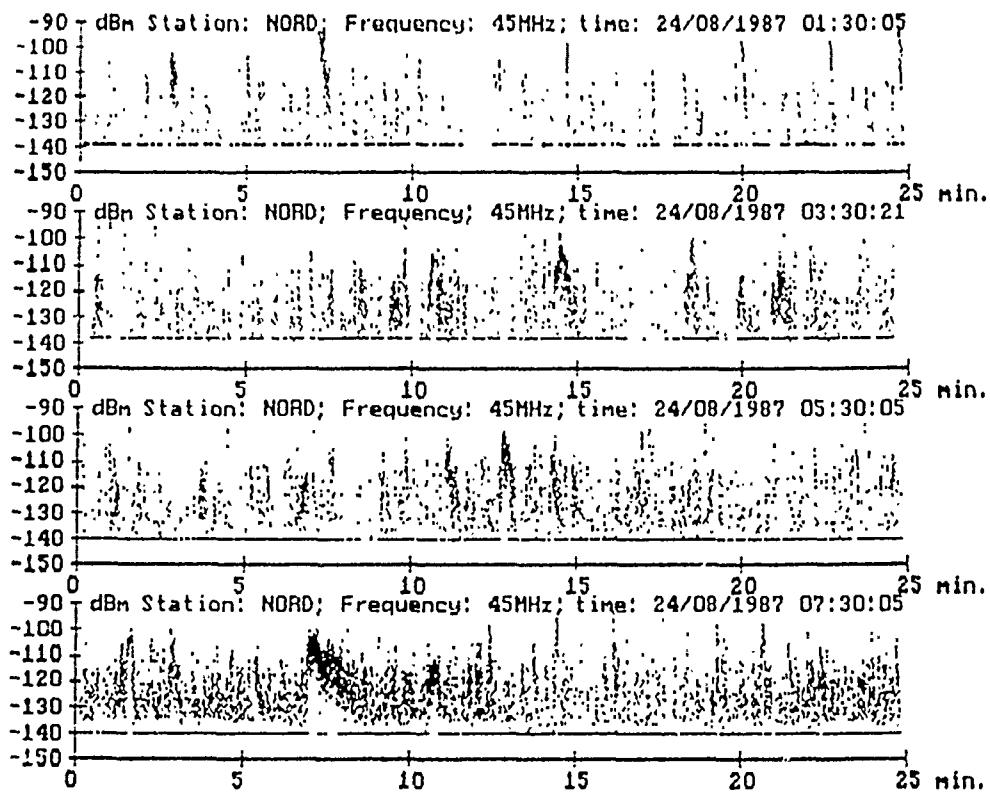


Figure 5.3 Low Resolution Plots of Signals Received at Station Nord
August 24, 1987

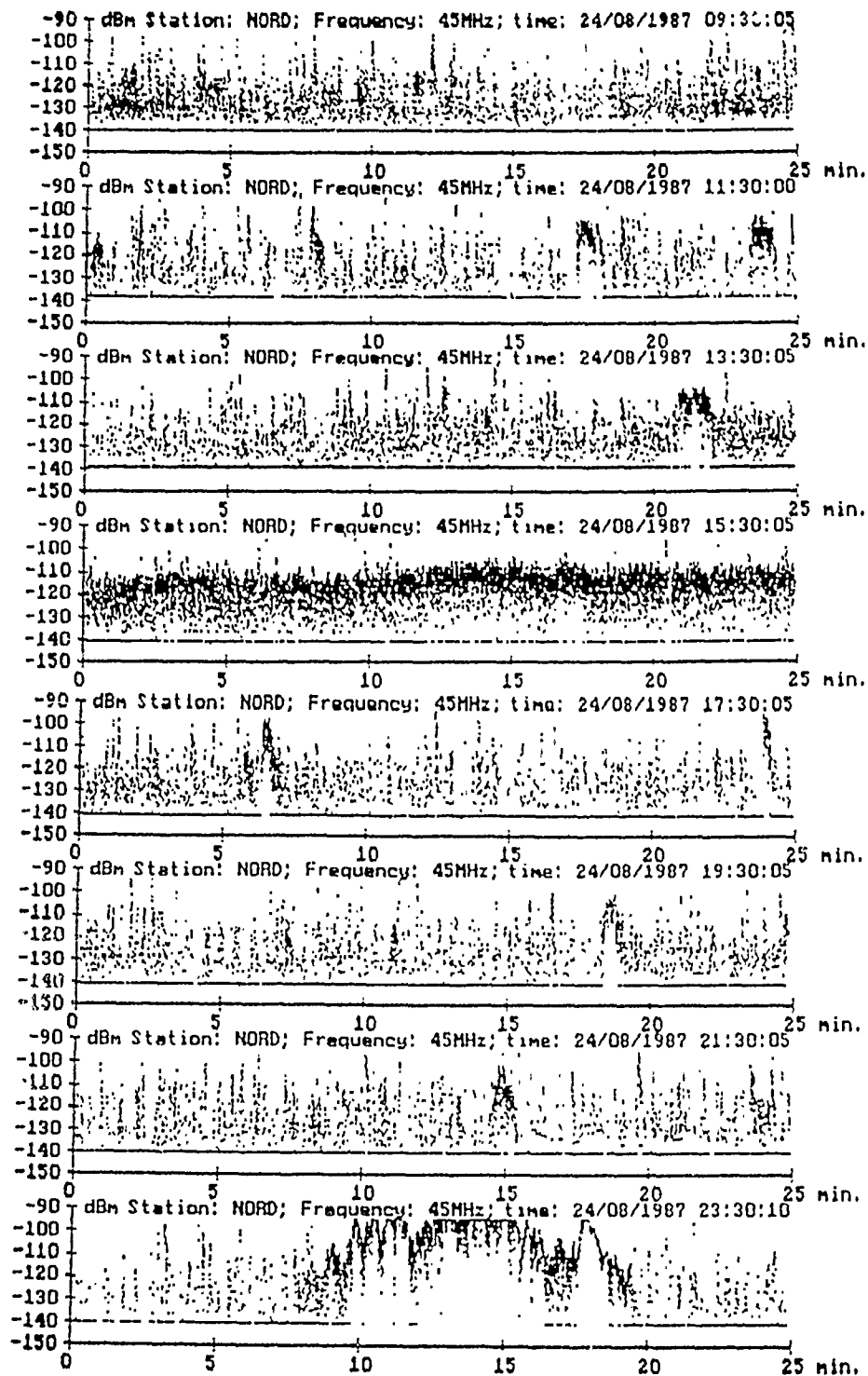


Figure 5.3 Low Resolution Plots of Signals Received at Station Nord August 24, 1987 (Continued)

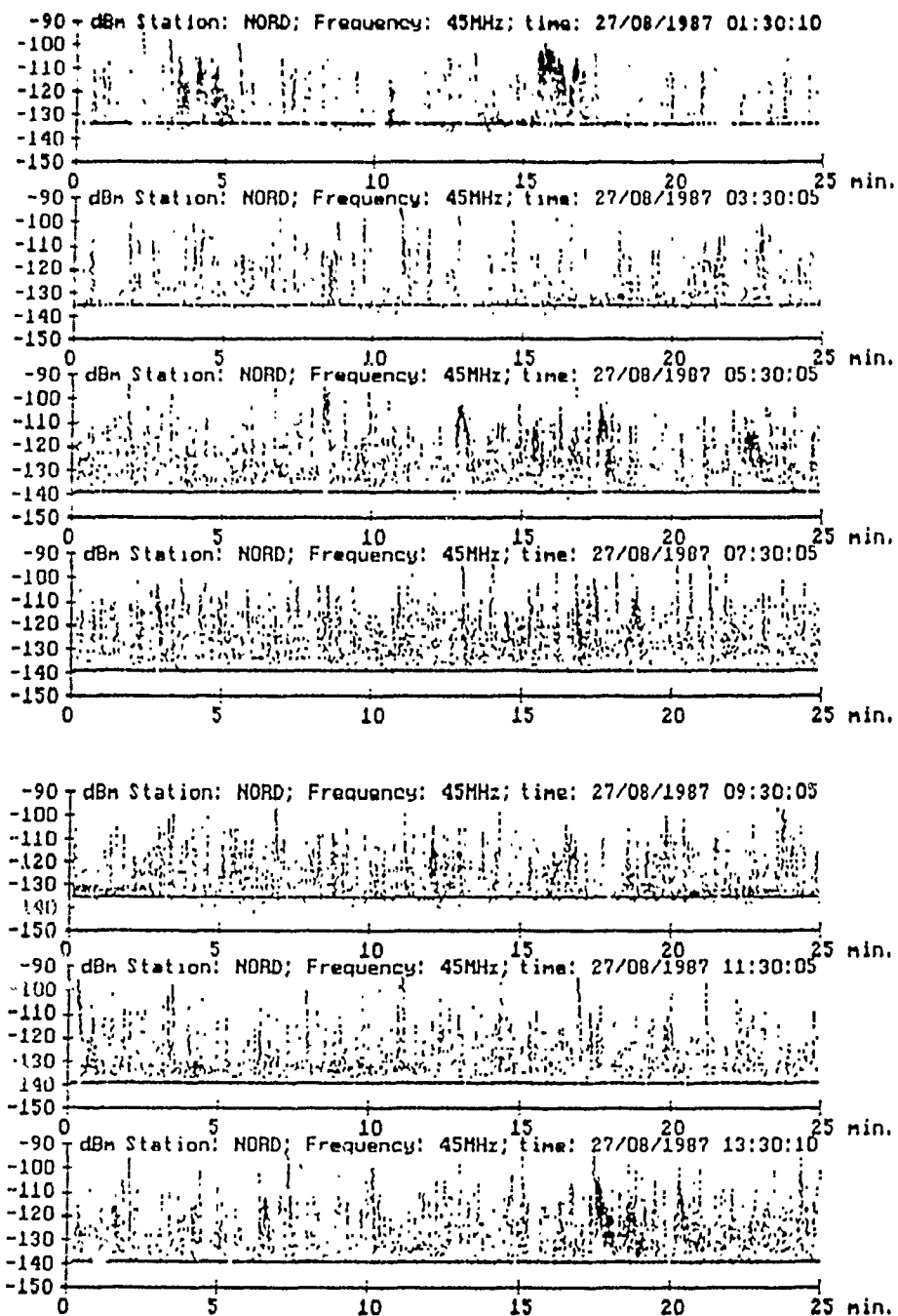


Figure 5.4 Low Resolution Plots of Signals Received at Station Nord
August 27, 1987

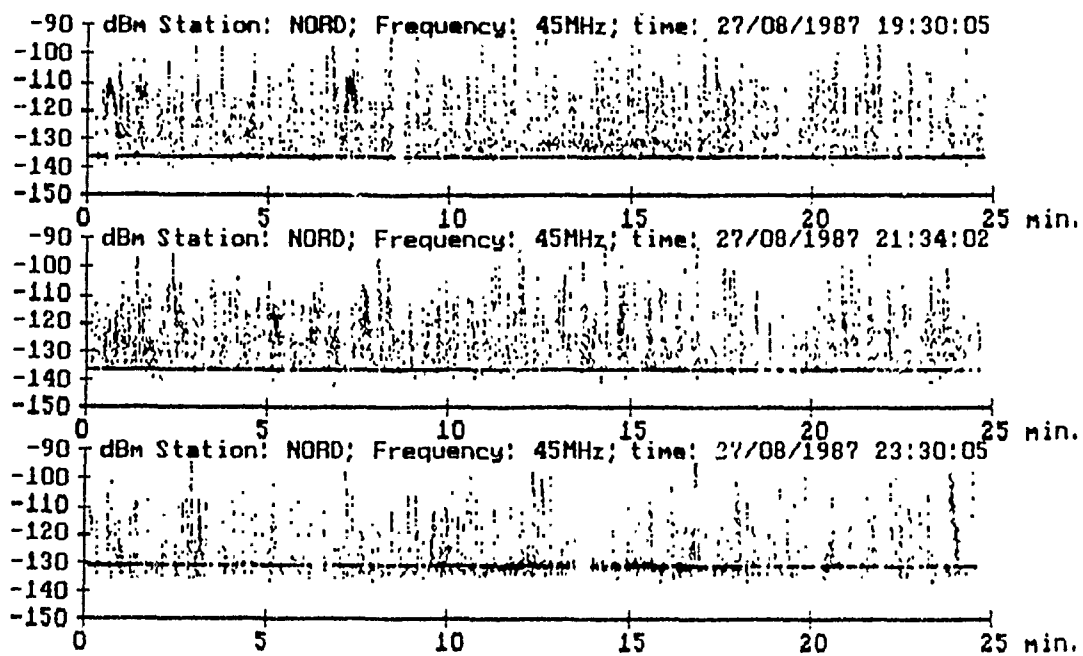


Figure 5.4 Low Resolution Plots of Signals Received at Station Nord
August 27, 1987 (Continued)

Figure 5.5. These signals were also present on the remaining days of the measurement period.

The majority of meteor trail signals observed at station Nord did not look like the idealized underdense and overdense signal waveforms predicted by theory. Rather, fades in one form or other are present on most. Also, a number of meteor trail signals that were presumably formed in a location not supporting propagation between Thule and station Nord, but shifted into such a position by high altitude winds at a time after the formation were observed. Finally the receiving system was so sensitive that a very weak ionospheric scatter signal of approximately the same amplitude as the channel noise, -140 dBm, could be observed regularly. Often this signal was not strong enough for the phase locked loop detector in the receiver to acquire lock, and the signal must be viewed as a noise signal without communication capacity associated with it. In the following, a number of meteor trail signal waveforms are presented to illustrate the various signal types observed during the measurements in August 1987.

A sequence of three underdense meteor trail signals occurring within a five second time interval are shown in Figure 5.6. The first signal is close to the theoretical expectations for underdense trail signals. The amplitude raises from the noise level to -108 dBm in less than 100 msec and then decays exponentially within the next 300 msec's. Such a trail is close to a "mean" underdense trail signal with a duration of 0.3 sec. The next underdense trail signal has the same characteristics of formation, but deep fading most probably caused by the parts of the trail being relocated by high altitude winds begin 0.7 sec after formation. The signal continues to exist for another 1.2 seconds, but has recurrent, deep fades. The third trail signal shows a shallow fade 0.2 seconds after formation and then a short enhancement. This may be due to the simultaneous occurrence

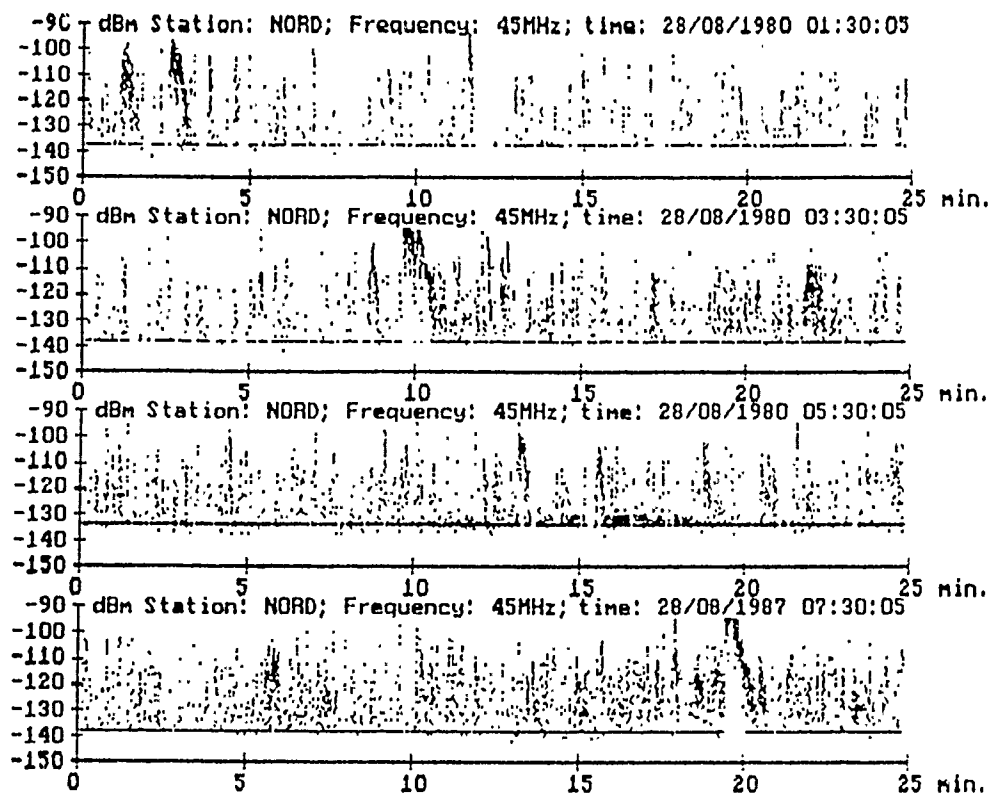


Figure 5.5 Low resolution plots of signals received at station Nord August 28, 1987. The measurements ended at 08 UT.

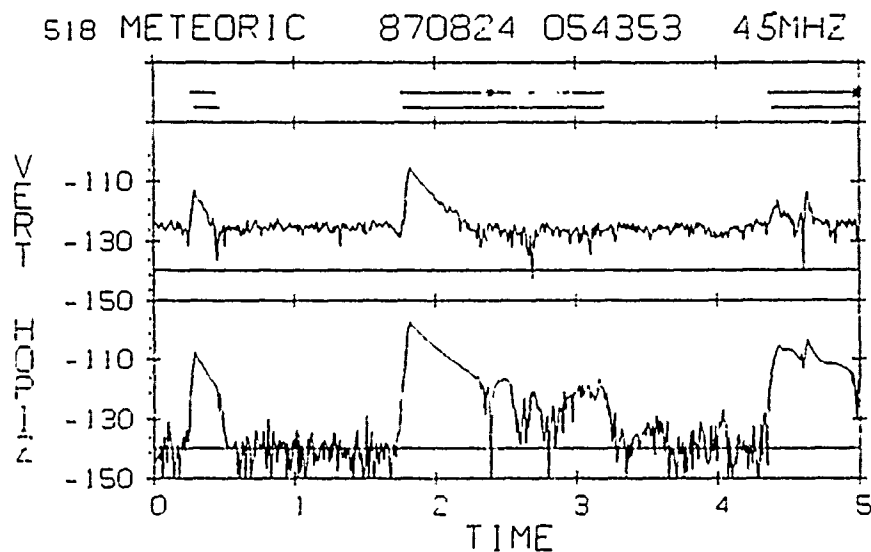


Figure 5.6 Example of a Series of Three Underdense Trail Signals Occurring Within a Five Second Time Interval

of two meteor trails that both supported propagation between Thule and station Nord. A better example of this is shown in Figure 5.7.

A long lasting underdense trail signal was formed at the beginning of second four in the sequence. The signal had a slow diffusion and lasted more than two seconds with only a 4 dB loss of amplitude. After two seconds an overdense meteor trail signal was received in addition to the underdense trail signal. The overdense trail signal had a very large amplitude, -92 dBm, just after formation, but began to fade after approximately 0.6 seconds. The overdense trail signal lasted for six seconds but was broken up into segments due to the fading. The simultaneous occurrence of two meteor trail signals can lead to destructive multipath propagation if the signal amplitudes are comparable. In this case the overdense signal is much stronger than the underdense signal during the first 0.5 seconds, but some of the fading observed thereafter might well be

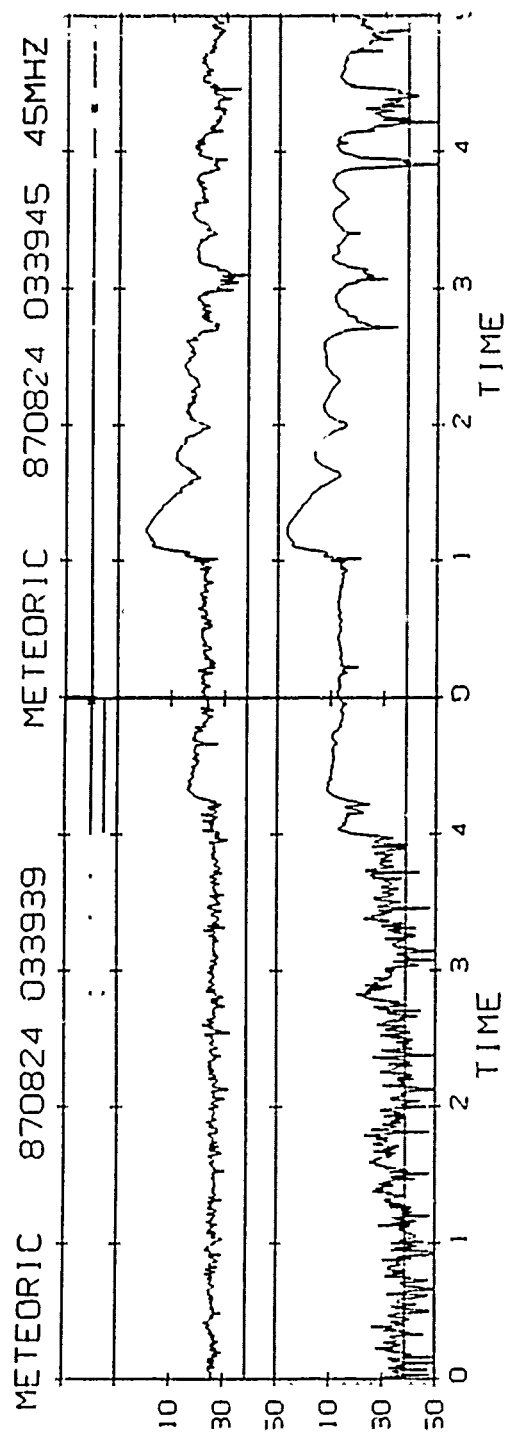


Figure 5.7 A Ten Second Time Interval Where a Long Lasting Underdense Meteor Trail Signal is Being Overlaid by an Overdense Trail Signal

caused by interference between the two signals as they could have been moved relative to each other by high altitude winds.

Figure 5.8 shows an overdense meteor trail signal that was shortened appreciably by fading. It is of course impossible to project how long the signal would have been if it had not faded, but judged from the development of the fading signal, it might have lasted two seconds instead of the 0.5 seconds seen on the figure.

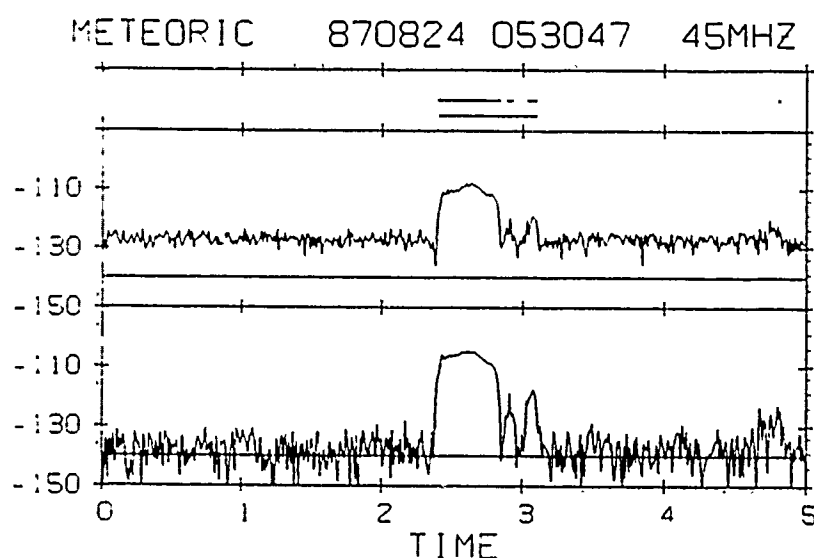


Figure 5.8 Example of an Overdense Meteor Trail Shortened by Fading

A long lasting overdense meteor trail signal with a more regular fading is shown in Figure 5.9. The fresnel zone fading is seen in the first 0.1 second after trail is formed and the amplitude continues to increase for the next 0.3 seconds until a combination of diffusion and fading reduces the amplitude of the signal. The total endurance of the trail signal was almost two seconds, but a communication system might have lost lock during some of the fades and have experienced the signal as a sequence of shorter signals. A

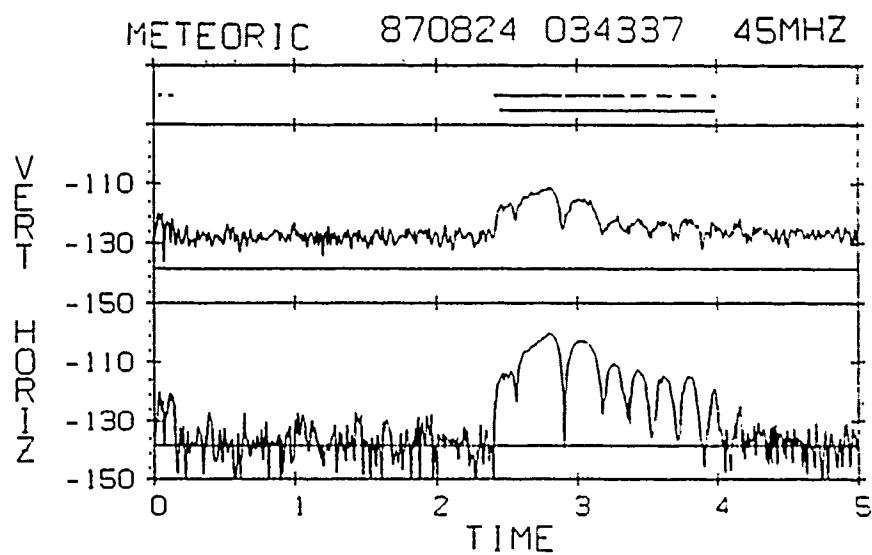


Figure 5.9 Example of an Overdense Trail Signal With Fading

communications processor is needed to control the exchange of information on a meteor scatter link and this processor can use a number of techniques such as error correcting codes and interleaving to combat fades. The processor must also be capable of acquiring a signal and establishing handshake with the other terminal in a link. This follows from the waveforms presented in this section. The signal is very variable and fast acquisition of the signals is essential due to the short duration either of the signals as such or the duration between deep fades within a trail signal.

Figure 5.10 shows an example of an overdense trail signal that was possibly formed in a location not quite good enough to support propagation between Thule and station Nord and then shifted into a better position by high altitude winds. The shift may have warped the trail to produce several independently reflecting segments and this in turn has produced the fading seen on the signal.

Finally Figure 5.11 shows an example of the weak ionoscatter signal such as is often observed on meteor scatter links with high sensitivity. The signal is just a few dB stronger than the noise level, and it is difficult to determine if it is composed from a number of weak underdense meteor trail signals or it is a weak continuous signal embedded in the noise. The signal is not useful for communication and would not have been detected by a receiver with a larger bandwidth such as would be used in a communication system.

Figures 5.12.A, B, C show a sequence of five second records of the long lasting high level signal observed August 24 at 1147 UT. The signal started with a fast fading prelude at 114715 UT which was very different from the Fresnel Zone fadings observed on meteor trail signals. The signal then gained amplitude and the fading rate slowed. A slow fading signal with high amplitude was then observed for 50 seconds, an endurance very seldom observed for

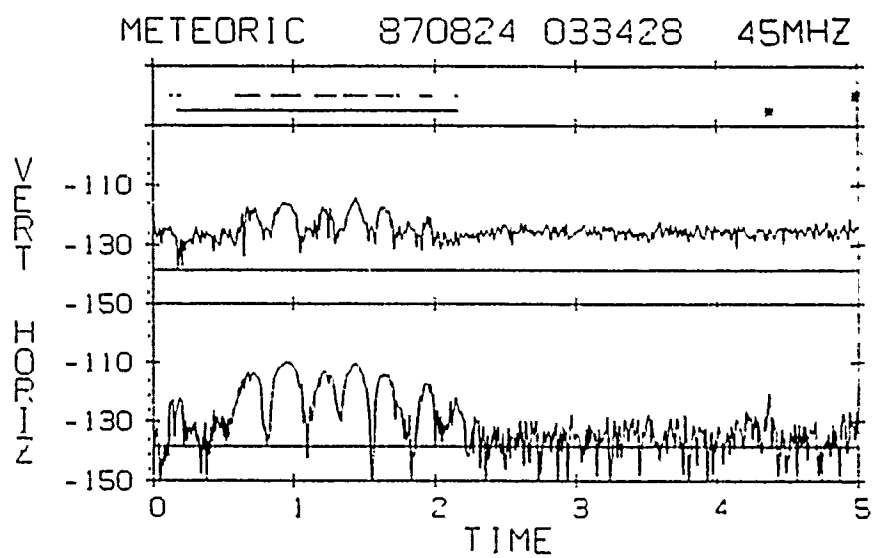


Figure 5.10 Example of an Overdense Meteor Trail Signal With Severe Wind Distortion

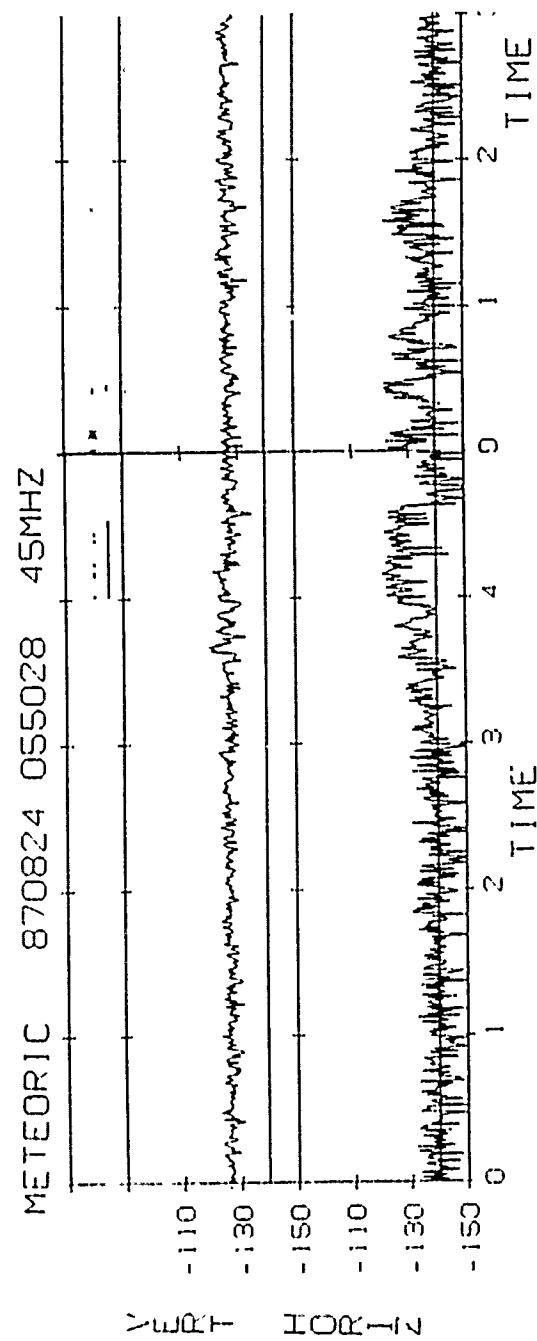


Figure 5.11 Example of a Weak Ionosscatter Signal Often Observed on Very Sensitive Meteor Scatter Links

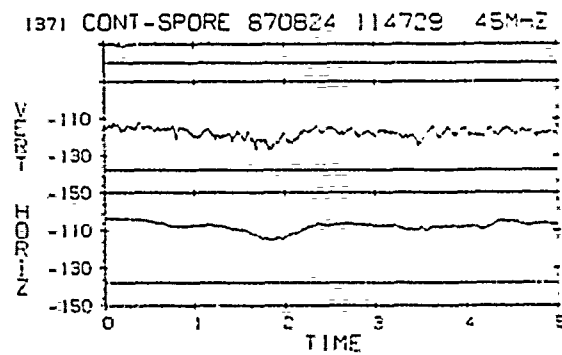
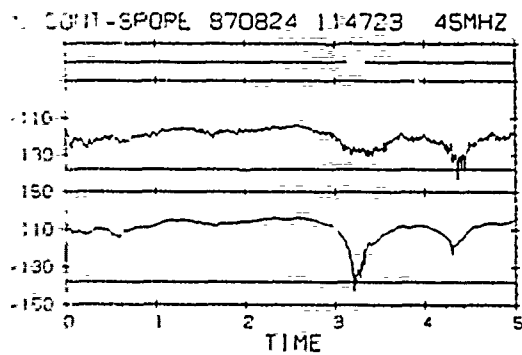
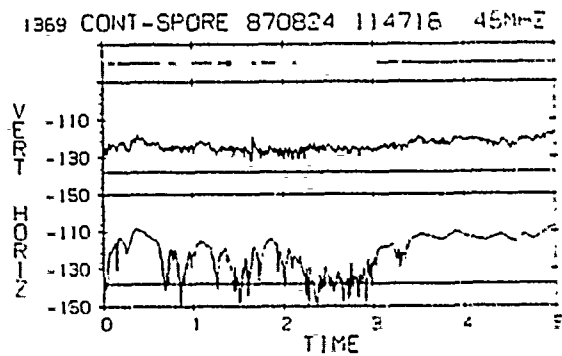
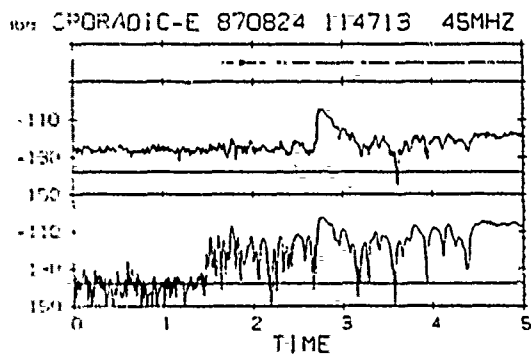


Figure 5.12A Sequence of Received Signals Showing the Long Enduring High Level Signal Observed on August 24 at 1147 UT

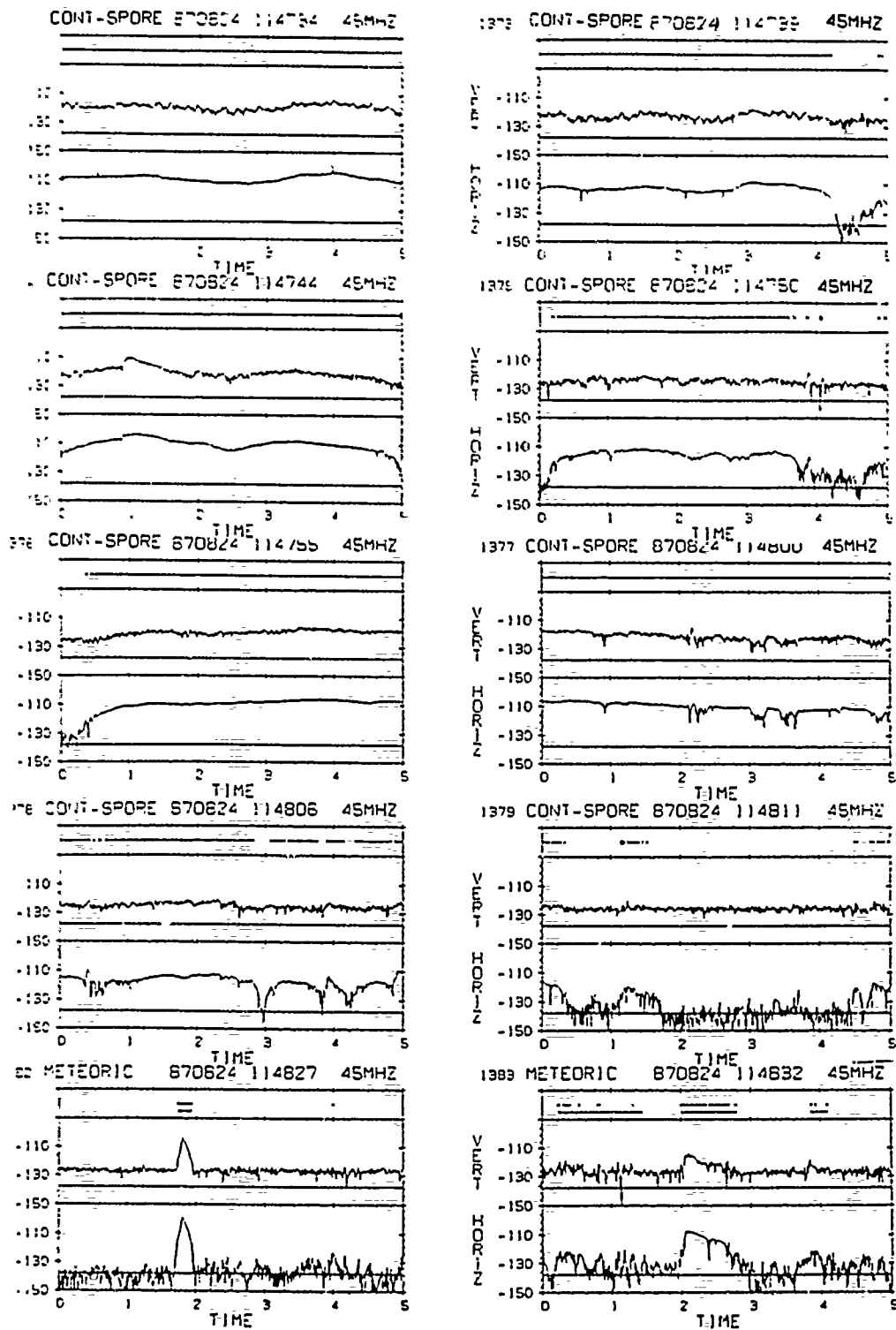


Figure 5.12B Sequence of Received Signals Showing the Long Enduring High Level Signal Observed on August 24 at 1147 UT

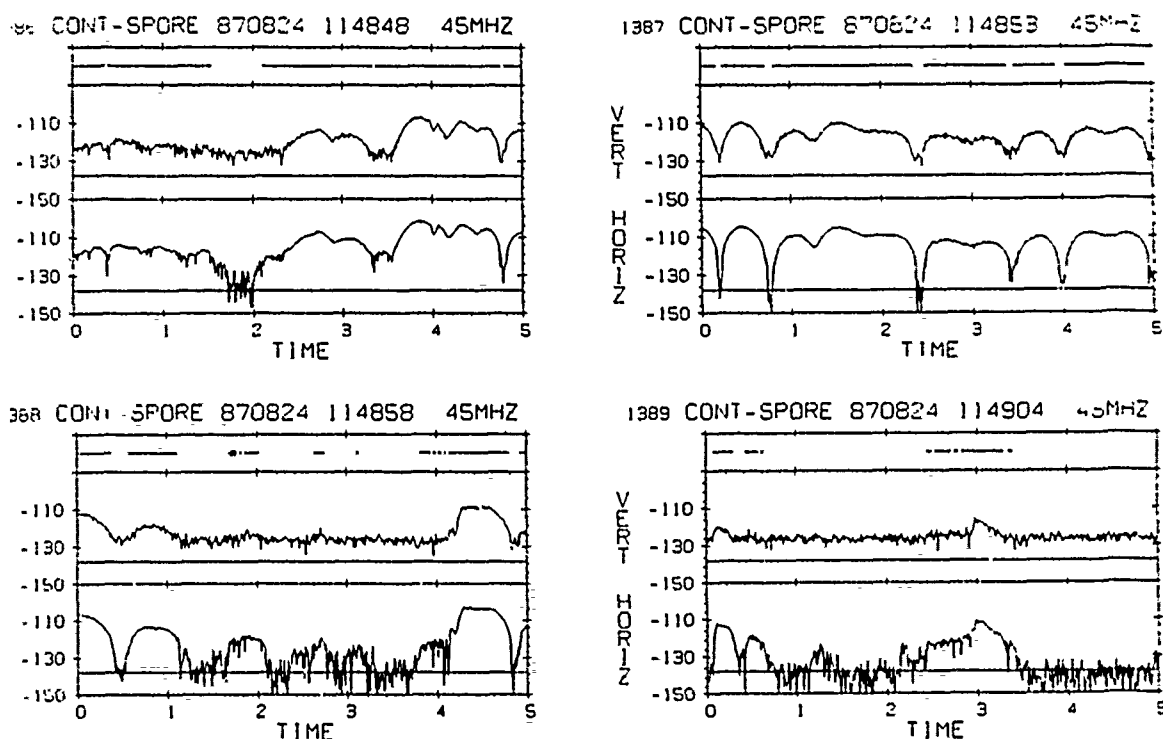


Figure 5.12C Sequence of Received Signals Showing the Long Enduring High Level Signal Observed on August 24 at 1147 UT

meteor trail signals. The signal all but disappeared at 114811 UT and regular meteor trail signals were observed until 114848 UT when the slow fading signal reappeared for another twenty seconds. The event was then over and more regular meteor scatter trail signals followed. The endurance of the signal was clearly much longer than the endurance of the meteor trail signals occurring in the same time frame and a substantial communication capacity would have been associated with it. Also, the signal amplitude behaved much like the sequence of sporadic E-layer reflected signal shown in Figure 1.5. Although these signals may or may not be caused by a

propagation mode different from sporadic E-layer propagation they will not be different from a communications point of view. A communication protocol which will be able to utilize meteor trail signals and sporadic E-layer signals will be able to utilize these signals as well.

After this rather extensive discussion of non-meteor trail signals it is reasonable to add a few comments as to whether the signals received at station Nord were propagated on a meteor scatter channel, or if it was rather an ionoscatter channel. Overall, it was a meteor scatter channel because the majority of the ionoscatter signals were so weak that they did not have much communication capacity associated with them except if a combination of very high transmitter power and high gain antennas would be used for an operational system. This, however, would be true of any meteor scatter communication system. It has been observed at other locations that the connectivity of a meteor scatter system increases from a few percent for an exclusively meteor scatter propagation channel to a large fraction of the time when power is increased but the increase in connectivity is associated with ionoscatter or a multitude of very short meteor trail signals.

What was different from a meteor scatter channel was the additional capacity obtained from sporadic E-layer propagation which is well known from other high latitude locations is a "bonus channel" of good value at high latitudes especially for a link such as the proposed Thule station Nord channel that has primary emphasis on capacity. Also the occurrence of the shorter lasting but high level signals speculated to be caused by Auroral arcs are a bonus at high latitudes.

6.0 THE PROPAGATION STATISTICS

The signal waveforms acquired at station Nord have been processed into a data base at GL in Boston. The data base can be queried to produce both propagation and communication related statistics. This section presents the propagation statistics of: Meteoric arrival rates, duty cycles, durations, fades and underdense time constants. These statistics describe the time and bandwidth properties of the meteor scatter channel provided no dispersion is present. Measurements have shown this to be true for bandwidths exceeding 100 kHz (Weitzen, 1985).

The data acquired at station Nord were transferred to the GL VAX computer and the date, time, noise level, transmit power, frequency, and other information was attached to each data record. The next step was classification in which the dominant propagation mechanism in each data record, or sequence of records, was identified. Classification is an important element of the analysis procedure because several different propagation modes are observed at high latitudes. Due to differences in propagation mechanisms these modes have different communication and propagation characteristics. In addition to underdense and overdense meteor trails, sporadic-E and low level ionospheric scatter propagation occur frequently.

If the dominant mechanism in a record or sequence of records was meteor propagation, the type of each meteor trail (underdense or overdense) was identified and entered, along with the time of the trail and its duration. Other propagation mechanisms such as sporadic E-layers and ionosscatter require special treatment. Arrival rates cannot be defined for these and the statistics include duty cycles, durations and fades. The end product for this portion of the data analysis was a data base for the period of the investigation.

The final step in the processing procedure was statistical analysis of the classified data bases. Information in the data base was retrieved and processed interactively using a menu-driven program. Output of the analysis program is presented in either table form or in files which can be plotted using a number of different routines. The statistical analysis options are divided into two general categories; propagation analysis and communication analysis.

The propagation statistics allow analysis of the arrival rate of trails, their duration and duty cycle as a function of trail type, signal level, time of day and day. The Communication statistics allow a user to infer the performance of a specified link from the actual data. Parameters which can be defined by the user are the data rate, modulation, bit error rate, packet structure, and signalling protocol. Users can specify either a fixed data rate system or an adaptive data rate system. Available statistics include time to deliver a message, and throughput as a function of time of day, event type (underdense, overdense, sporadic-E, or low level scatter), frequency, data rate, packet duration, error rate and packet structure. Selected communication statistics are presented in Section 7.0 of this report.

The arrival rate for signals are defined as the number of signals received each minute which exceed a defined threshold. Such a description is linked to the mass of the micro-meteorite creating the trail and to the scattering geometry. The arrival rate can be referenced to a Received Signal Level RSL in dBm, or to the Signal to Noise Ratio existing in the channel expressed in dB. The arrival rate can be in, but is not limited to, the range 0.1 to 20 meteors/min.

The duty cycle is defined as the percentage of the total time the meteor scatter channel is open, and the signal level or signal to noise ratio in the channel exceeds some required value either above a RSL or an SNR. The duty cycle does not describe the duration of the individual signals. These are determined mostly by

the fading associated with long lasting trails. The duty cycle covers the range 0% to 100%.

The duration of a meteor signal above a threshold of either RSL or SNR in the channel is defined as the continuous period of time, the signal level remains above the threshold. The duration is determined by the endurance of signals without fades and the time between fades for signals with fades. The average endurance of underdense trails is approximately 0.4 sec, and fading rates between 0.1 and 1 fades/sec are common. The distribution of signal duration is therefore expected to have a mean of approximately 0.5 sec and cover the range 0 to and exceeding a few seconds. Occasionally a very long meteor trail signal without fades can be observed. Although such signals are spectacular, the rate of occurrence is so small (one a week to one a month) that they are not relevant for link design.

Most meteor scatter signals fade, so the durations are generally shorter than the life time of the individual meteor trails or sporadic E events. The duration of a fade is defined as the continuous period of time the signal remains 3 dB or more below a threshold. The fade durations are of interest to the communication systems designer, because the communication system must be designed to cope with both shallow and deep fades. This means, that both coding to overcome short fades and frequent resynchronization due to deep, long lasting fades must be incorporated in the communication protocol. Underdense meteor trail signals are characterized by a fast rise of the received signal power, followed by an exponential decay. The decay time constant theoretically describes the signal duration above a threshold. However, some underdense trail signals fade, so the durations may not be expressed by the exponential decay. The statistics analysis package extract the underdense trail signal decay time constant as least mean squares fit to the decay process.

Figure 6.1 illustrates the derivation of the various quantities from the classified waveforms.

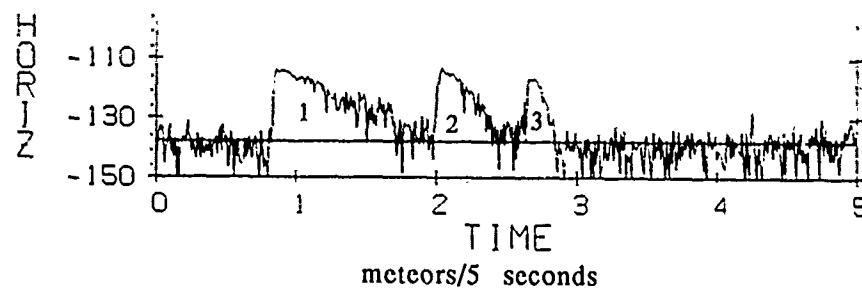
All propagation statistics presented in this section describe the horizontally polarized signal. The period of measurement did not contain any ionospheric disturbances with expected depolarization effects.

6.1 Arrival Rate Statistics

The average arrival rate of underdense and overdense meteor trails has been computed as a function of Received Signal Level and Signal to Noise Ratio for the measurement period in August 1987. The results are presented in Figures 6.1.1, 6.1.2.

The arrival rate of underdense trails exceeds that of overdense trails at low SNR's as expected. The arrival rate of overdense trails exceeds that of underdense trails at high SNR's. The crossover point is at 33 dB SNR. According to Forsyth et al. (Proc IRE Dec. 1957, p. 1650) the asymptotic slopes of the total arrival rate in double logarithmic coordinates should be approximately -1 and -4 for the part dominated by underdense and the part dominated by overdense trails. Slopes close to these numbers are present in Figure 6.1.1 and Figure 6.1.2.

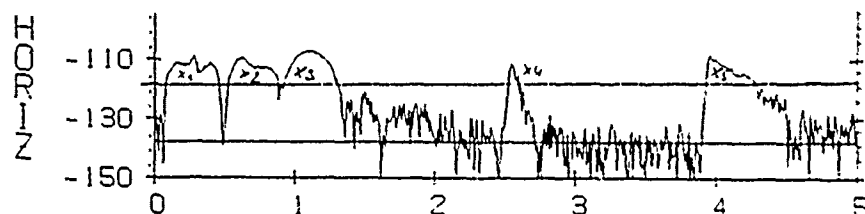
The change from underdense to overdense scatter occurs at a electron line density of approximately 10^{14} electrons/cm at 45 MHz, and it could be expected that very few overdense trails were found at low SNR's, and conversely very few underdense trails were found at high SNR's. However, the peak amplitude of a meteor scatter signal is not solely dependent on the electron line density of the trail. It also depends on the orientation of the trail with respect to the plane of propagation, and the forward scattering angle. Thus a significant number of overdense trails are found at low SNR's, but it



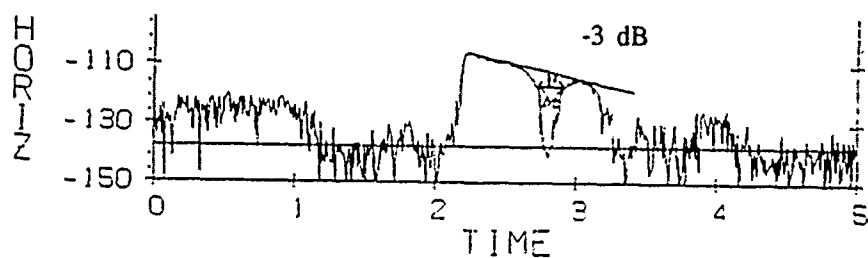
Arrival rate,
duty cycle,
durations:

$$\text{Duty Cycle} = 100 \sum X_i / 5\%$$

Durations: X_1, X_2, X_3, X_4, X_5 seconds



Fade durations: $t_f = \Delta t @ -3 \text{ dB}$



Underdense time constants: $t_c = \Delta t / 8.68 \text{ dB}$

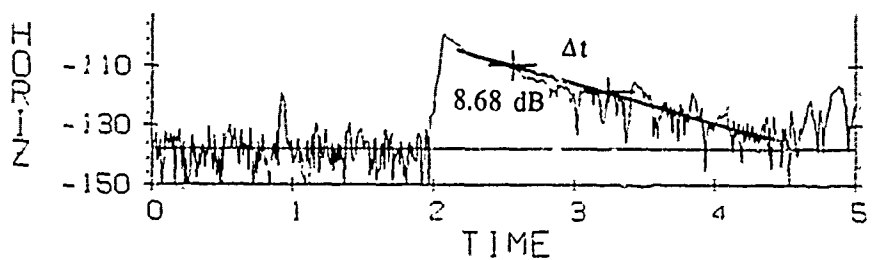


Figure 6.1 Derivation of Arrival Rate, Duty Cycle, Duration, Fades, and Underdense Time Constants from the Classified Waveforms

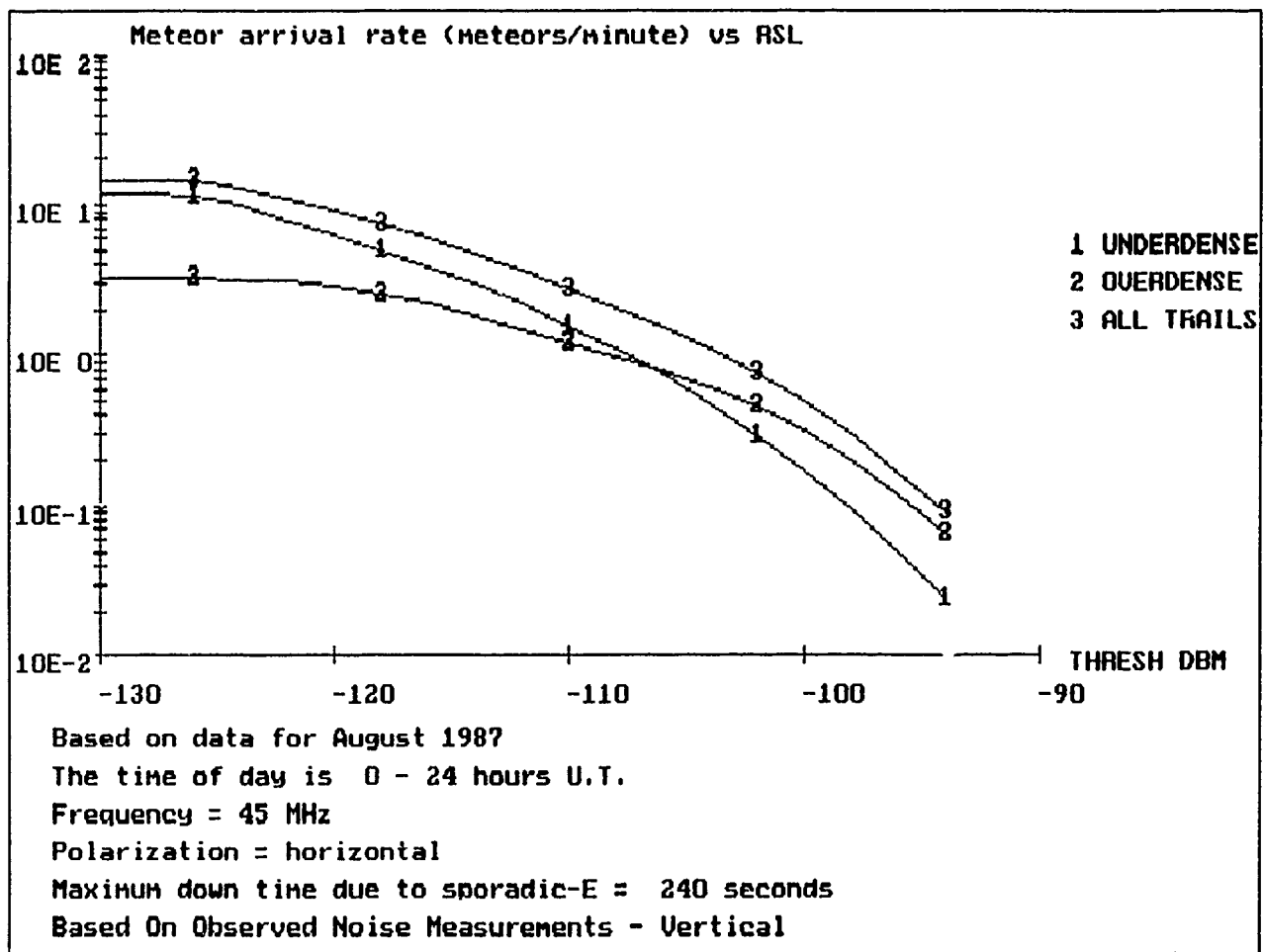


Figure 6.1.1 Meteor Arrival Rate as a Function of RSL for August 1987 at Station Nord

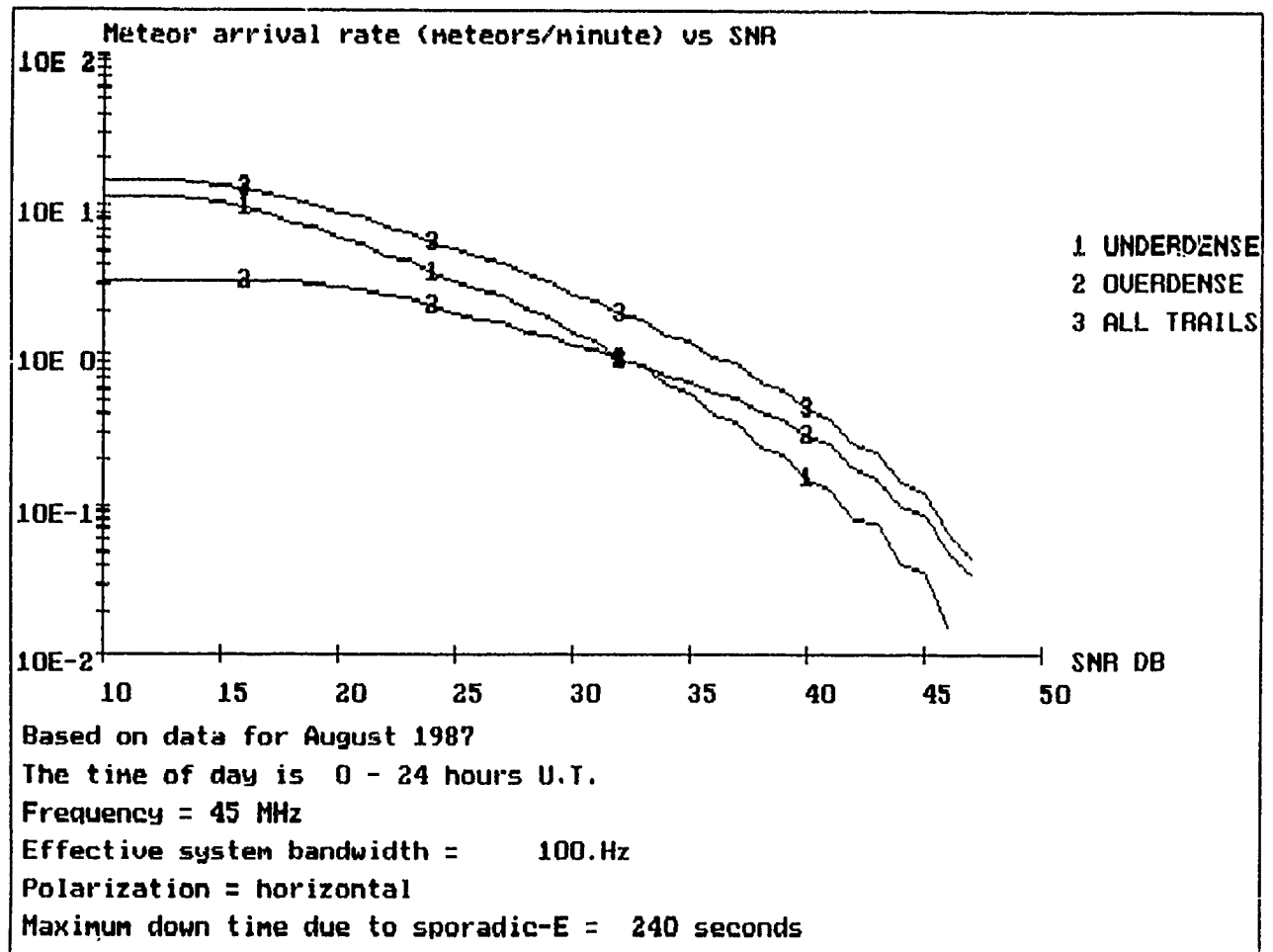


Figure 6.1.2 Meteor Arrival Rate as a Function of SNR for August 1987 at Station Nord

is seen from Figures 6.1.1 - 6.1.2 that no overdense trails with peak amplitudes less than -124 dBm are found. The arrival rate of the underdense trails continue to increase with decreasing SNR until the receivers triggering level of -127 dBm is reached.

A meteor scatter communication system transmitting 8000 bits/sec, with a target bit error rate of 10^{-3} requires a SNR of 26 dB relative to the SNR of the test link having a 100 Hz noise band width. Thus, with 10000 W and 1000 W of transmitter power, the arrival rate should be dominated by underdense trails. With a transmitter power of 100 W and 10 W the arrival rate will be more and more dominated by overdense trails. This has implications for the waiting time to transfer short messages. The overdense trails are generally longer lasting than the underdense trails and generally provide larger communication capacity by supporting large signaling speeds. A communication system relying predominantly on overdense trails due to either a low transmitter power or a high signaling rate can exhibit prohibitive waiting times for transfer of short messages due to the low arrival rate of overdense trails. The tradeoff between transmitter power, waiting time and capacity are investigated and quantified in Section 7.0 of this report.

The average diurnal variation of the arrival rate for signals exceeding -100 dBm, -110 dBm, and -130 dBm RSL are presented in Figures 6.1.3 - 6.1.5. A diurnal maximum is expected at approximately 08 UT, when the path between Thule and station Nord is at the Earth's apex to its orbit around the sun. In this position the Earth sweeps up meteors. At 20 UT a diurnal minimum would be expected, as the path is at the Earth's antapex, where the Earth moves away from the meteors. It is seen from the figures, that the expected maximum occurs at 08 UT, but that a second maximum occurs at approximately 20 UT and the expected diurnal minimum at 20 UT is not present. It is believed that the second diurnal maximum is due to trails generated by meteors arriving over the

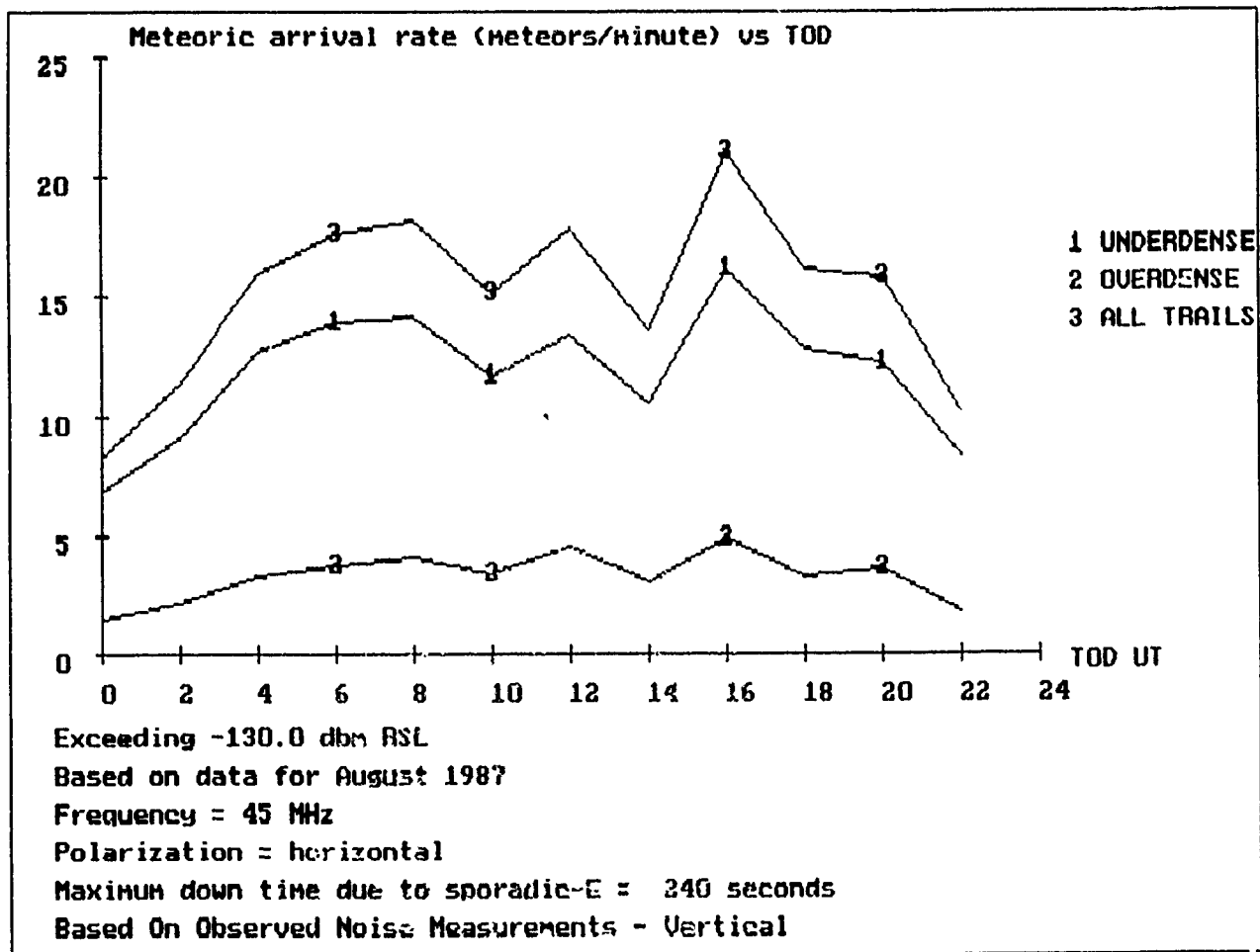


Figure 6.1.3 Arrival Rate vs. Time of Day for Signals Exceeding -130 dBm for August 1987 at Station Nord

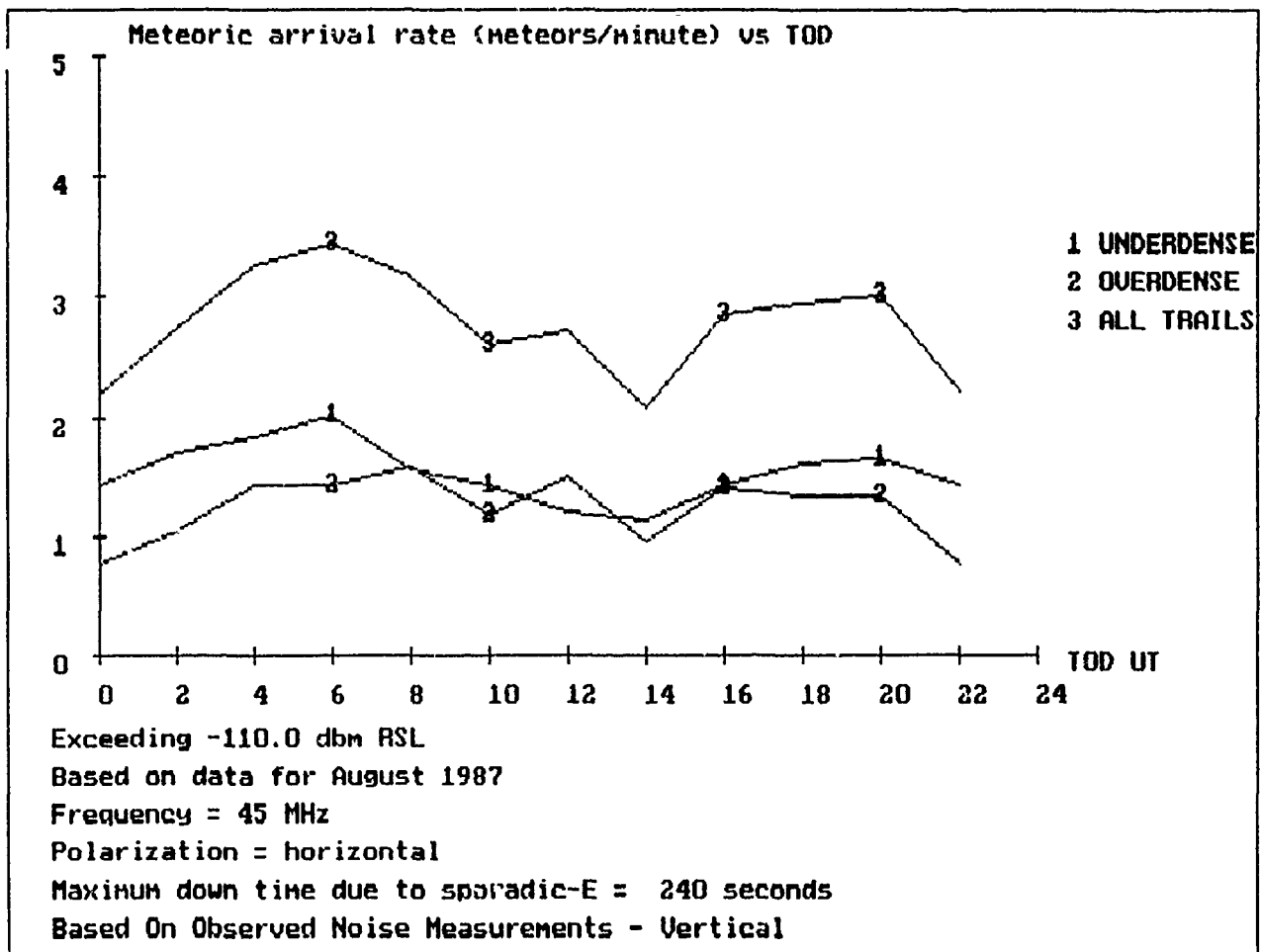


Figure 6.1.4 Arrival Rate vs. Time of Day for Signals Exceeding -110 dBm for August 1987 at Station Nord

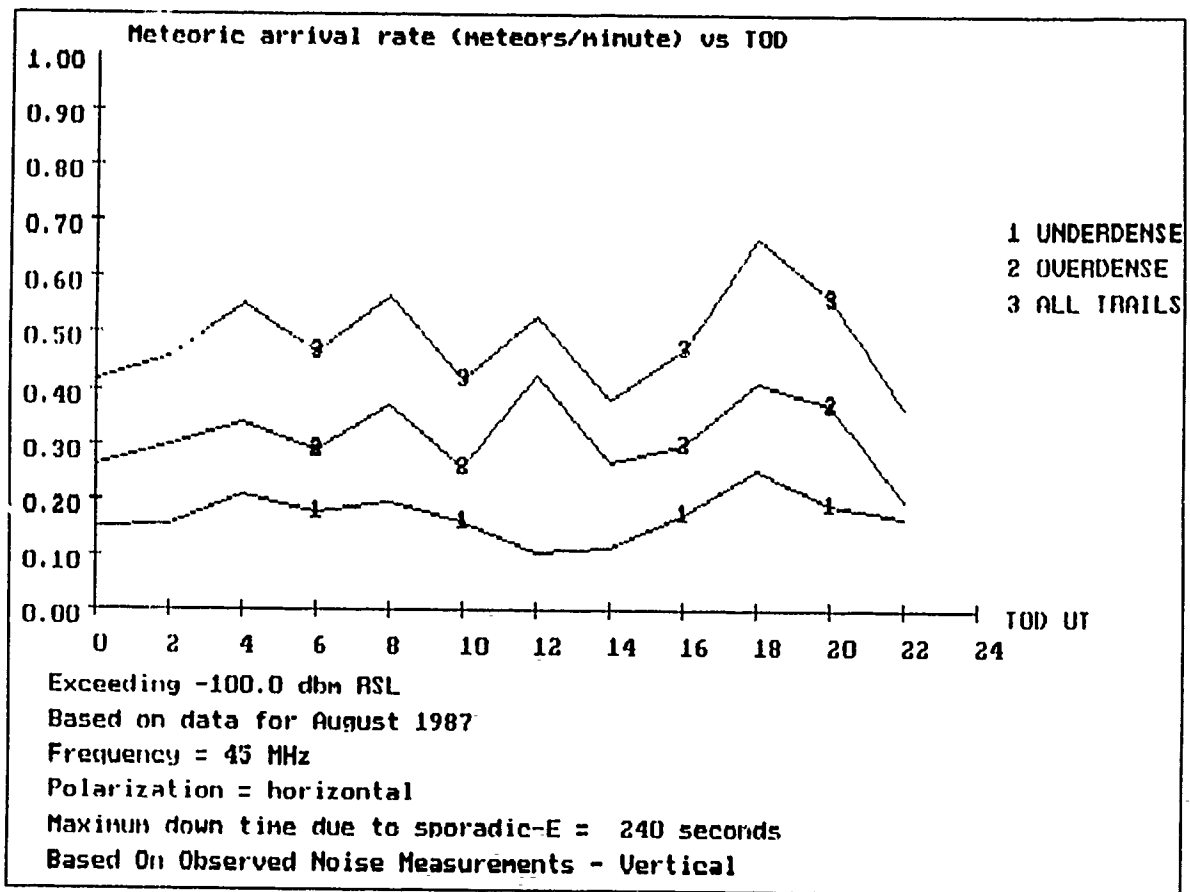


Figure 6.1.5 Arrival Rate vs. Time of Day for Signals Exceeding -100 dBm for August 1987 at Station Nord

North Pole from the morning side of the earth. Computer models of meteor arrival rates anticipates this for a link at such high latitude as the Thule station Nord link. The late afternoon meteors arriving from the morning side presents an advantage for a meteor link into station Nord. The capacity of the link will have little diurnal variation due to the arrival of meteors, and also added capacity in the afternoon.

The average diurnal variation of the arrival rate for signals exceeding 20 dB and 30 dB SNR are presented in Figures 6.1.6 and 6.1.7. The diurnal variation is similar to the variation found for the arrival rates exceeding RSL in the range -130 to -100 dBm. The

arrival rate vs. SNR statistics are included to enable a comparison with the derived communication statistics presented in Section 7.0 of this report.

Figures 6.1.8, 6.1.9 present the arrival rates for signals exceeding -110 dBm RSL and 30 dB SNR for the measurement period. Day to day variations of the diurnal average arrival rate are seen. The arrival rate of underdense trails decrease during the period.

6.2 Duty Cycle Statistics

The average diurnal variation of the duty cycle exceeding -110 dBm for the period of measurement August 20 - 28 1987 for the Thule station Nord link is presented in Figure 6.2.1. The meteoric signal duty cycle shows a maximum around 08 UT, and another maximum at 20 UT, consistent with the diurnal variation of the meteoric arrival rate. The total duty cycle is dominated by the duty cycle of the overdense trail signals. Although the arrival rate of overdense trails at this signal level is less than half of the arrival rate of underdense trails, they generally last much longer. The duty cycle of sporadic-E signals is dominated by the sporadic-E events occurring August 24 and 25, and by the long lasting signals described in Section 5.0, postulated to originate from Auroral arc scatter.

The average diurnal variation of the duty cycle exceeding 10, 20, 30, and 40 dB SNR for the period of measurement August 20 - 28, 1987 for the Thule station Nord link are presented in Figures 6.2.2 - 6.2.5. The meteoric signal duty cycle shows a maximum around 08 UT, and another maximum at 20 UT independent of SNR. The diurnal variation is similar to the diurnal variation of the duty cycle exceeding -110 dBm. However, the passage of the Galactic noise maximum between 00 and 04 UT create a relative decrease of the duty cycle vs. SNR during this time period. The total duty cycle is again dominated by the duty cycle of the overdense trail signals.

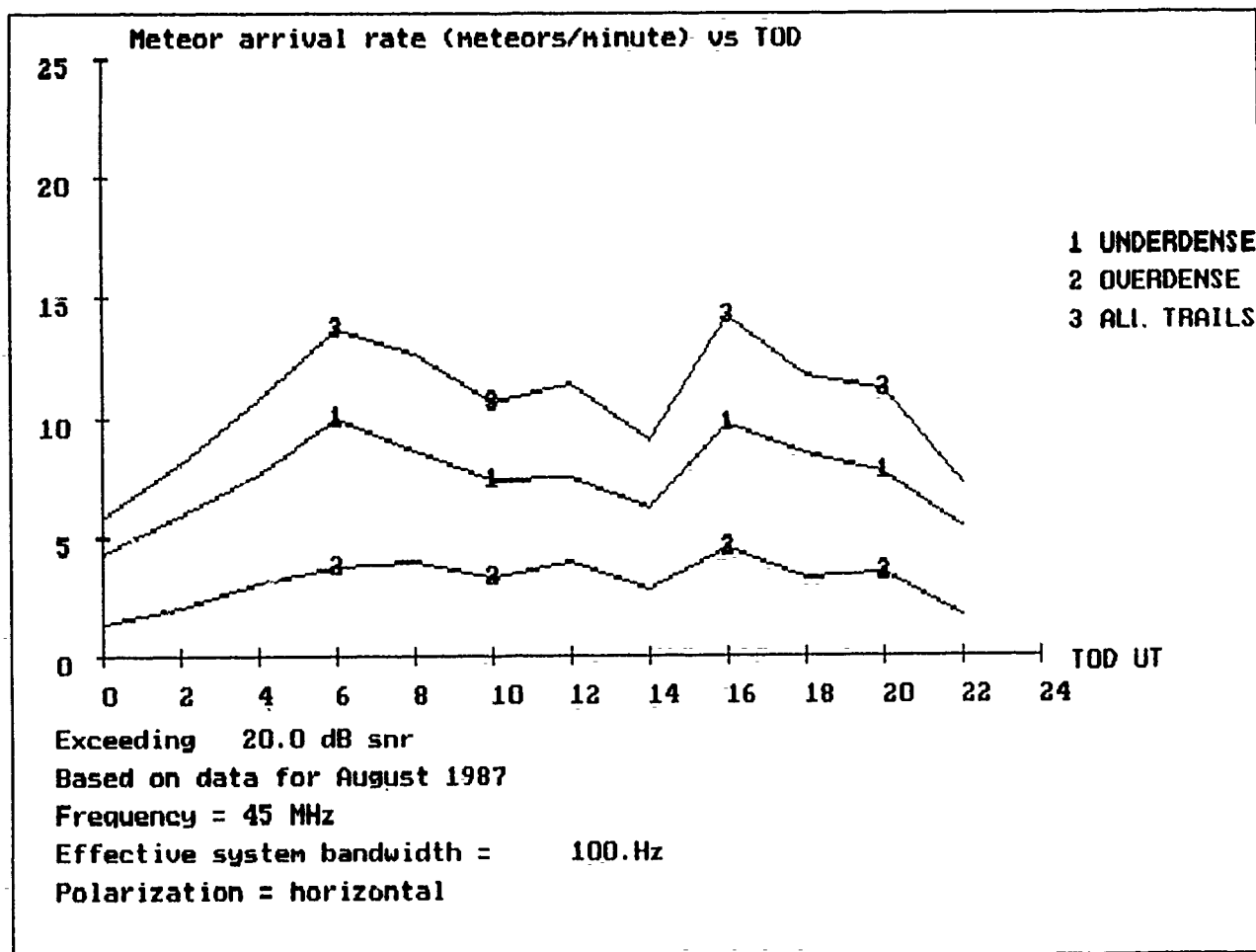


Figure 6.1.6 Arrival Rate of Signals Exceeding 20 dB SNR for the Period 20 - 28 August 1987 at Station Nord

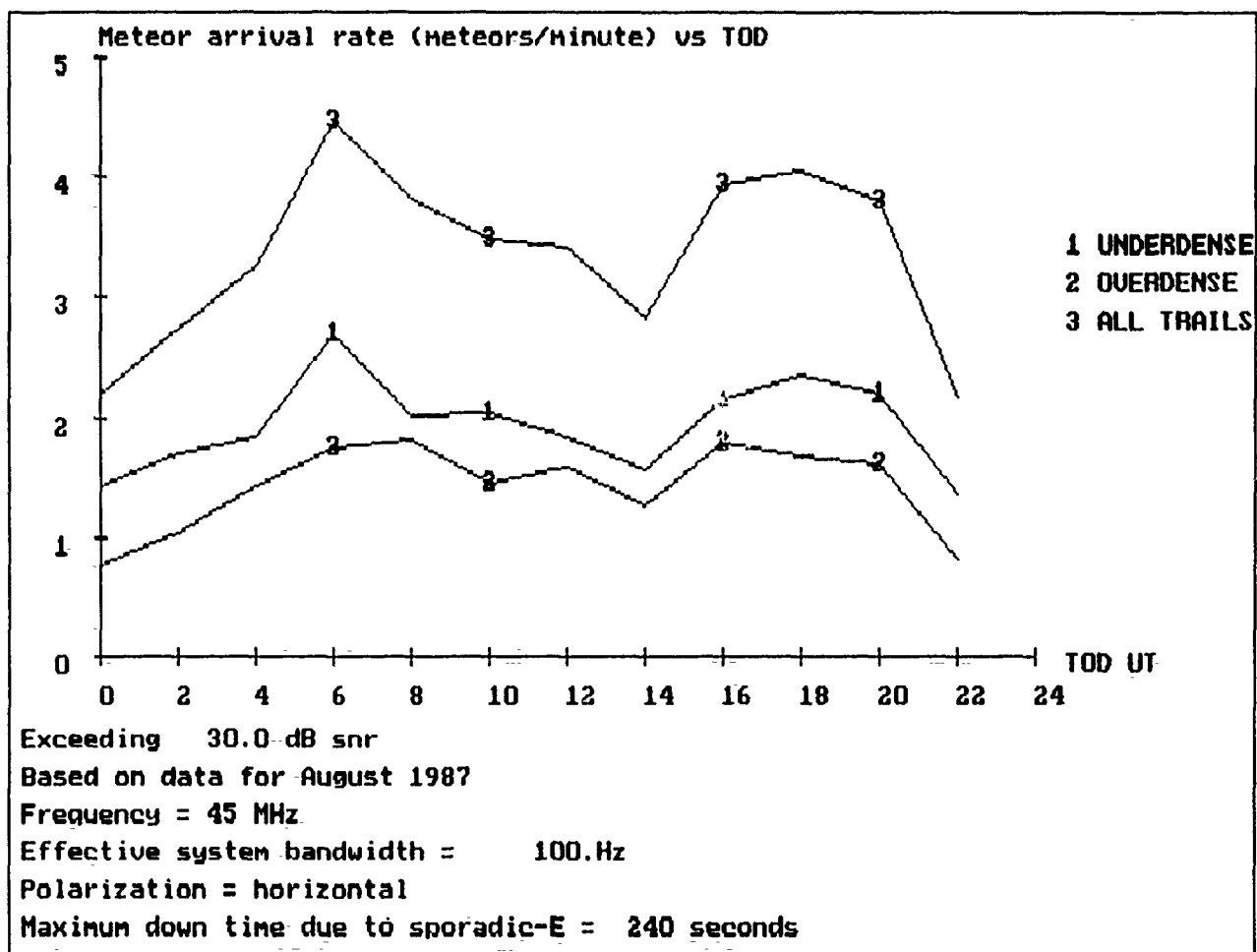


Figure 6.1.7 Arrival Rate of Signals Exceeding 30 dB SNR for the Period 20 - 28 August 1987 at Station Nord

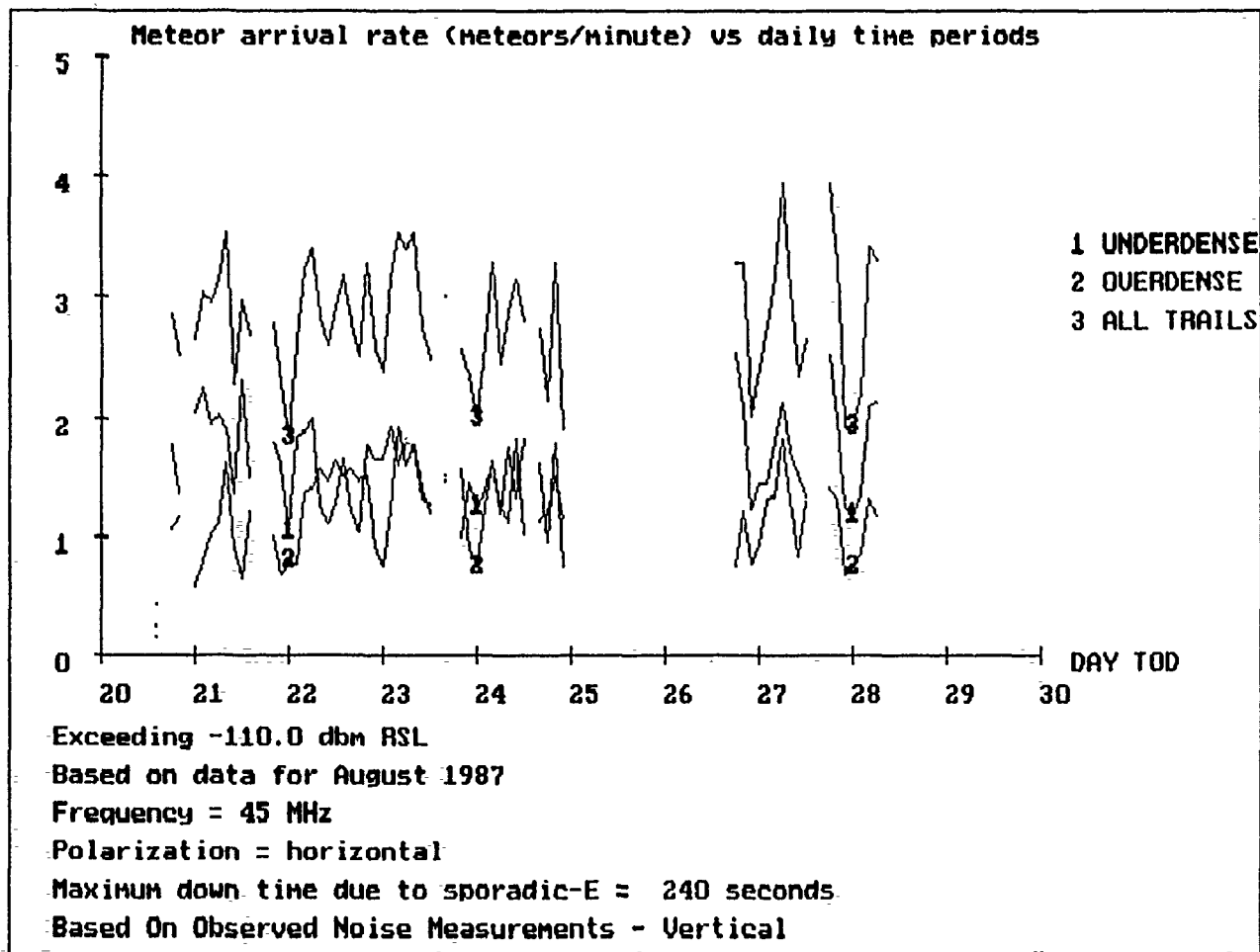


Figure 6.1.8 Arrival Rate of Signals Exceeding -110 dB RSL for the Period 20 - 28 August 1987 at Station Nord

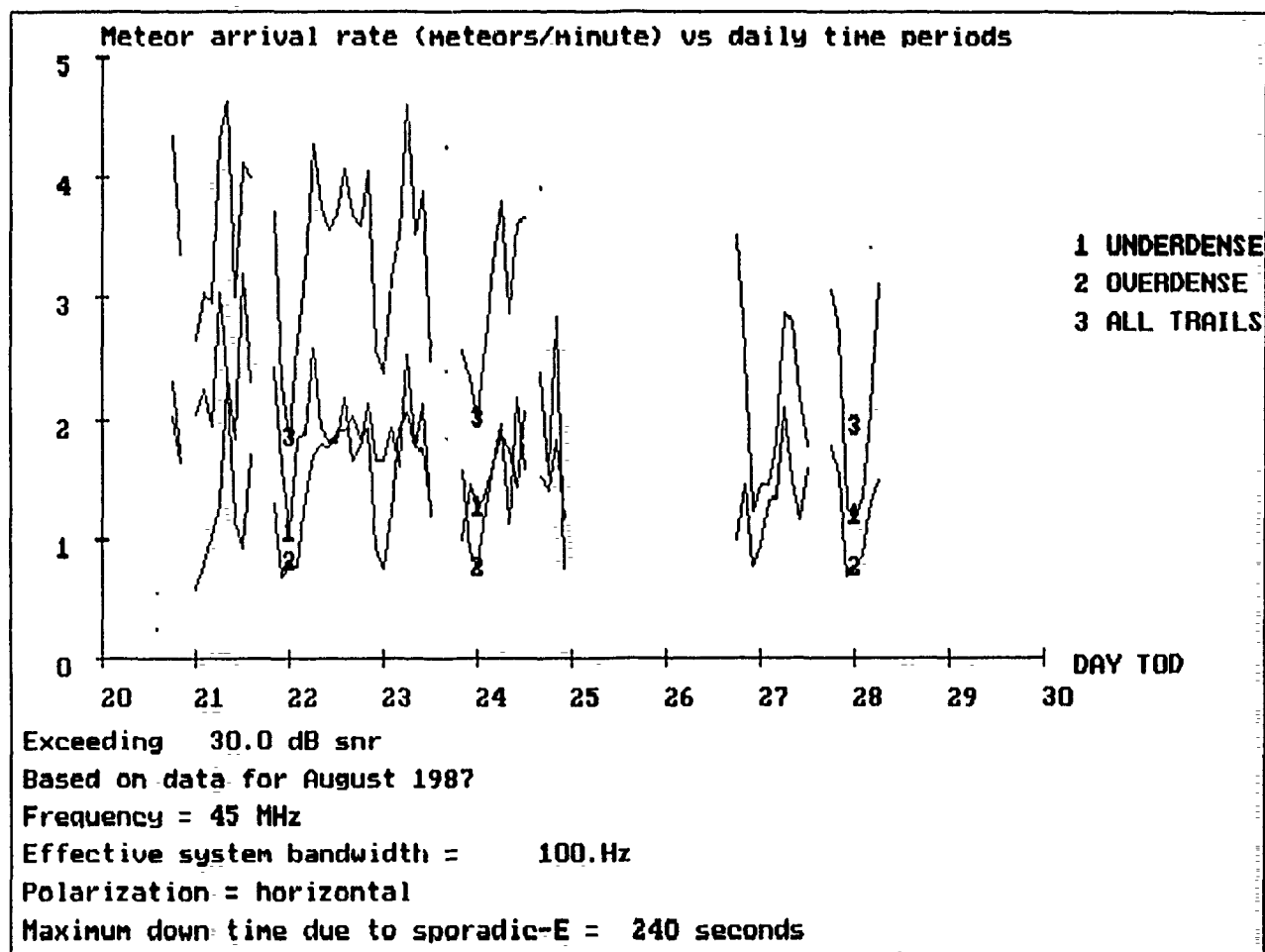


Figure 6.1.9 Arrival Rate of Signals Exceeding 30 dB SNR for the Period 20 - 28 August 1987 at Station Nord

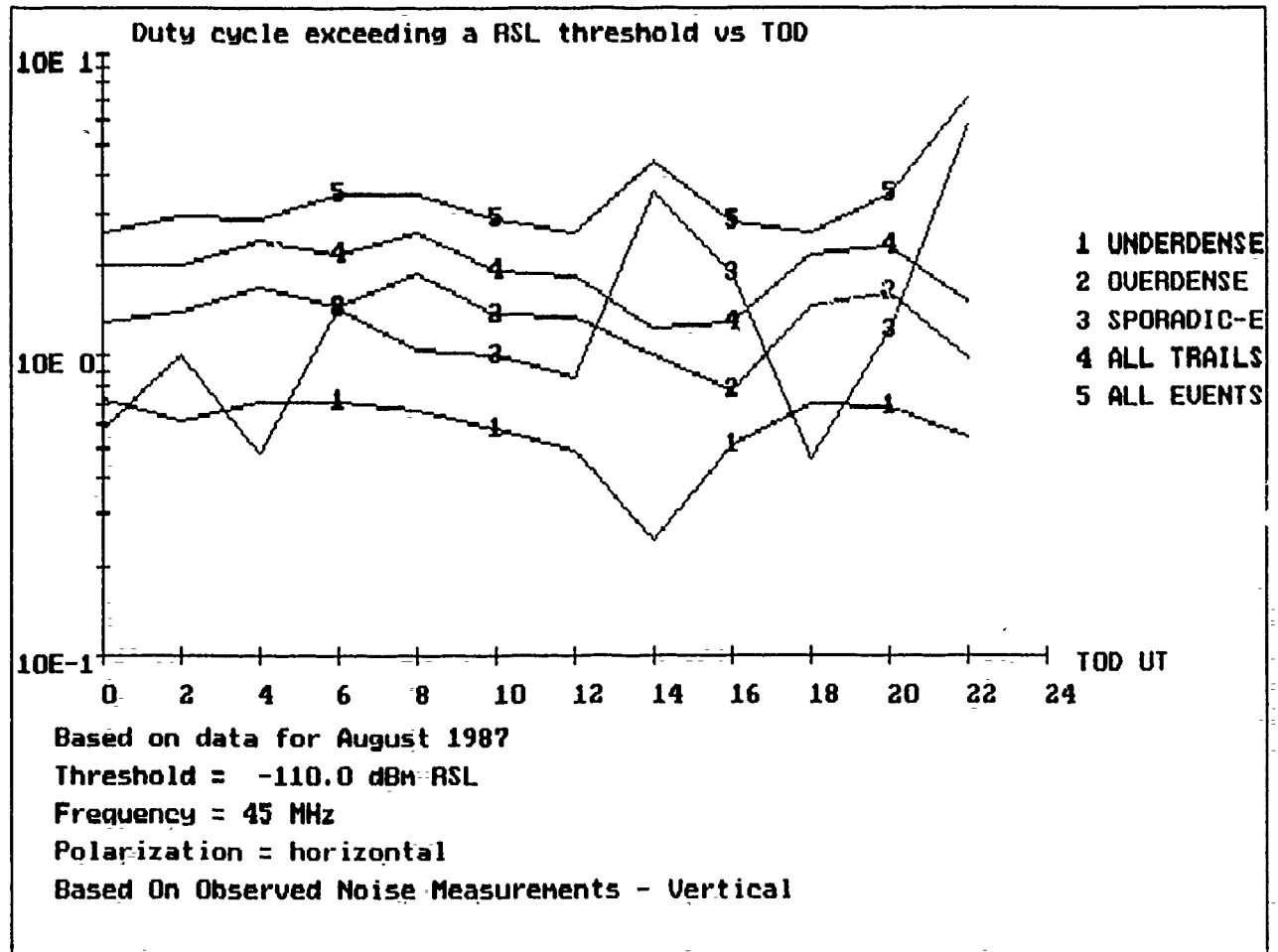


Figure 6.2.1 Diurnal variation of the duty cycle exceeding -110 dBm. August 1987 at station Nord.

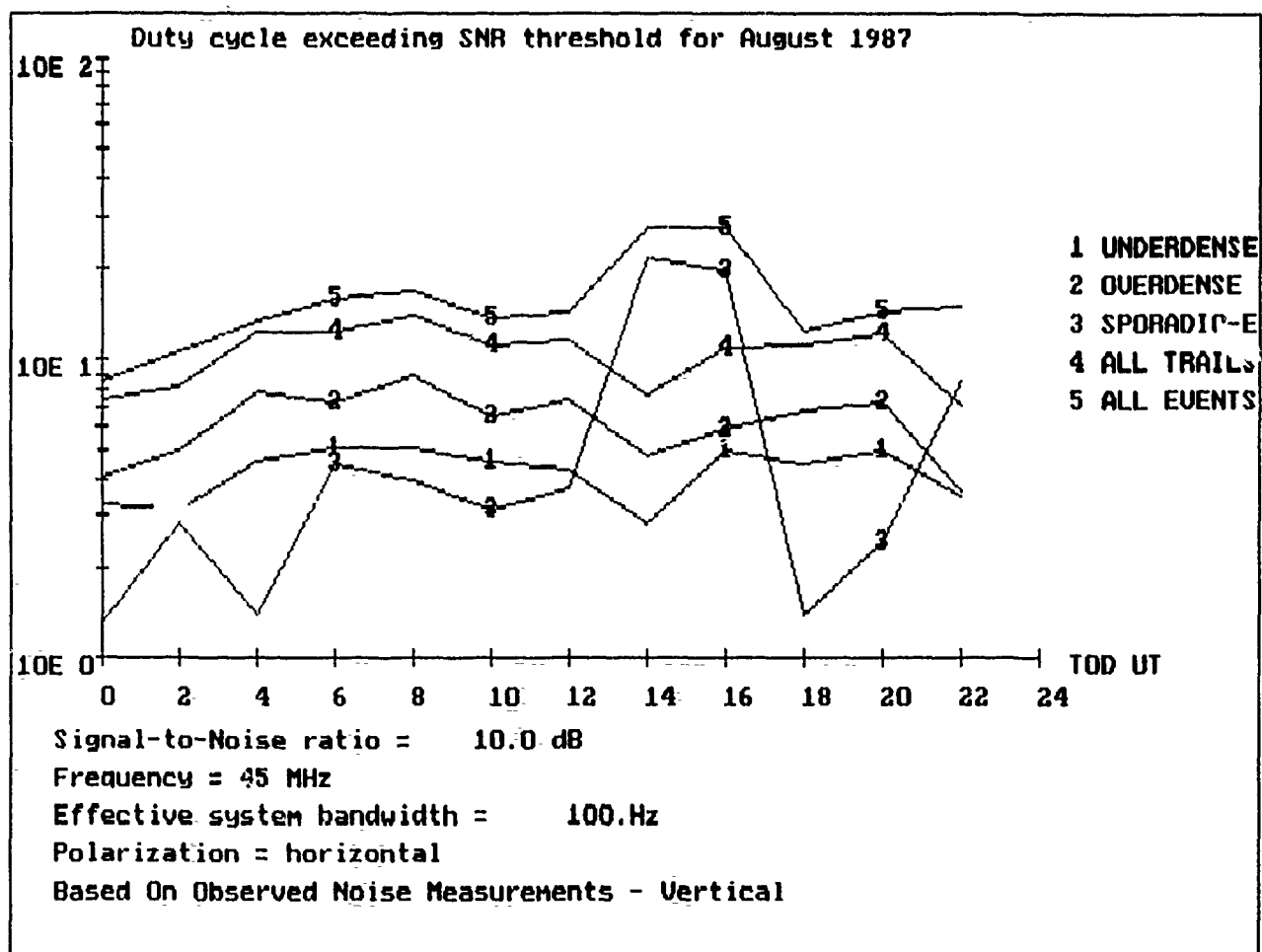


Figure 6.2.2 Diurnal variation of the duty cycle exceeding a SNR of 10 dB. August 1987 at station Nord.

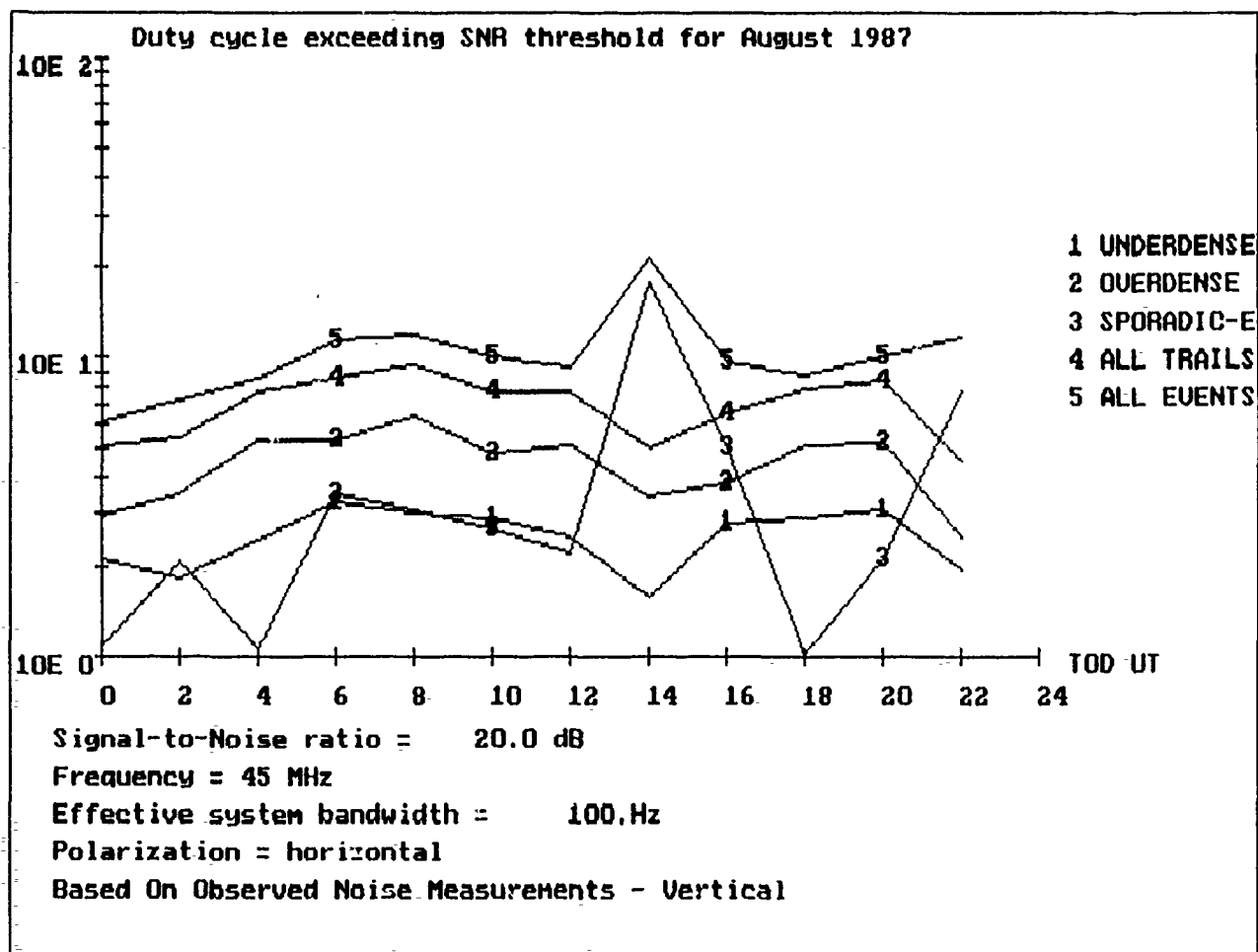


Figure 6.2.3 Diurnal variation of the duty cycle exceeding a SNR of 20 dB. August 1987 at station Nord.

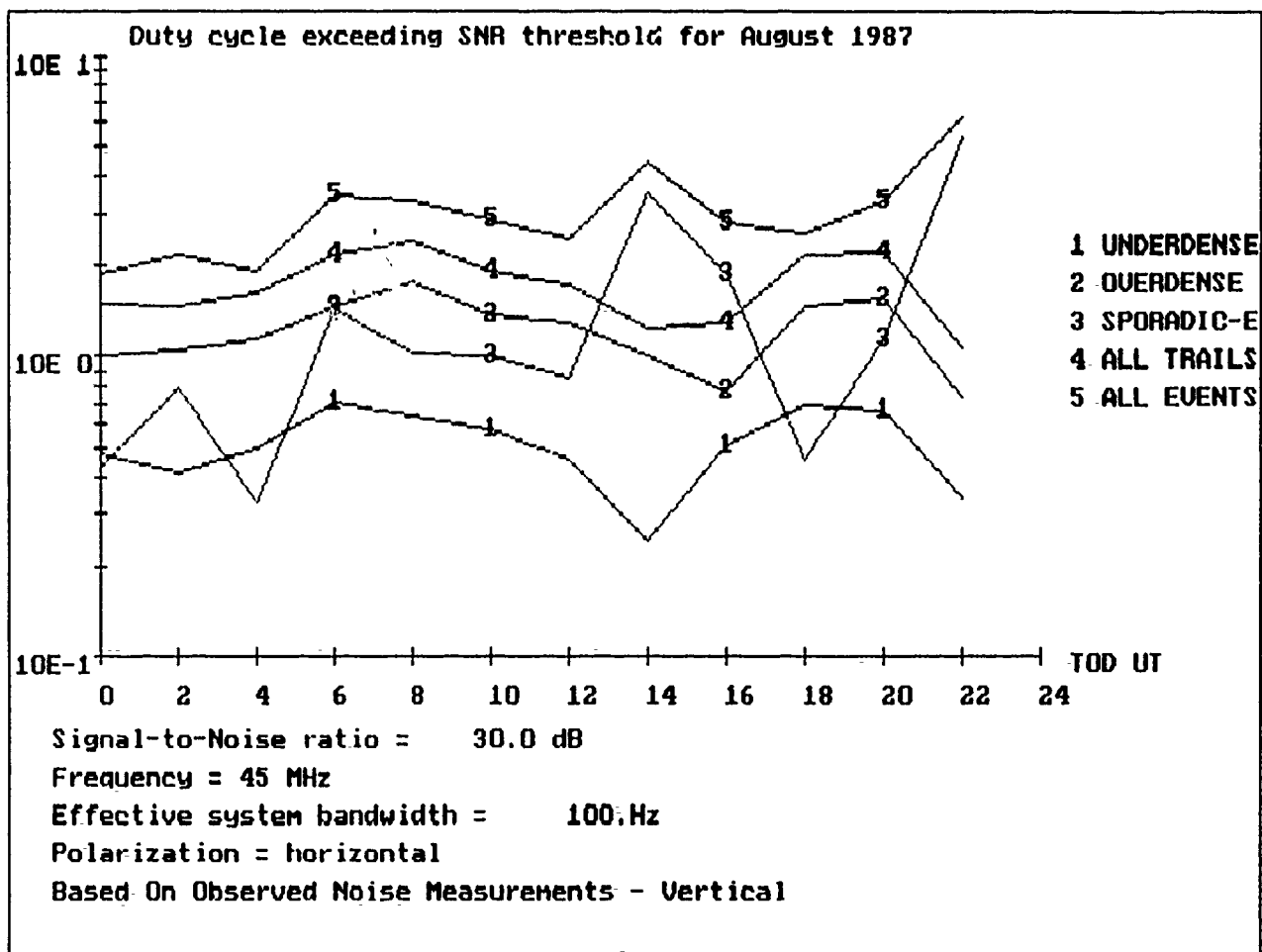


Figure 6.2.4 Diurnal variation of the duty cycle exceeding a SNR of 30 dB. August 1987 at station Nord.

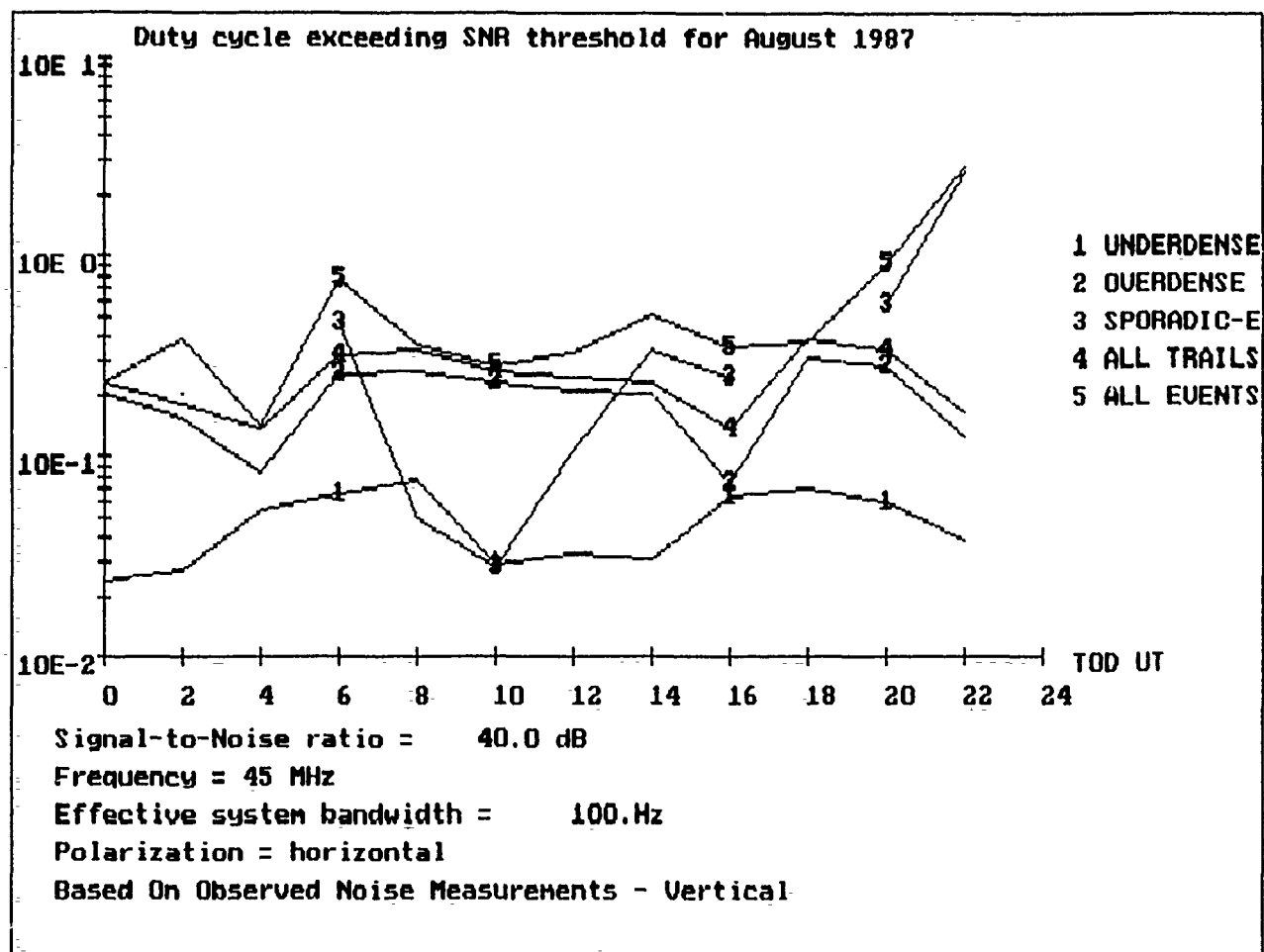


Figure 6.2.5 Diurnal variation of the duty cycle exceeding a SNR of 40 dB. August 1987 at station Nord.

The duty cycle of sporadic-E signals is again dominated by the sporadic-E events occurring August 24 and 25, and by the long lasting signals described in Section 5.0, postulated to originate from Auroral arc scatter.

The average communication capacity of a meteor scatter link is determined by the average duty cycle at the SNR required for the specified Bit Error Rate. Thus the average, long term capacity for a meteor scatter link can be evaluated from a presentation of the monthly mean duty cycle as a function of SNR. Figures 6.2.6 and 6.2.7 present the mean duty cycle for the measurement period as a function of RSL and SNR respectively. The two statistics are identical when RSL is translated into SNR by subtraction of the mean noise level of -140 dBm. The duty cycle of overdense trail signals exceed the duty cycle of underdense trail signals for all SNR levels, and dominates the meteoric duty cycle at high SNR levels.

The duty cycle of sporadic-E layer signals dominate the total duty cycle at very high SNR's, reflecting the long lasting, high level of the sporadic-E event of August 24. Thus, sporadic-E layers when available can support a much larger communication capacity than meteor trails. This extra capacity is difficult to incorporate in daily average throughput calculations, as it occurs much less frequently than meteor trails.

An increase of 10 dB SNR is not accompanied by a decrease of a factor 10 in the duty cycle. This means that a increase of signaling speed for a given modulation and Bit Error Rate performance results in a net increase of the average channel capacity. The waiting time for short messages will, however, also increase, as an increase in SNR is accompanied by a decrease of the arrival rate.

The general trend, that the capacity of a meteor scatter link increases with signaling speed, that the overdense trails carry

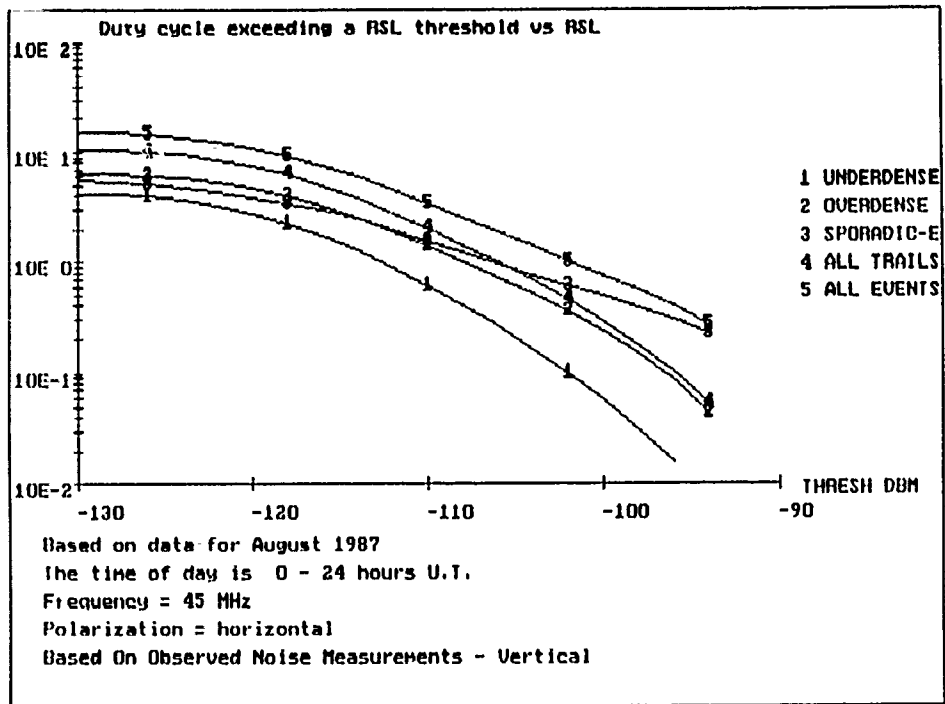


Figure 6.2.6 Duty Cycle Exceeding a RSL Threshold for August 1987 at Station Nord

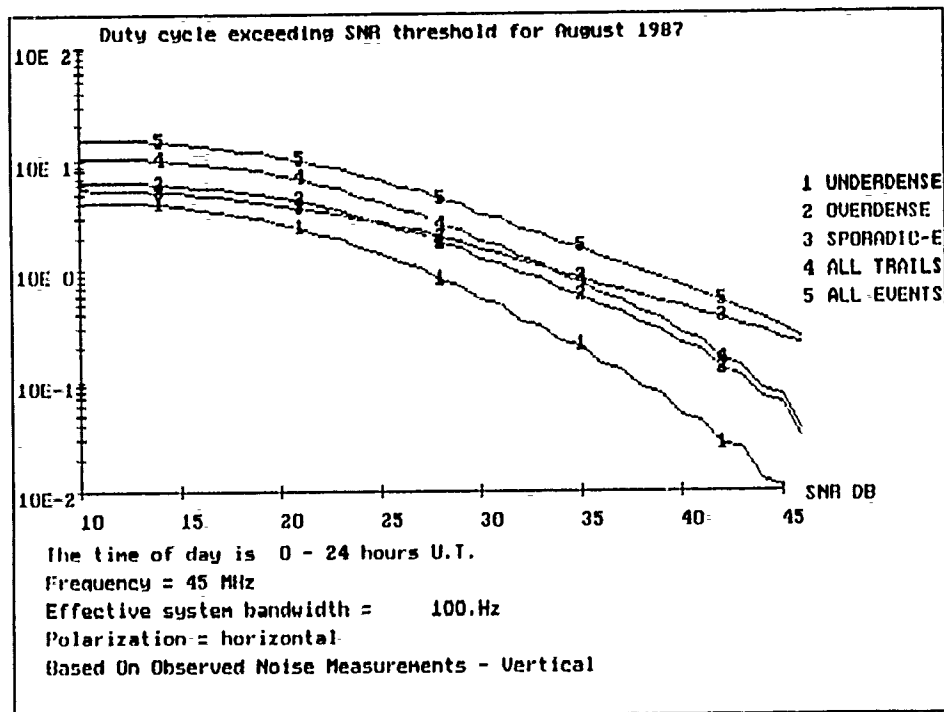


Figure 6.2.7 Duty Cycle Exceeding a SNR Threshold for August 1987 at Station Nord

by far the largest part of the throughput, and that the waiting time for short messages increase with signaling speed follow from the arrival rate and duty cycle statistics.

The duty cycle exceeding -110 dBm RSL for the Thule station Nord meteor scatter link as a function of time of day for the measurement period is presented in Figure 6.2.8. The time variation of the duty cycle is dominated by the overdense trails, which generally last longer than the underdense trails. Sporadic-E layer propagation provides a large increase in the duty cycle on August 24 when extended sporadic-E events occurred at noon, and near midnight. Smaller peaks found on the curve expressing the duty cycle for all events are contributed by the long lasting signals described in Section 5.0 postulated as Auroral arc scatter. The daily fluctuations of the duty cycle of the overdense trails has an average value almost independent of day. However, the average duty cycle of the underdense trails decreases markedly from August 21 through August 25, and increases again through the rest of the period. The variation is almost a factor of two and it is independent of the occurrence of sporadic-E signals.

The duty cycle exceeding a SNR of 30 dB for the same period is shown in Figure 6.2.9. The average noise power is -140 dBm, so a SNR of 30 dB is equivalent to a RSL of -110 dBm. The duty cycle variations are very similar to the duty cycle exceeding -110 dBm, but the influence of the daily Galactic noise peak at 02 UT can be seen every day, as a decrease in the duty cycle relative to the -110 dBm duty cycle presented in Figure 6.2.8. The variation of the daily average underdense trail duty cycle is also seen.

6.3 Duration Statistics

Duration is defined as the continuous time interval where the SNR exceeds a certain value. As a meteor signal theoretically has

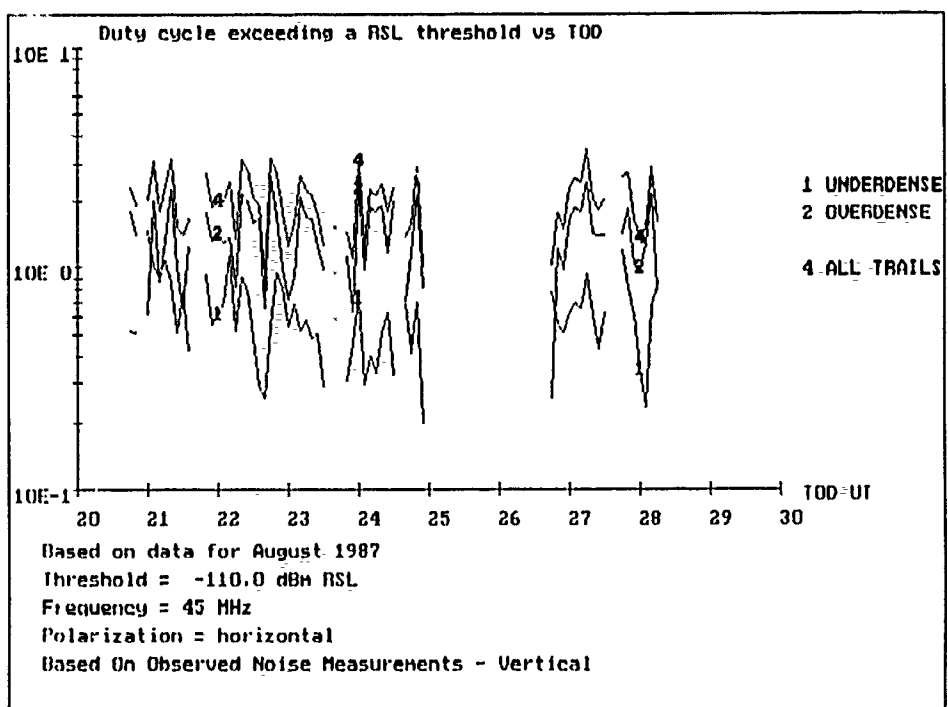
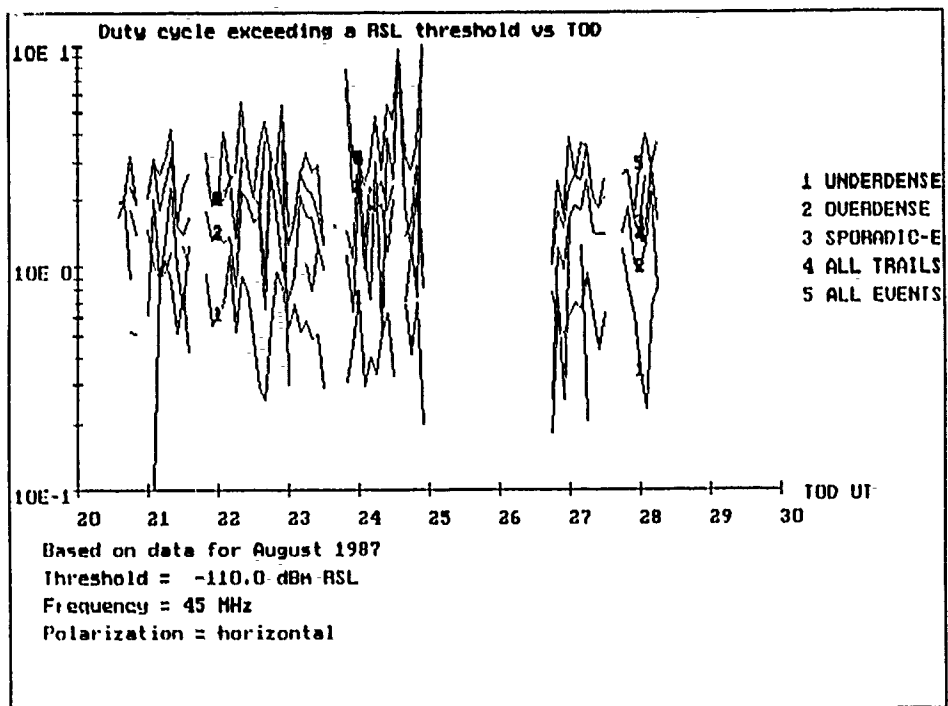


Figure 6.2.8 Duty cycle exceeding a RSL threshold vs. time of day for the period August 20-29, 1987 at station Nord. Top: For all events. Bottom: For meteor trails only.

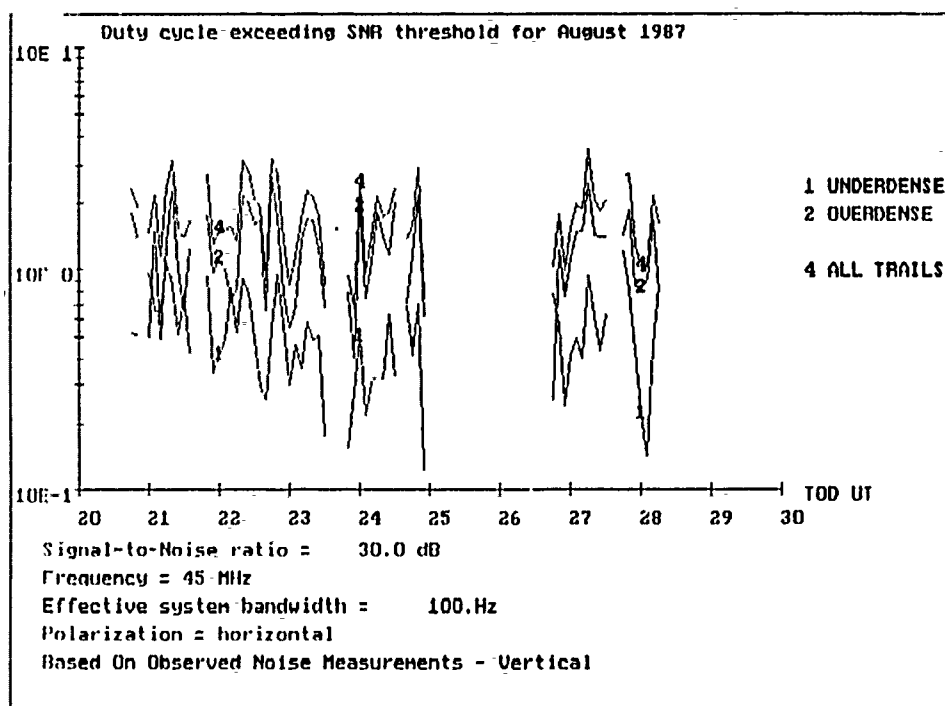
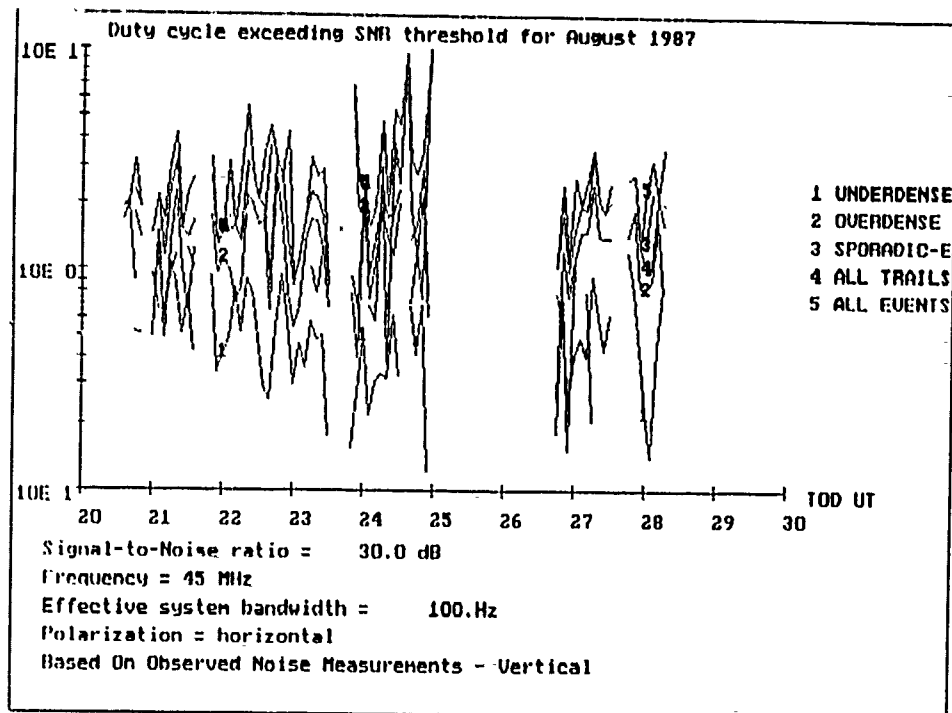


Figure 6.2.9 Duty cycle exceeding a RSL threshold vs. time of day for the period August 20-29, 1987 at station Nord. Top: For all events. Bottom: For meteor trails only.

a exponential decay, the duration could be expected to decrease with an increase of the specified SNR. This is true for the individual trails, but the arrival rate increases as the threshold is decreased, so more, short lasting trails are added at low thresholds. Also, at high thresholds, few trails will endure very long. The analysis of the dependence of the average duration of meteor trails on signal level thresholds show this to be independent of the threshold for the simple underdense trail model. Finally, meteor trail signals fade and are broken up into segments of shorter duration than the endurance of the trail signal. These count as individual contributions to the duration statistics. The average duration of meteor signals as a function of Received Signal Level RSL and Signal to Noise Ratio, SNR for August 1987 at station Nord are presented in Figures 6.3.1, 6.3.2.

It is seen that the average duration is not a monotonic function of SNR. The duration decreases with an increase of the SNR for low values of the SNR, but increases slightly again for large values of the SNR. The reason for this is the combined effect of short trails with little fading, and the fading associated with the long lasting and high power trails. Thus even if the lifetime of the meteor trails often by far exceeds the average duration, long lasting signals without fades are a rare occurrence. In general the average duration is almost independent of the signal level supporting the classical analysis of Sugar.

The sporadic-E signals have a much larger average duration than the meteor scatter signals, and show a large increase at high signal levels. A sporadic-E event generally lasts several minutes or even half an hour. Still, the average duration of the signal does not exceed 1.5 seconds. The duration of sporadic-E signals are thus determined by fading.

The normalized distributions of signal durations exceeding an SNR of 10, 20, 30, and 40 dB for August 1987 at station Nord are presented in Figures 6.3.3 - 6.3.6. The normalized

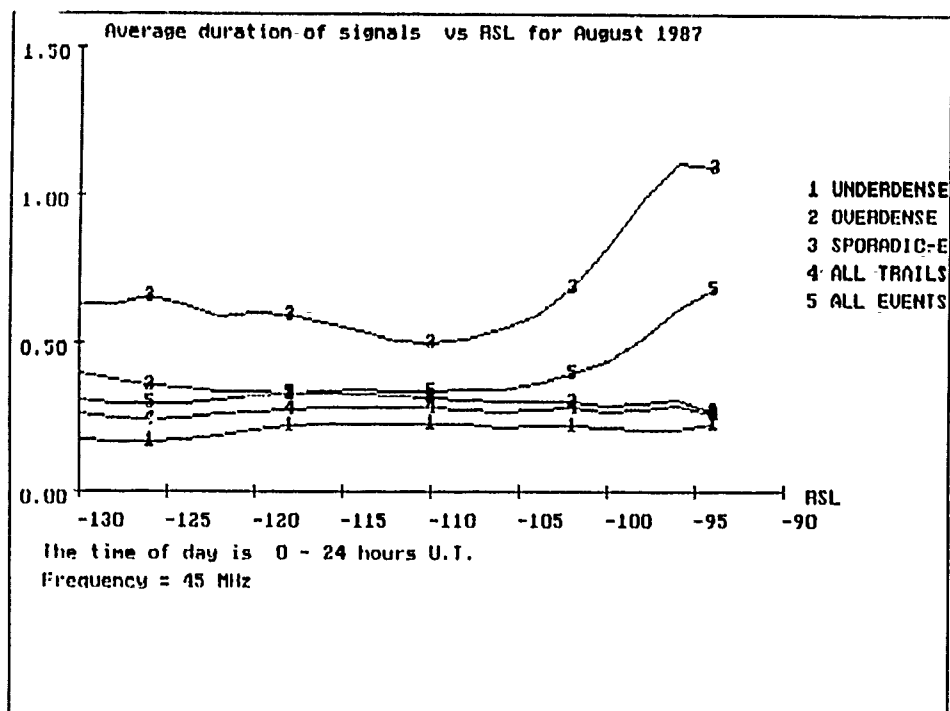


Figure 6.3.1 Average Duration of Meteor Signals as a Function of RSL for August 1987 at Station Nord

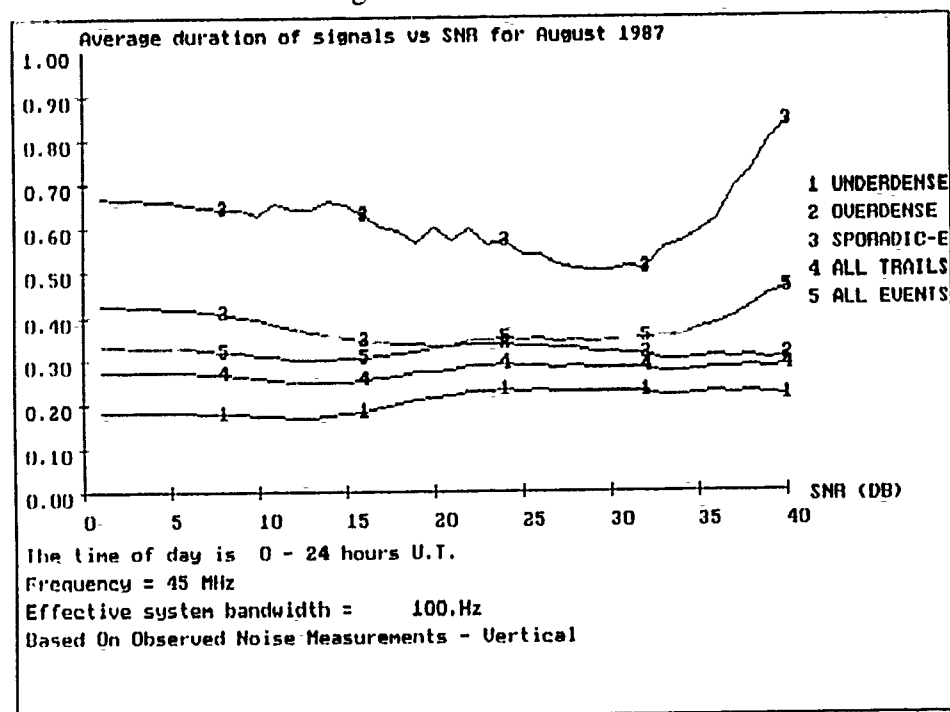


Figure 6.3.2 Average Duration of Meteor Signals as a Function of SNR for August 1987 at Station Nord

distributions show two main features. The distributions of signal durations is almost independent of the SNR level chosen throughout the 30 dB range presented. Also, the increase in duration of the sporadic-E signals at high SNR's is very noticeable. At 40 dB SNR 10% of the durations of sporadic-E signals exceed 3 seconds, compared to 0.9 seconds for the overdense trail signals. Thus the sporadic-E signals on the average fade less often than do the meteor scatter signals.

The diurnal variation of the average duration of signals exceeding -120 dB RSL and 30 dB SNR are shown in Figures 6.3.7 and 6.3.8. Virtually no diurnal variation is seen for the meteor trail signals. The sporadic-E signals show a large decrease in duration between 18 UT and 22 UT. This is in part due to the sporadic-E event occurring late in the day on August 24. For reasons unknown signals during this event had slower fading than other sporadic E-layer events observed. The data sample is too small to evaluate the long term variation of the properties of sporadic-E signals, so the statistics only show what durations can be observed for the sporadic-E signals.

6.4 Fading Statistics

The average number of fades per trail observed at station Nord is presented as a function of time of day in Figure 6.4.1. The underdense trails show almost no fading, but the number of fades for the overdense trails vary between 4 and 8. This reflects that the underdense trails are mostly short lasting and the high altitude winds will not be able to shift and warp the trails, a process that results in fades, before the trails have diffused. The overdense trails on the other hand generally last longer than the underdense trails, and are more prone to wind distortion.

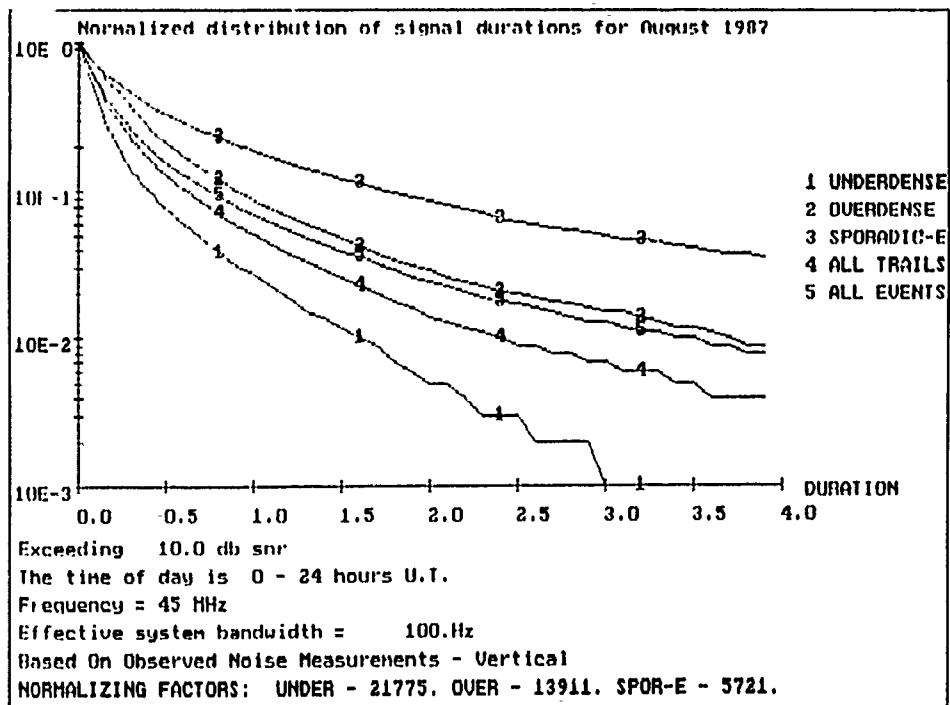


Figure 6.3.3 Normalized Distribution of Signal Durations Exceeding 10 dB for August 1987 at Station Nord

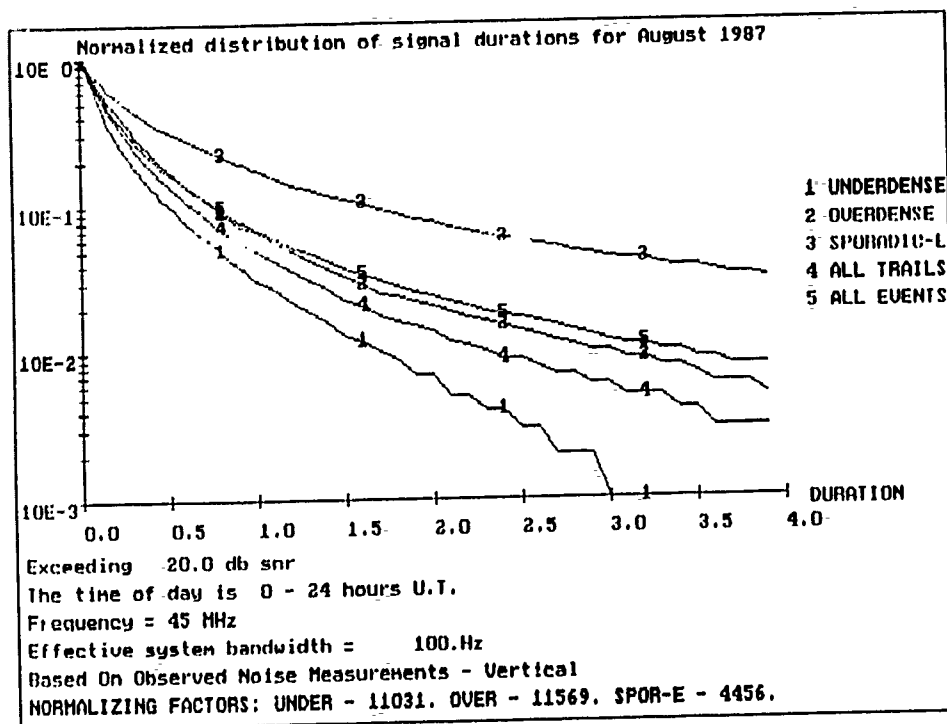


Figure 6.3.4 Normalized Distribution of Signal Durations Exceeding 20 dB for August 1987 at Station Nord

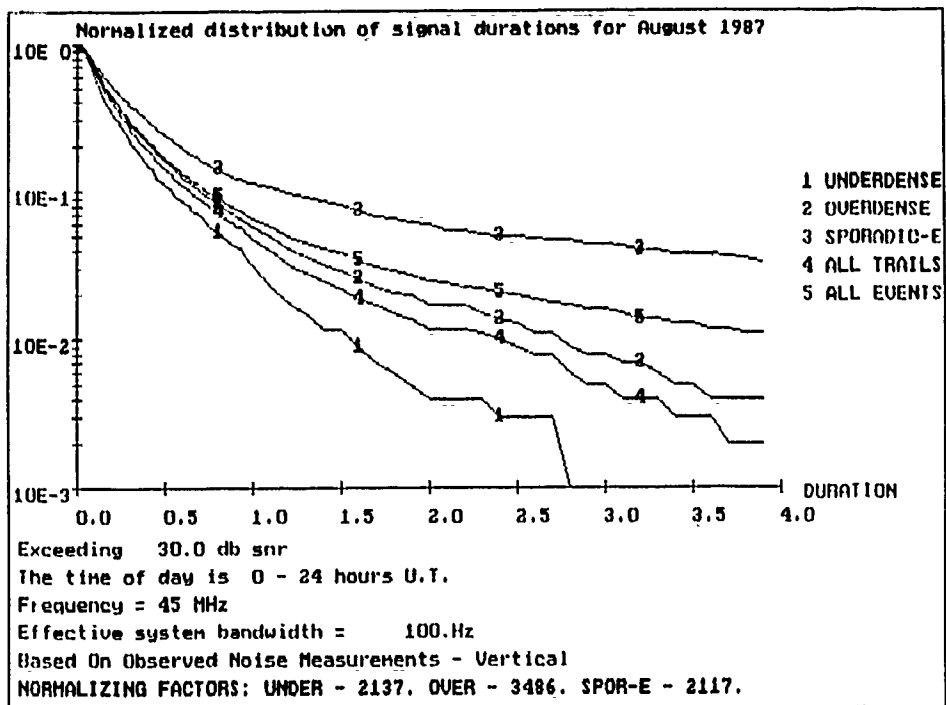


Figure 6.3.5 Normalized Distribution of Signal Durations Exceeding 30 dB for August 1987 at Station Nord

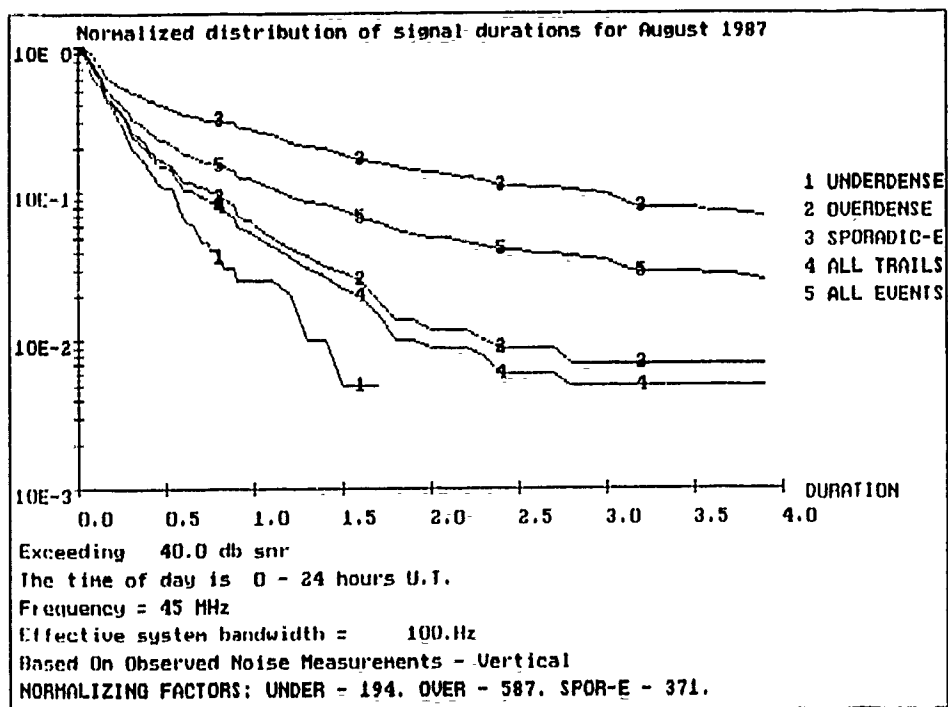


Figure 6.3.6 Normalized Distribution of Signal Durations Exceeding 40 dB for August 1987 at Station Nord

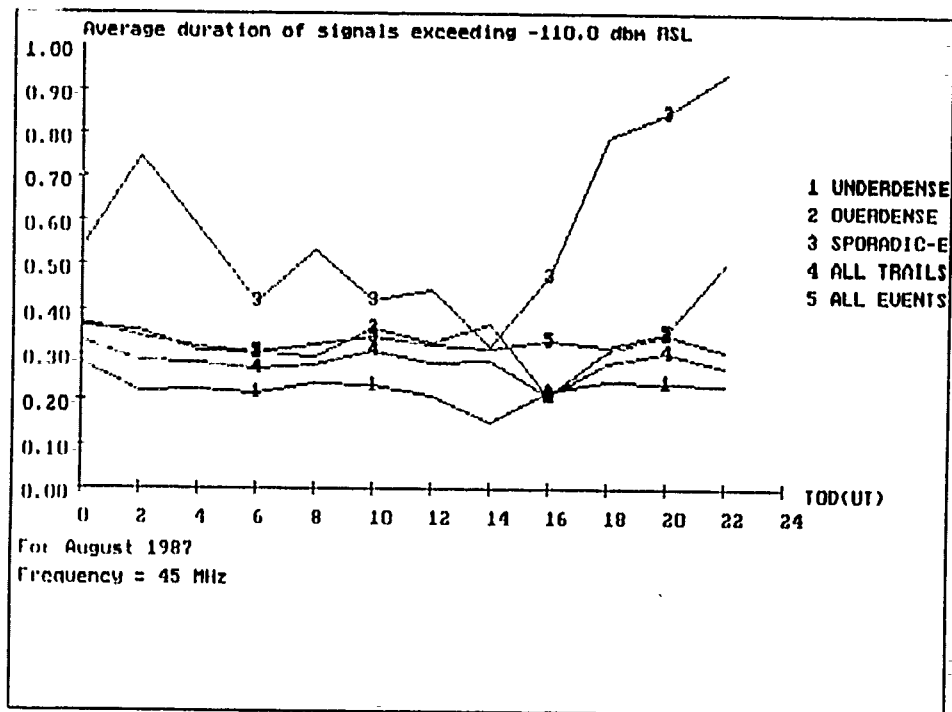


Figure 6.3.7 Diurnal variation of the average duration of signals exceeding -120 dBm at station Nord. August 1987.

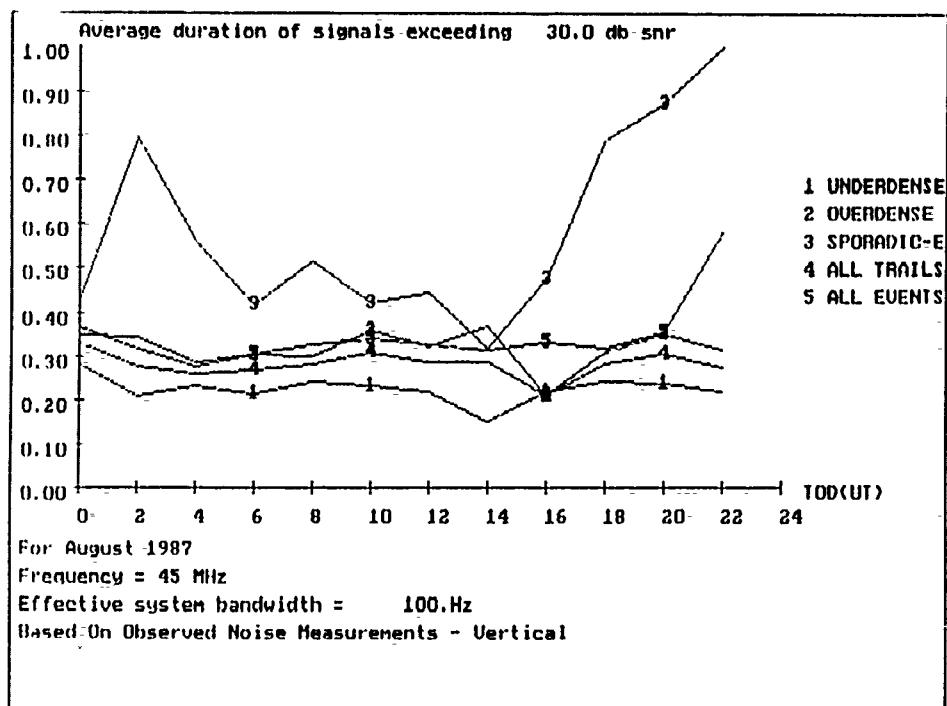


Figure 6.3.8 Diurnal variation of the average duration of signals exceeding 30 dB SNR at station Nord. August 1987.

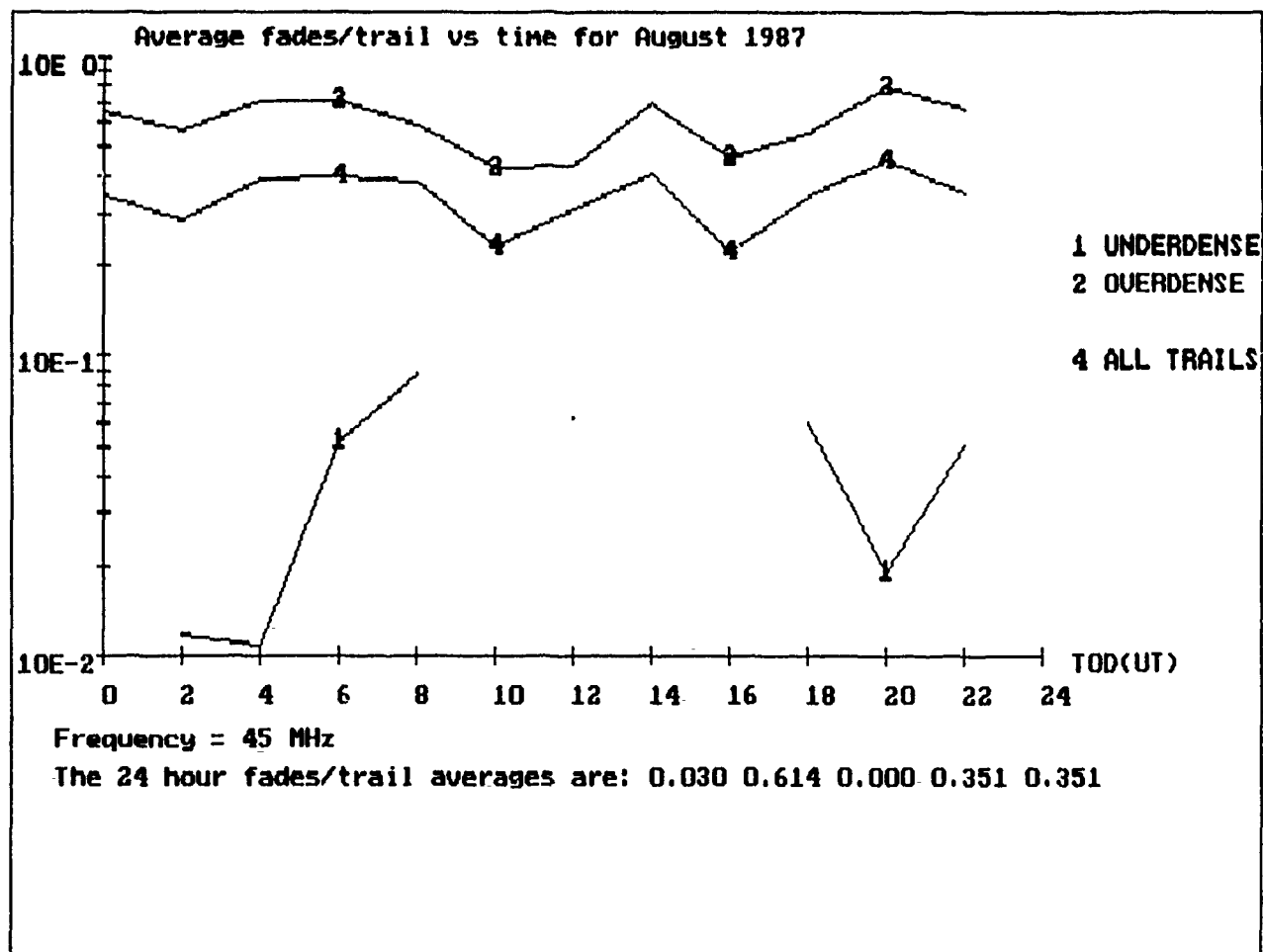


Figure 6.4.1 Average Number of Fades/Trail vs. Time of Day for August 1987 at Station Nord

The average number of fades/second for underdense trails, overdense trails and sporadic E-layer reflected signals are presented in Figure 6.4.2 as a function of time of day. Little diurnal variation is seen in the rate of fading for the meteor trail signals. The underdense trails do not show any fades at all for a large part of the day consistent with Figure 6.4.1. The overdense trails had fade rates between 1 and 2.5 fades/sec and a maximum is seen in the afternoon. The low values of the fade rates are linked to the endurance of the trail signals. On the average, few overdense trails endure more than one second, and as the average average number of fades per trail is approximately 0.8, lower fade rates are implausible. The average fade rate for the sporadic E-layer signals is much less than the average fade rate for the meteor trail signals. The sporadic E-layer signals last much longer than the meteor trails, so fade rates of fractions of one fade/second are possible. The fact that the fade rate is very low also indicates that the coherence bandwidth of sporadic E-layer channel is large. Measurements of the coherence bandwidth using low band TV signals confirm that the sporadic E-signals can have a large bandwidth. Thus, the occurrence of sporadic E-layers constitutes a "Bonus channel" for a meteor scatter communication system if it is not accompanied by interference from other users. The capacity will increase dramatically due to the endurance of the signals, and the meteor scatter signaling scheme will also be useful on the sporadic E-layer channel.

The normalized distributions of fade rates for meteor trail and sporadic E-signals presented in Figure 4.6.3 shows that the fade rate for sporadic E-signals is indeed much lower than the fade rate for the meteor signals. Only 10% of the intervals between fades were shorter than 0.5 seconds while this is true for 35% of the meteor signals. Few signals have more than 3 fades/second regardless of the propagation mechanism.

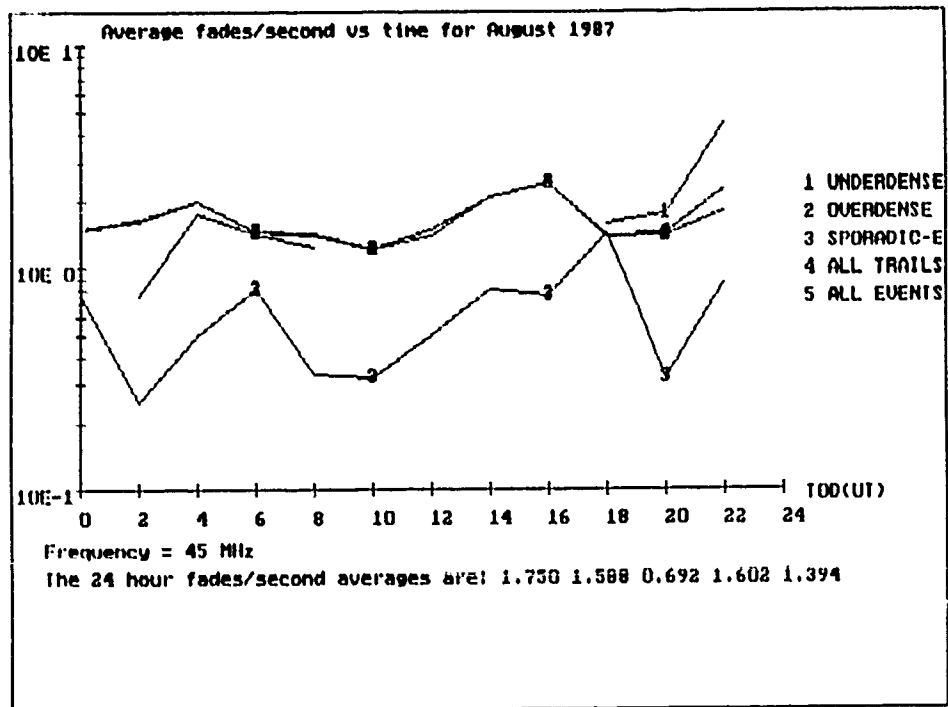


Figure 6.4.2 Average Number of Fades/Sec vs. Time of Day for August 1987 at Station Nord

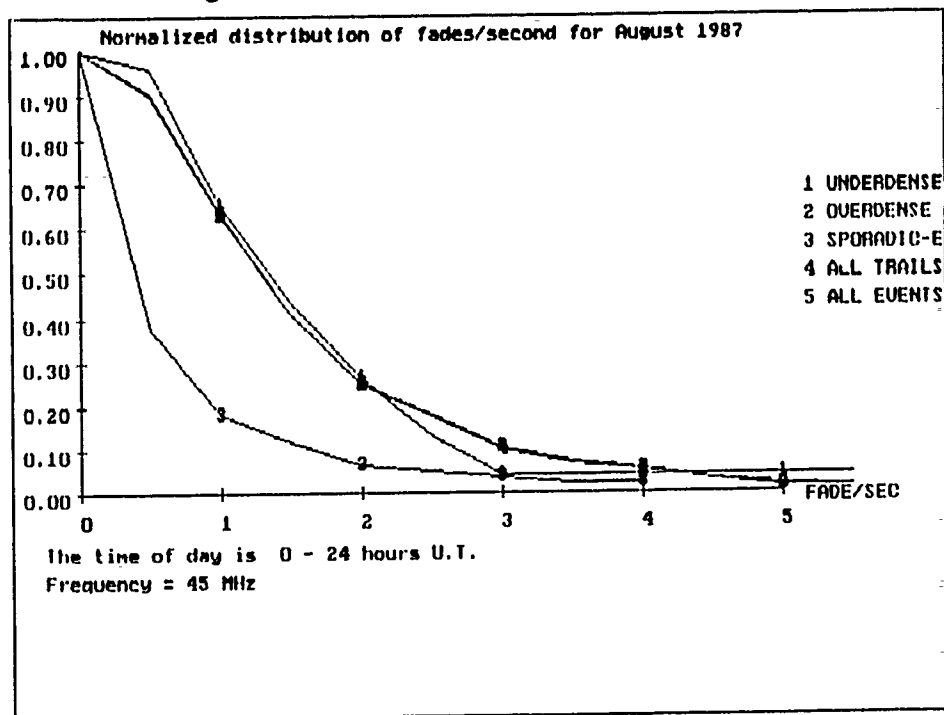


Figure 6.4.3 Normalized Distribution of Fades/Seconds for August 1987 at Station Nord

The normalized distributions of fade durations for signals received at station Nord in August 1987 are presented in Figure 6.4.4. The distribution of fade durations is essentially independent of the propagation mechanism. The distribution for underdense trail signals is uneven compared to the distributions for overdense trail signals and sporadic E-signals. This is caused by the small number of underdense trail signals having any fades at all. 50% of the fades last longer than 150 msec and 10% of the fades last longer than 0.5 seconds. The duration and depth of a fade that a communication system can work through without losing synchronization is dependent on the modulation and coding used. The distributions presented here can be used as a guide to the expected fade durations when selecting a signaling scheme to combat fading on a meteor scatter link.

6.5 Underdense Decay Time Constants

The exponential decay of underdense meteor trail signals is characterized by a time constant determined by the frequency of the forward scattering angle and the diffusion constant of the atmosphere surrounding the trail. A detailed discussion of the underdense decay time constant is found in McKinley's Book: Meteor Science and Engineering. His treatment is used here to illustrate implications of the underdense decay time constant.

The mathematical expression for the underdense decay time constant is:

$$C = \text{wavelength}^2 \sec^2(\theta) / 16 \pi^2 D$$

where C is the decay time constant, θ the forward scattering angle, D the diffusion constant, and wavelength is the wavelength of the signal. An empirical average value for the diffusion constant D in the height range 80 - 110 km can be obtained as:

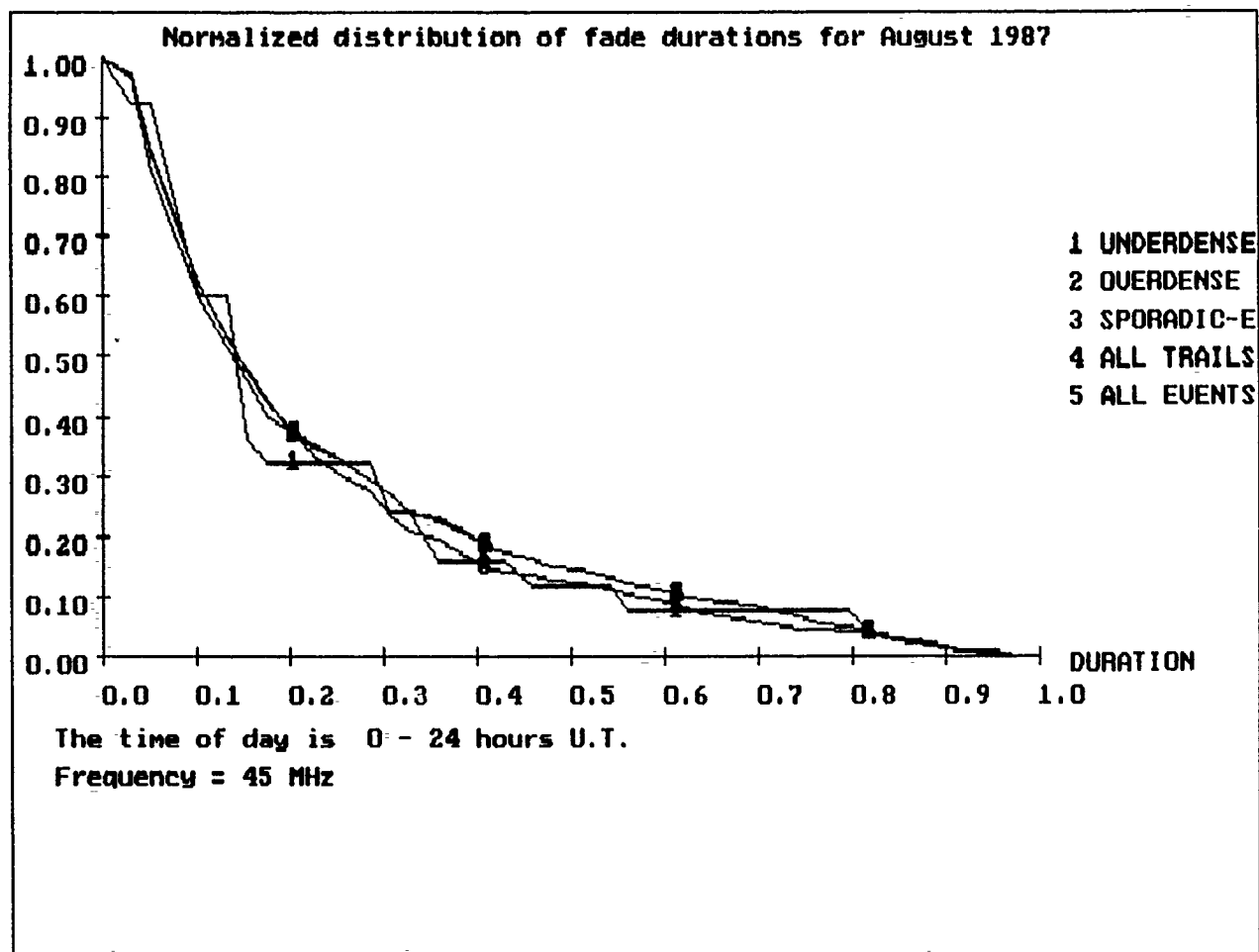


Figure 6.4.4 Normalized Distribution of Fade Durations in Seconds
for August 1987 at Station Nord

$$\log_{10}(D) = 0.067H - 5.6$$

where H is the height of the trail in km.

This relation can be used to compute the average height distribution of the meteor trails, provided the forward scattering angle is known, and that D is accurately obtained from the above formula.

Figure 6.5.1 presents the normalized distribution of the underdense trail decay time constant for the measurement period. The mean value is 0.2 seconds and the 10% and 90% values are 0.6 sec and 0.05 sec respectively.

The weak point in the height range calculation is the determination of the diffusion constant D. Significant variations of D with local atmospheric conditions are known, so analysis of the variation of the height distribution of meteor trails must be performed with caution. This is illustrated by the average diurnal variation of the underdense decay time constant shown in Figure 6.5.2, and the daily variation of the decay time constant throughout the period of observation presented in Figure 6.5.3. Very little diurnal variation is apparent in Figure 6.5.2, indicating a almost invariant value of D and the height distribution of trails. However, Figure 6.5.3 shows large daily fluctuations and day to day variability of the decay time constant. A trend similar to the one found for the arrival rates and durations, i.e. a decrease during the period 20 - 23 August followed by an increase at August 26 - 28 is present in the decay time constant day to day variation. Attempts to further analyze the arrival rate, duty cycle and decay time constant relations to the local atmospheric conditions are beyond the scope of this report. Interested readers are referred to McKinley.

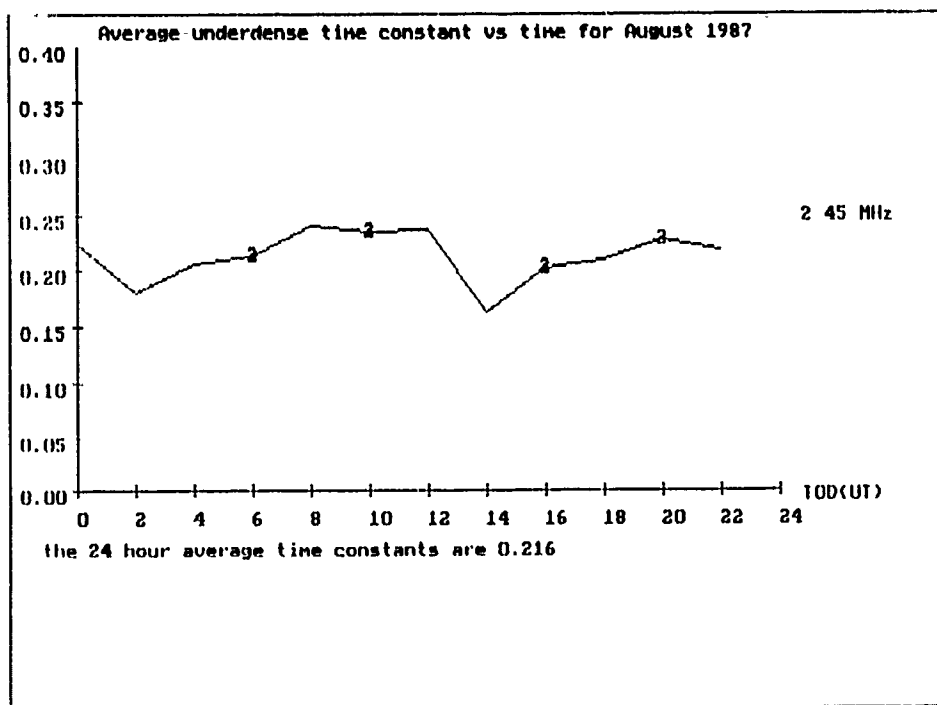


Figure 6.5.1 Normalized Distribution of Underdense Meteor Trail Decay Time Constants for August 1987

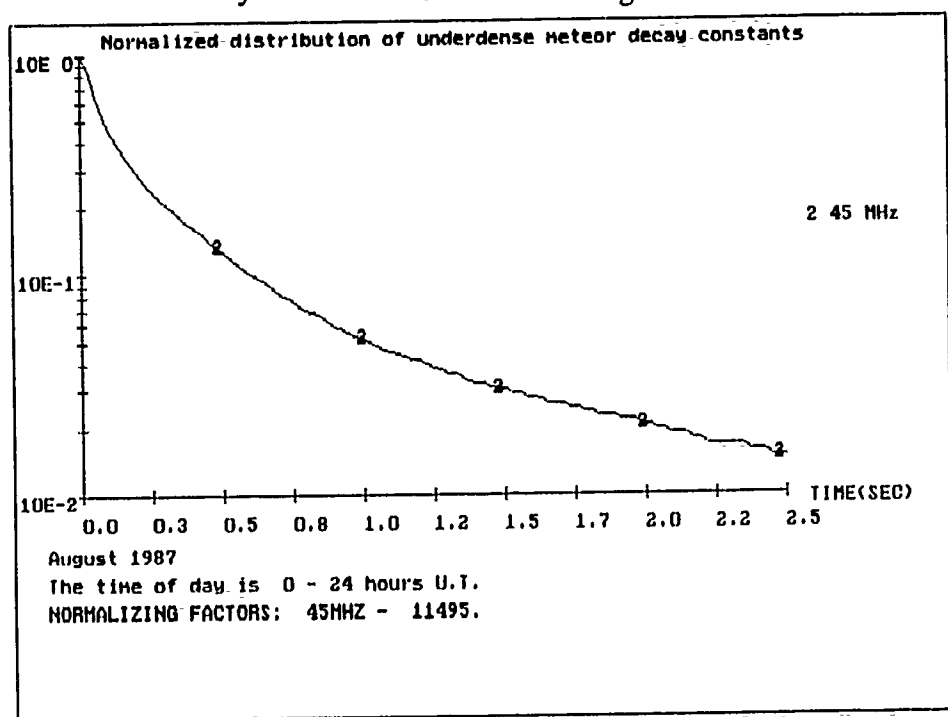


Figure 6.5.2 Average Diurnal Variation of the Underdense Decay Time Constant for August 1987

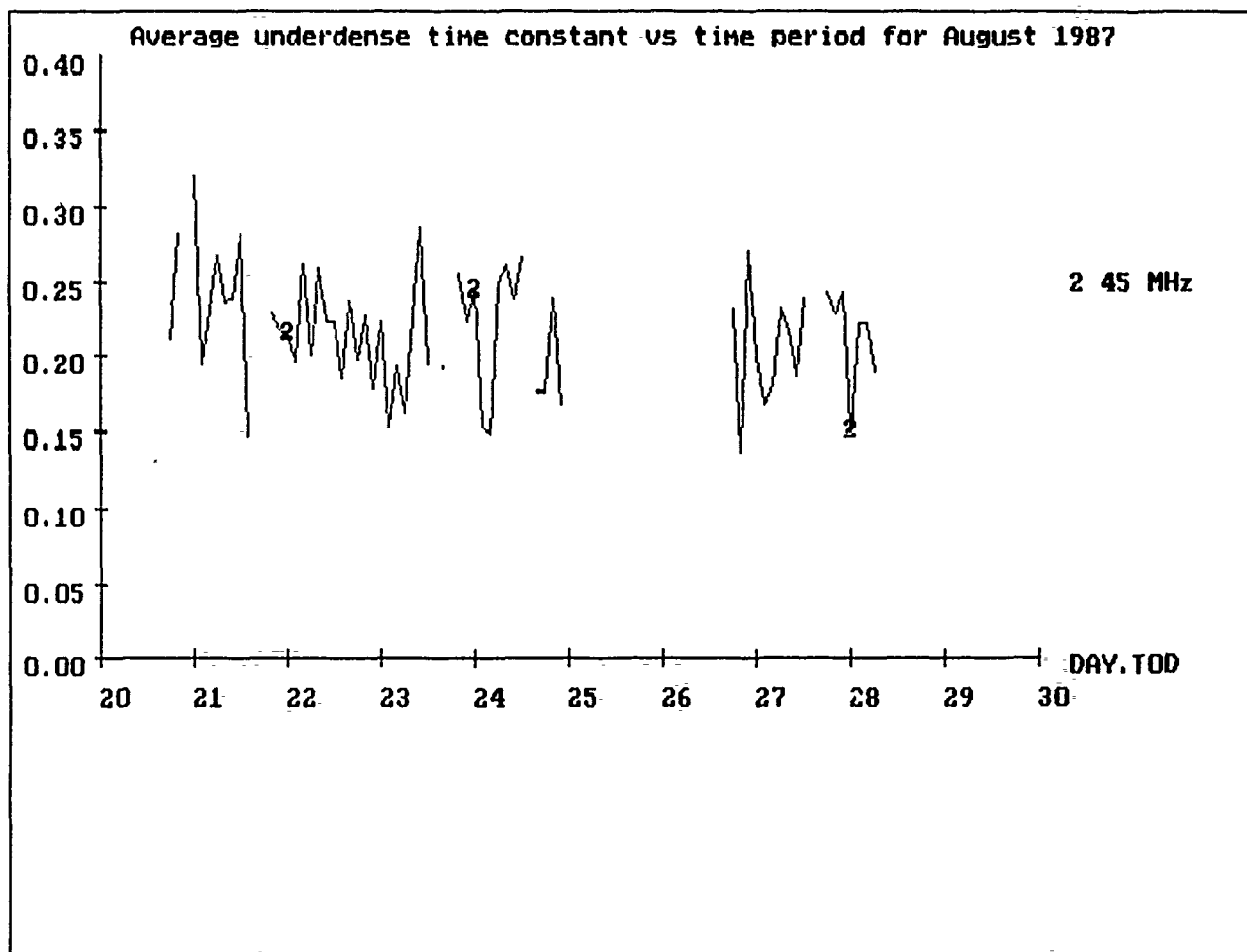


Figure 6.5.3 Daily Variation of the Underdense Decay Time Constant for the Period 20 - 30 August 1987

7.0 DERIVED COMMUNICATION STATISTICS

The AFSC/GL meteor scatter statistics analysis package includes provisions to derive the performance of meteor scatter communication systems from the basic propagation statistics. This feature can be used to examine different configurations of meteor scatter communications for use in Greenland.

The analysis is based on the assumption that no dispersion exists in the channel, and that the system noise is additive and Gaussian distributed. This has been found to be valid for galactically noise limited systems with signaling rates up to at least 250 Kbits/sec. Such systems are assumed to cover the range of systems of interest for operation in Greenland. Also, the derived statistics are descriptive of a system installed between the terminals of the test link only. The antennas must be identical, as different antennas will create different illumination of the common volume, and different distances and locations of the terminals will imply a different diurnal and seasonal variation of the capacities.

Even with these limitations, the derived communication statistics are useful in two situations. If a data base exists for a target meteor scatter link, direct evaluations of the communication properties can be evaluated. The data bases can also be used to validate prediction models, which can then be used to predict the performance of other links.

A limited number of such prediction models exist, and their accuracy is being improved through experiments such as the AFSC/GL meteor scatter test-bed in Greenland. In the future, planning of new meteor scatter links may be assumed to rely more and more on modeling computations. However, verification of the results of modeling will still be important for some time to come.

Two systems of interest for Greenland are examined in this section. One is a high capacity system intended for data transfer between station Nord and Thule, the other is a simple system intended for data collection from unmanned weather stations or geophysics sensors. The first system requires a high average capacity, whereas the waiting time for short messages, power consumption and antenna sizes are of less importance. The other system requires the shortest possible waiting times for short messages, and the allowable power consumption and antenna sizes set limits to the system configuration.

7.1 The Dependence on Transmitter Power

When planning a meteor scatter link, the required transmitter power and antenna gain and their interaction are important issues. The transmitter power essentially determines the power consumption of the radio equipment, and the antenna size must be chosen to illuminate the common scattering volume properly. At the same time, antennas must have a manageable physical size and be able to withstand the climatic conditions present at the terminals.

The most commonly used antennas for terminals on land are horizontally polarized Yagi's with 4 to 6 elements. The gain of such Yagi's are 9 - 11 dBi. As a rule of thumb, the gain of a Yagi or an array of Yagis increases 3 dB when the number of elements are doubled, or equivalently if the boom length of the Yagi is doubled. This puts some constraints on the size of antennas feasible for a meteor scatter link.

A six element Yagi for 45 MHz has a boom length exceeding 6 m. A ten element Yagi for 45 MHz would be a very large structure, and antennas with more than six elements might be easier to construct as arrays of stacked six element Yagis. At the higher

frequencies, antennas with more than six elements are easier to deploy, as their size decreases with frequency. Still, the antenna gain can not be increased indefinitely, as the illumination of the common scattering volume must be appropriate for the particular link.

Thus antenna gains for meteor scatter links will for all practical purposes be limited to 14 - 16 dBi, and smaller antennas may be required for many links either to properly illuminate the common scattering volume for a short link, or to keep the physical size of the antenna small.

Power amplifiers suited for meteor scatter transmitters are available through a range of power levels. Broadband Semiconductor devices are available for power levels of 10 W, 50 W, 100 W, and 300 W. A combination of such devices can yield 1 kW, whereas powers exceeding 1 kW are usually obtained with tuned tube type transmitters. Such transmitters are available with power levels of 1 kW, 2 kW and 10 kW. Transmitter powers in excess of 10 kW, must be considered impractical for meteor scatter links.

The power efficiency of meteor scatter transmitters range from 45% solid state amplifiers to 60% for tuned tube type amplifiers. Battery operated transmitters for intermittent use will for all practical reasons, be limited to power levels not exceeding 500 W, and transmitters for continuous use must be supplied from main power supplies when the power level exceeds 10 W.

These power levels may at a first glance seem very high for a battery operated communication system, but 500 W transistor amplifiers are not much more complicated technically than 50 W amplifiers, and the transmitter at a remote station need only transmit when polled by a master station. The transmission time needed to transfer synoptic data is then a few seconds every three hours, and a 500 W transmitter driven from a 24 V battery will consume 450 ampere hours a year and a comparable receiver would

consume an estimated 200 ampere hours a year. Such power consumption is feasible either with primary batteries or solar cells. Substantial power savings can be obtained if less transmitter power is sufficient. Even a 500 W transmitter need not be very large or heavy as little more than a heatspreader is needed for cooling. Such transmitters have been produced for balloon payloads where weight and volume are prime concerns. The SNOTEL meteor scatter network operated by the US Dept. of Agriculture has two master stations and 500 remote, battery operated stations scattered in the Rocky Mountains. The remote stations use 100 W transmitters and the terminal including transmitter, receiver and data storage is contained in a box $25 \times 25 \times 5$ cm.

The communication system statistics presented in the subsequent two sections are based on transmitter powers of 1000 W, but provisions exist to interpret these in terms of different transmitter powers, as long as the antenna configuration is not presumed different from the one used for the measurements. Such interpretations are discussed where appropriate.

7.2 Communications Properties of a Thule Station Nord Link

The following section presents the communication properties of a meteor scatter link operated between Thule and station Nord as derived from the August 1987 data. The communication system configuration includes six element Yagi antennas mounted 1.5 wavelengths above the ground, 1000 W transmitter power, galactically noise limited receivers, MSK modulation and a bit-error-rate performance requirement of 10^{-3} or 10^{-4} .

Provided the communication channel distortion is only due to additive Gaussian distributed noise, the instantaneous capacity of a meteor scatter communication system is dependent on

the signal-to-noise ratio required for a given bit-error-rate performance. This is the case for meteor scatter signals using bandwidths less than approximately 250 kHz. For example a bit-error-rate of 10^{-4} when binary PSK or MSK modulation is used requires a signal-to-noise ratio of 8.7 dB in a bandwidth equivalent to the signaling rate. The signal-to-noise ratio varies throughout the lifetime of a meteor trail signal. It is high in the beginning of the trails lifetime and decreases as the trail diffuses. In addition the signal-to-noise ratio varies widely from trail to trail, so only a subset of the available meteor trail signals will have a signal-to-noise ratio high enough to support a given signaling rate. When the signal-to-noise ratio exceeds what is needed to support a given signaling rate and bit-error-performance then the signal has more communication capacity than is being utilized, and larger signaling speeds can be supported. The signaling speed must be continually adjustable to fit the instantaneous signal-to-noise ratio in the channel if the available communication capacity is to be fully utilized. This is called adaptive signaling and will theoretically give both the largest throughput and the shortest waiting times for transfer of messages. It is, however, also difficult to implement, both because the instrumentation is difficult to build and because adaptive signaling requires wide band frequency allocations. For these reasons fixed rate signaling is most often used when the large throughput of adaptive signaling is not required. The advantages of adaptive signaling has been known since the late 1950's but only recently have adaptive signaling communication systems become commercially available. The concepts of adaptive and fixed signaling are illustrated in Figure 7.2.1.

The derived communication capacity for a meteor scatter link using a fixed signaling rate between Thule and station Nord in August 1987 is presented as a function of signaling rate in Figure 7.2.2. The required capacity of 100 bits/sec could be obtained with a signaling rate of 5000 bits/sec if only the contribution of the meteor

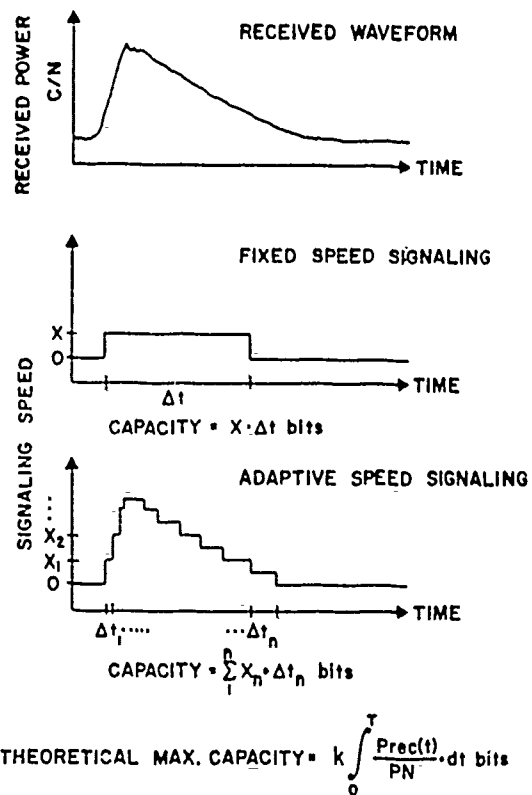


Figure 7.2.1. Illustration of the Communication Capacity of a Underdense Meteor Trail Signal When Adaptive and Fixed Signaling Rates are Used

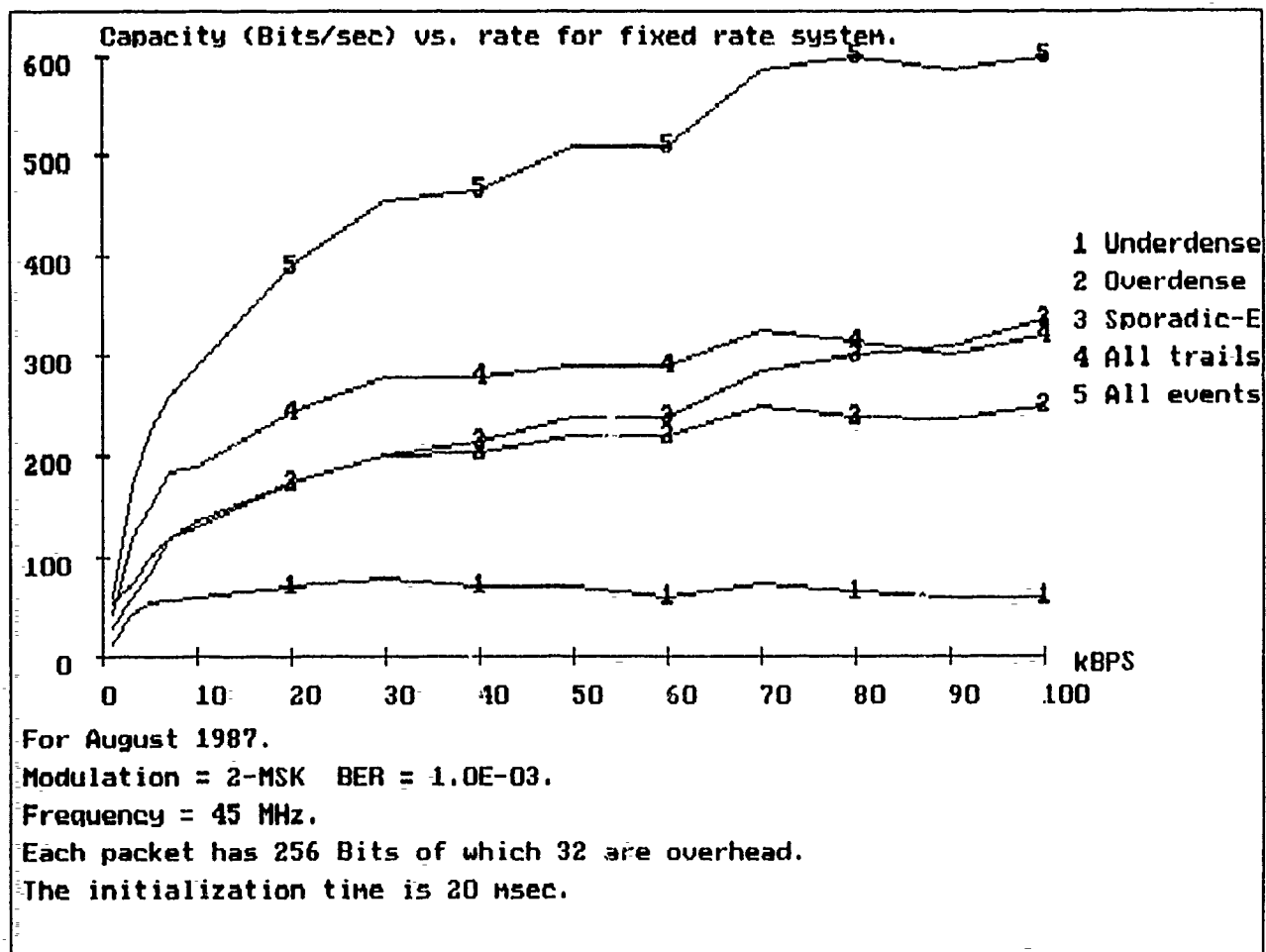


Figure 7.2.2 Derived Capacity for a Meteor Scatter Link Between Thule and Station Nord for August 1987 as a Function of Signaling Rate

trail signals were included. The target capacity of 300 bits/sec could be obtained with a signaling rate of 64 Kbits/sec. At low signaling rates the underdense and overdense meteor trail signals contributed approximately equal amounts of the capacity, while the contribution of the overdense trail signals dominated at the higher signaling rates. This is consistent with the larger part of the duty cycle being contributed by the overdense meteor trail signals at high SNR's. The sporadic E-signals contributed approximately the same capacity as the meteor trail signals and with a signaling rate of 32 Kbits/sec the capacity exceeded 400 bits/sec when the contribution of all propagation mechanisms were added. It seems thus, that the required communication capacity for a Thule to station Nord meteor scatter link can be obtained with a quite low, fixed signaling speed. However, a sufficient margin must be included to compensate for the seasonal and day to day variation of the capacity and allow room for future needs. Also the contribution of the sporadic E-signals will be less in winter and during low solar activity years. A signaling rate of 64 Kbits/sec seems a good choice balancing the need for capacity and at the same time not requiring a very large bandwidth.

The derived fully adaptive communication capacity for a Thule to station Nord meteor scatter link in August 1987 is shown in Figure 7.2.3 as a function of time of day. Only the contribution of the meteor trail signals is included. The capacity is much higher than the capacity obtained with a fixed signaling rate transmission scheme. A daily average capacity of approximately 1000 bits/sec is obtained. This may not be fully obtainable in practical applications, however, due to difficulties implementing a communication processor that will efficiently utilize the highest signaling rates. Few adaptive meteor scatter communication systems have yet been offered by manufacturers, but new systems may be expected to be available in the future. The fully adaptive capacity when the contribution of the sporadic E-signals were included in August 1987 is presented in Figure 7.2.4. These signals contributed on the average as much as

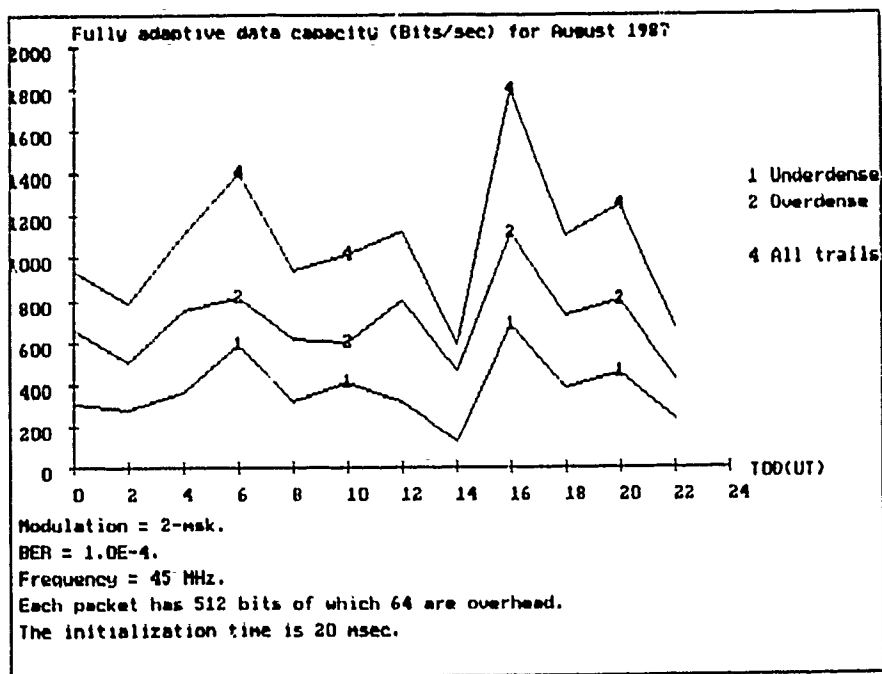


Figure 7.2.3 Derived fully adaptive capacity for a meteor scatter link between Thule and station Nord in August 1987. Meteor trail signals only.

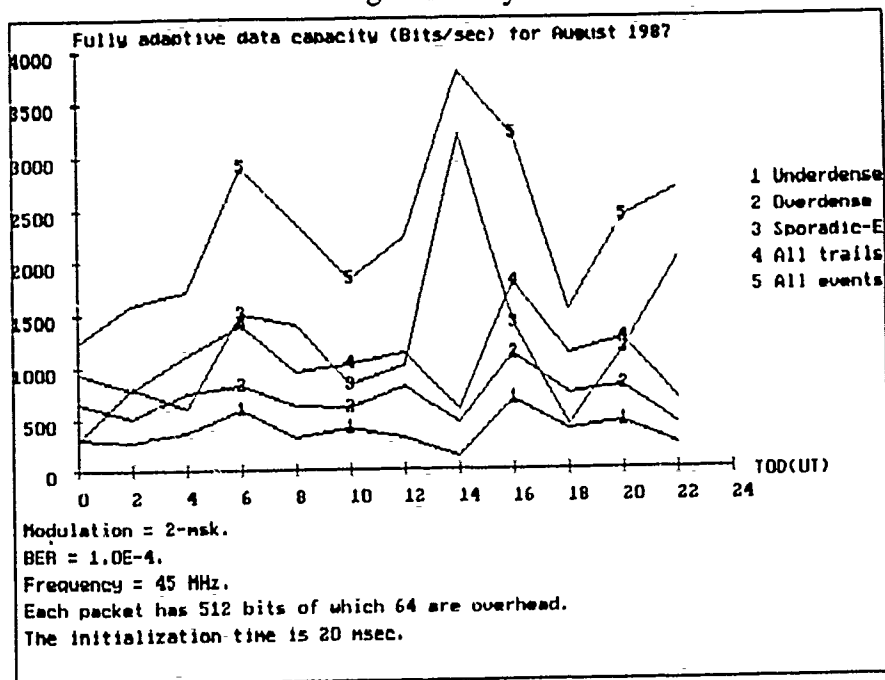


Figure 7.2.4 Derived fully adaptive capacity for a meteor scatter link between Thule and station Nord in August 1987. Meteor trail and sporadic E-signals are included.

the meteor trail signals, and a large enhancement is seen in the early afternoon. This enhancement is due to the sporadic E-event on the 24th and cannot be considered a recurrent phenomenon although a large fraction of the sporadic E-events can be expected to occur around noon.

The distribution of signaling rates used by the fully adaptive communication system is presented in Figure 7.2.5. The Y-axis is in arbitrary units. It is seen that the meteor trail signals predominantly supported signaling rates less than 50 Kbits/sec, but the sporadic E-signals supported much higher signaling rates. An adaptive communication system must have an upper limit to the signaling speed due to the obtainable bandwidth allocation and the cost of the communication system components. It is difficult to determine this limit, which is most probably rather low in areas of the world where VHF frequencies are heavily used, but may be higher in North Greenland where this part of the radio spectrum is virtually unused. Such limitations will inevitably limit the capacity available from the sporadic E-signals and this should be kept in mind when planning systems.

In conclusion, the target communication capacity of 300 bits/sec for a meteor scatter link between Thule and station Nord was found to be available for the period of the August 1987 measurements. A fixed signaling rate transmission scheme with a signaling rate exceeding 32 Kbits/sec is required though to ensure this capacity during months of less meteor activity. The sporadic E-signals provide a bonus for such a link which will not be dependent on extended privacy. The expected seasonal variation of the communication capacity can be investigated with one of the several physical meteor scatter models that have become available since the measurements were performed in August 1987. The results presented in this report can be used as a calibration point for the month of August.

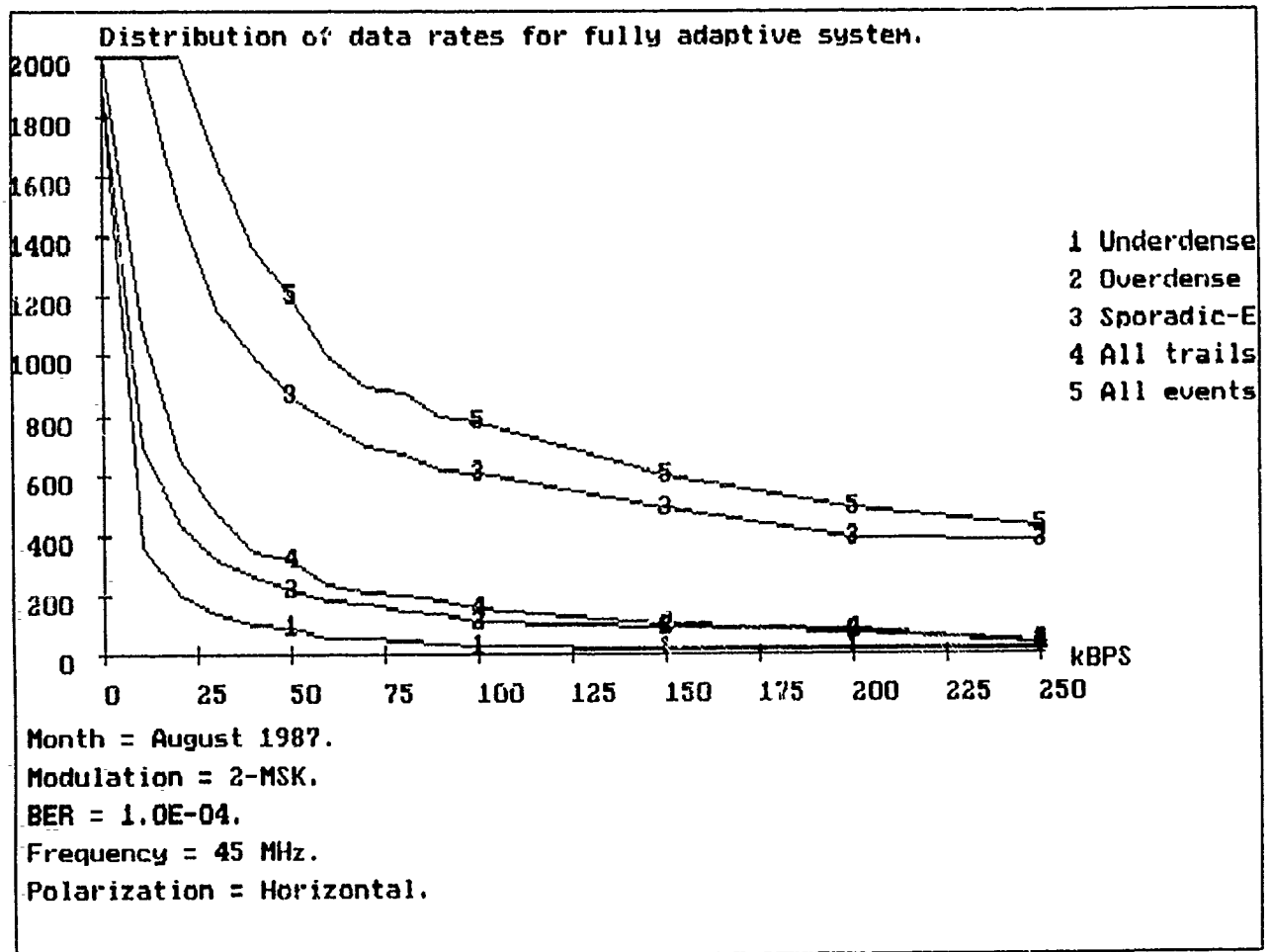


Figure 7.2.5 Distribution of Signaling Rates for a Fully Adaptive Meteor Scatter Link Between Thule and Station Nord August 1987

7.3 Properties of a Data Collection Link

Meteor scatter communication is currently being used for collection of environmental data from unmanned sensors. Such systems are characterized by short data messages, battery operation and often difficult climatic conditions and deployment. To be useful for forecasting, the data must be available in almost real time every three hours. This sets limits on the acceptable waiting time for transfer of the data messages from the sensor stations to the forecast centers.

The data collection can be performed in either a broadcast mode or a polled mode. When operated in a broadcast mode, the sensor stations are equipped with a meteor scatter transmitter only. The transmissions are controlled by a simple clockwork starting transmissions at proper intervals. The master station is equipped with a meteor scatter receiver only, continuously open for reception of data from the sensor stations. The sensor data is transmitted continuously for a period of time long enough to ensure reception at a master station with a high confidence. Compared to a polled mode of operation described below, the transmitter power consumption is entirely located at the sensor stations.

The waiting time calculation must be based on successful transmission during a time period containing at least two data messages, to ensure continuous transmission of at least one full message. Thus the lowest possible frequency of operation must be chosen to minimize the waiting time and transmitter power at the sensor stations. The main advantage of the broadcast mode of operation is the simple equipment needed, eliminating co-located receivers and transmitters, diplexors and handshaking processors. The main disadvantages are the power consumption at the sensor stations, and more elaborate networking schemes to reduce overlap of transmissions from separate sensor stations. Many sensor stations

can share a single frequency, if the links between the individual sensor stations and the master station are separated enough, so that only a small chance exists of coinciding meteor trails. Closely separated sensor stations should broadcast during separated time slots, but sensor stations separated a few hundred km can transmit simultaneous as they will be using different trails for the message transfer. A detailed analysis of the networking aspects of a Greenland network is beyond the scope of this report, however, and these explanatory remarks are only intended as a introduction to the operational aspects of a large network of sensor stations.

To operate in the polled mode, the unmanned sensor station is equipped with both a meteor scatter receiver and a transmitter. A master station, with access to the stations data transmits a probe signal containing the address and access key to one or a number of unmanned sensor stations. When a sensor station has received a probe signal and verified its own address and access to its data, these are immediately transmitted to the master station. The exchange of information can take place in semi-duplex, i.e. the sensor station either receives or transmits. This scheme relieves the need for diplexors at the sensor stations. The master station may or may not use semi duplex. If semi duplex is used, the probe signal is only sent once or twice before switching to a listen only mode. If the master station is equipped for full duplex, the probe can be sent until a sensor station responds. Then it should be stopped not to provoke responses from more sensor stations before communication has been exchanged with the station first to respond.

The polled mode of operation has the advantage, that only master stations with legitimate access to the sensor station data can obtain the data, and the polling can be continued until a very low probability of error in the data has been obtained. Also, the sensor stations transmit only when polled, and this conserves power to drive the transmitter, relative to a station operated in the broadcast

mode. The main complication of the polled mode is the need for a receiver and control processor at the sensor stations, which need not be a real cost disadvantage when the long term operating costs including power supply is calculated.

When deriving the waiting time for transfer of a full data message from a sensor station, an overhead long enough to successfully transmit two polling packages from the master station must be added to the synchronization overhead. The required time of transmission from a sensor station must be at least the time to send one full data message. However, some environmental sensor networks send two or three data packages and let the master station decide which message content is correct. A more modern method would be to include encryption and error correction coding, which will also add redundancy to the transmission. Such schemes will provide privacy and better performance than simple repetition.

The operating aspects of a large network of sensor stations in a polled mode are simpler and well proven compared to a network operated in the broadcast mode. Networks operated in the US in this mode, e.g. SNOTEL, handle up to 500 sensor stations with two master stations and a single pair of frequencies. When polling the sensor stations a strategy is used too simultaneously poll a number of sensor stations separated enough to avoid overlapping transmissions with a high probability, and at the same time obtain a higher polling efficiency than would have been obtained if the sensor stations were polled one after one in succession.

The complexity of broadcast and polled mode data collection systems vary for different configurations. One configuration envisioned uses non-coherently detected FSK modulation, having a modest SNR performance combined with very simple detection hardware. No overhead is required for carrier and bit clock synchronization. The receivers required for such a system will be very simple, needing only two integrated circuits. Another

possible configuration uses BPSK or MSK modulation, having 4 dB better SNR performance than non-coherently detected FSK. However, BPSK require a more elaborate detection scheme including both carrier and bit synchronization. An inherent feature of the meteor scatter channel aids the detection process, however. The SNR is usually high in the beginning of a meteor trail signal, and experience has shown, that a Costas loop detector performs well with a low bit error rate at the beginning of a signal even if the loop does not totally settle until some time later. By then the SNR may have decreased, but the loop operates at maximum performance.

Most current data collection systems using meteor scatter operate in the 40 - 50 MHz frequency band. Higher frequencies are less vulnerable to solar disturbances, and use smaller antennas, but support less communication capacity. This may not be a major concern, as the amount of data to be transferred is small. Of more concern is the waiting time and its interaction with the transmitter power.

Waiting time statistics derived from the data acquired at station Nord in August 1987 are presented and discussed in the following paragraphs. The waiting times have been calculated assuming a range of communication system parameters. A signaling speed of 8000 bits/second in combination with MSK modulation has been chosen. The basic bit error rate for the channel without distortion except for additive Gaussian noise was selected to either 10^{-4} or 10^{-2} . The messages have been divided up into packages of 256 or 512 bits including an overhead of 32 or 64 bits which are intended for synchronization and error correction. No other coding was assumed. 1000 W transmitter power and six element Yagi antennas were assumed. The waiting times are based on meteor trail signals only. Sporadic E-signals might decrease the waiting times, but for planning purposes it is important to evaluate waiting times in the context of meteor trail arrivals only.

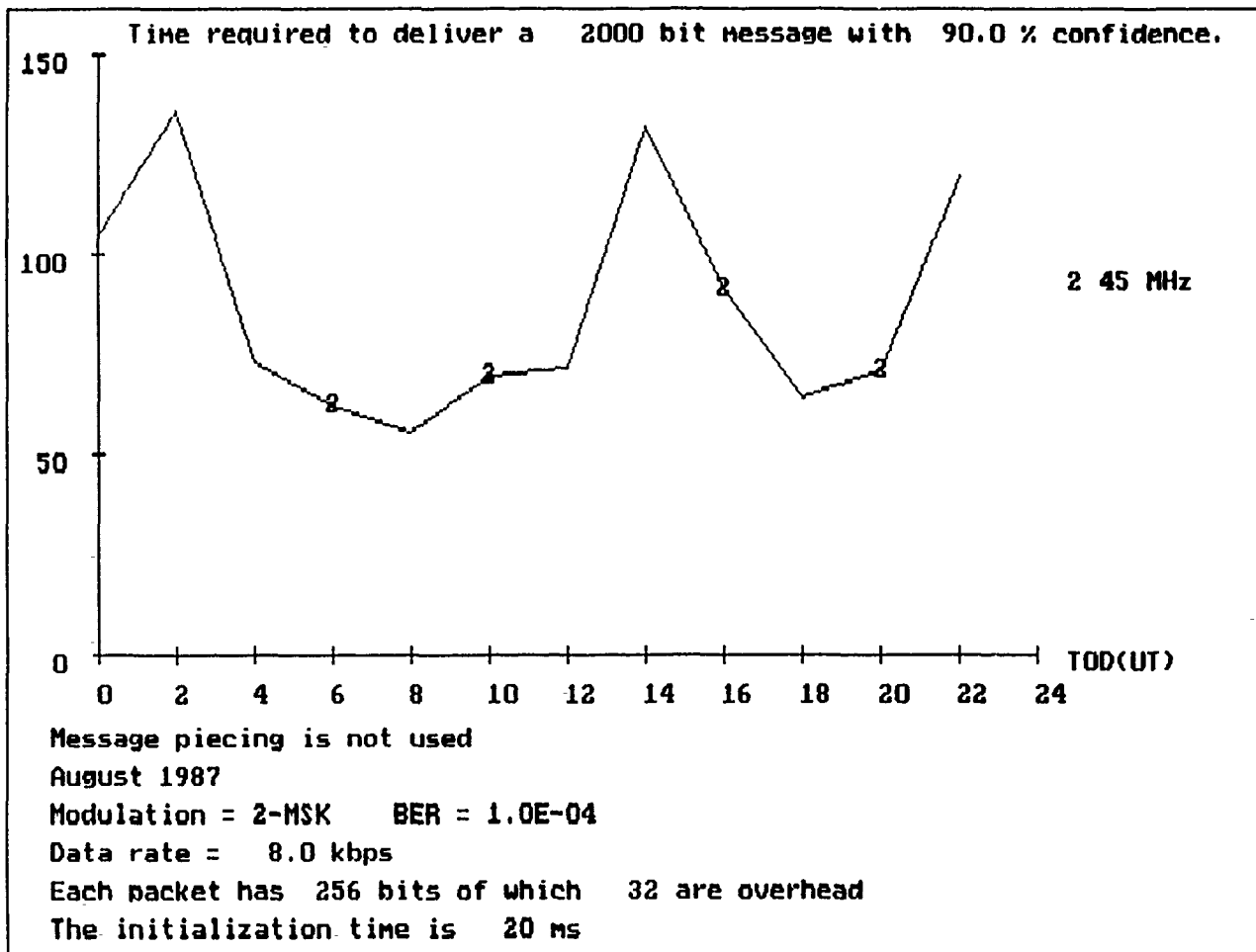


Figure 7.3.1 Waiting time for a 2000 bit message as function of time of day for August 1987 at station Nord. Message piecing is not used.

The waiting time to transfer a message of 2000 bits as a function of time of day is presented in Figure 7.3.1. The minimum waiting time was approximately 60 seconds between 6 and 12 in the morning and 18 to 22 in the evening coinciding with the periods of the highest arrival rates. The maximum waiting time was approximately 140 seconds at 03 UT in the morning and 15 UT in the afternoon. The package size was 256 bits including 32 overhead bits. The message was then transferred in nine packets. Message piecing was not used, and the message was transmitted on one meteor trail signal with a duration of at least 308 milliseconds. The duration must be long enough to accommodate 20 milliseconds to set up the link and 288 milliseconds to transfer nine packages. The confidence was chosen to be 0.9, i.e. 90% of the waiting times observed for a large amount of messages would be less than the waiting times in Figure 7.3.1.

It is not necessary to wait for a meteor trail signal long enough to transfer the whole message. A succession of trails can be used as well, as the information is packaged. The waiting time to transfer a 2000 bit message when message piecing is used is presented in Figure 7.3.2. Every trail signal long enough to transfer at least one package and the initialization sequence was used. The waiting time had the same general diurnal variation, but was half as long as when message piecing was not used. Message piecing is clearly an advantage, and the packages should be kept short enough to take advantage of the abundance of short trail signals available on a meteor scatter link. The procedure for choosing an optimum packet length for a given modulation and signaling speed is beyond the scope of this report and interested readers are referred to the many excellent texts on digital communication system design.

The derived waiting time in seconds for messages as a function of message length at station Nord in August 1987 is presented in Figure 7.3.3. The confidence is 0.95, packets are 512

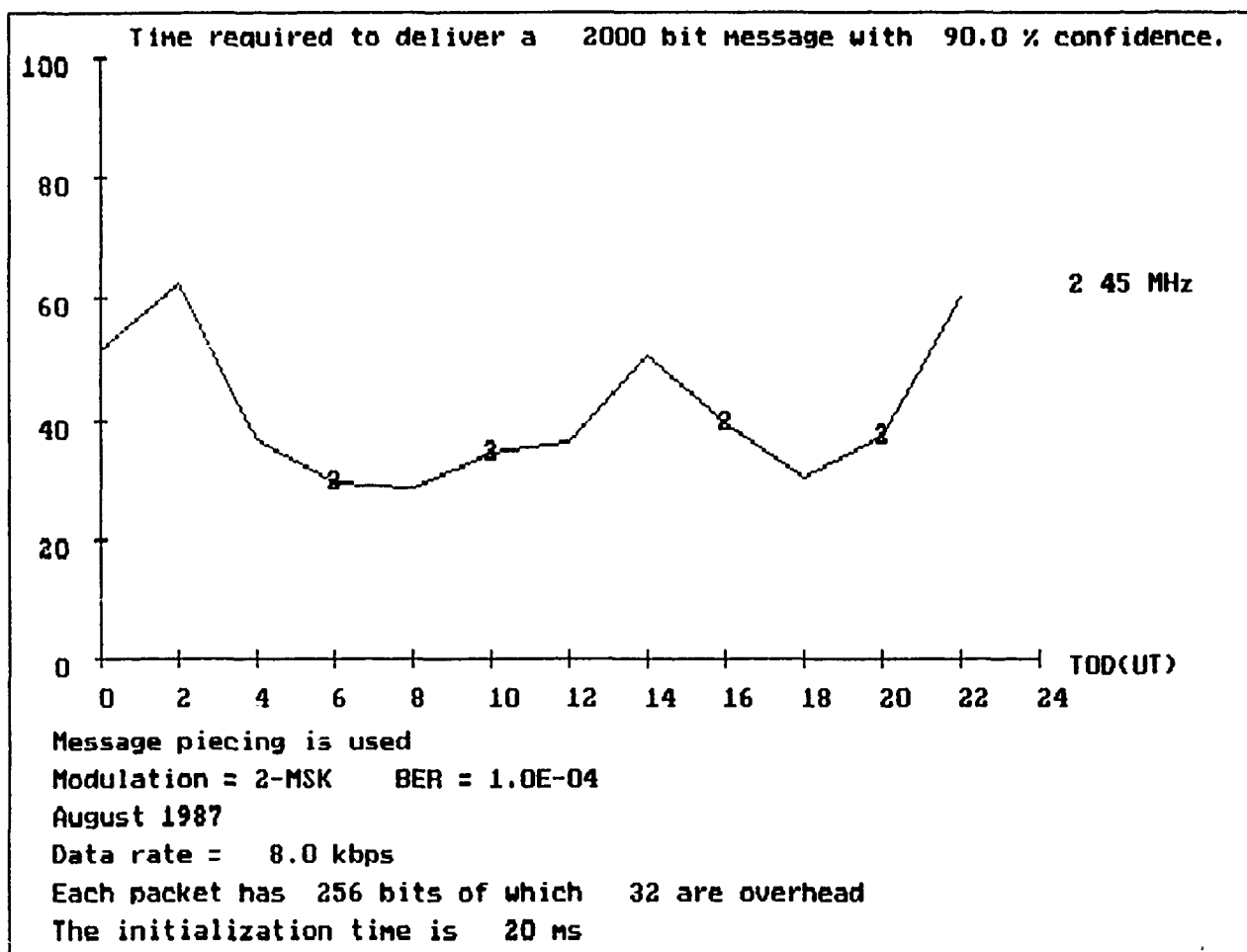


Figure 7.3.2 Waiting time in seconds for a 2000 bit message as function of time of day for August 1987 at station Nord. Message piecing is used.

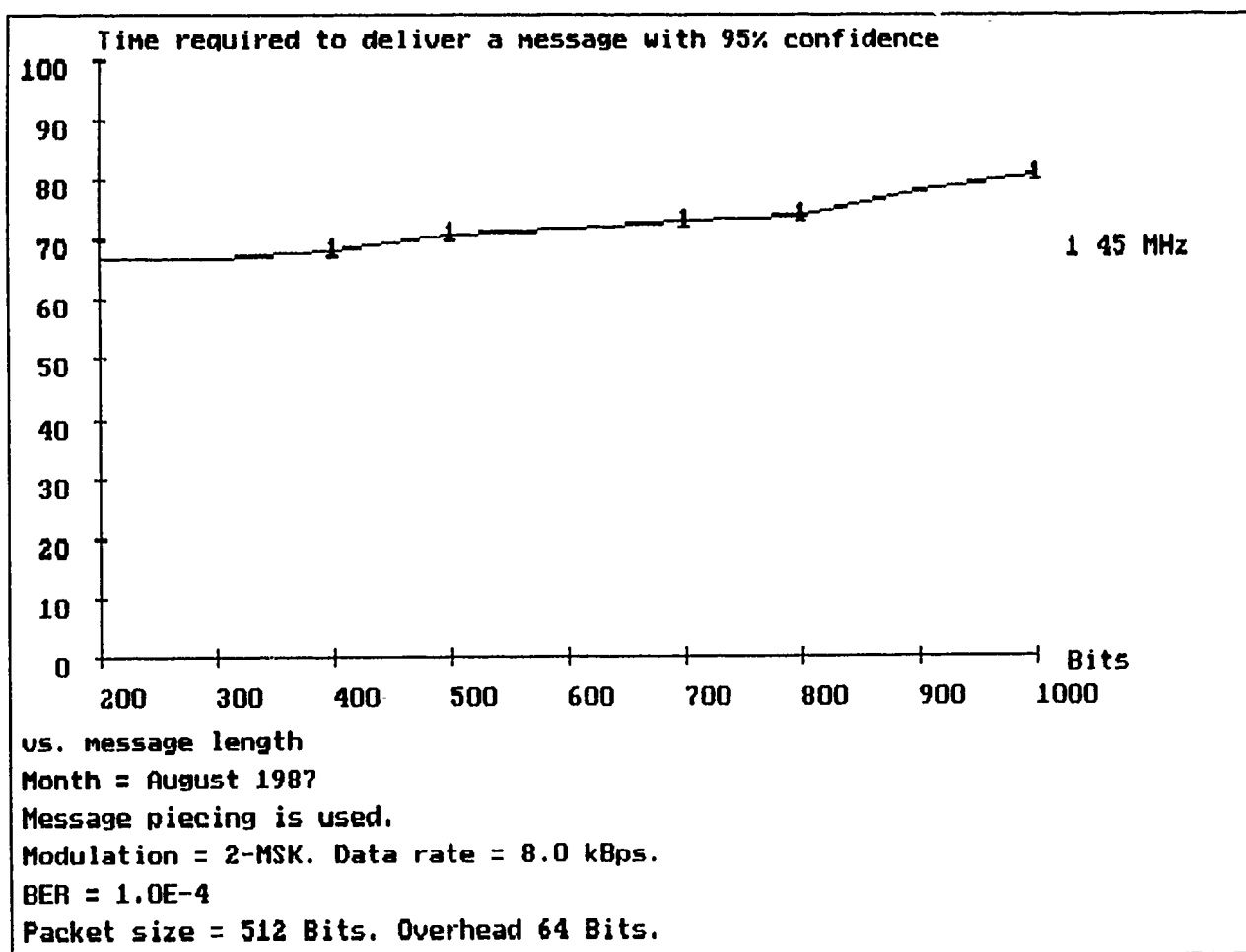


Figure 7.3.3 Waiting time in seconds for messages as function of message length for August 1987 at station Nord. Message piecing is used.

bits long including an overhead of 64 bits. Message piecing is used. Little dependence on message length is seen which is to be expected as one or two packets were needed to transfer messages of all lengths.

It was shown in Section 6.0 that the capacity of a meteor scatter communication system increased with increasing signaling speed up to speeds exceeding several hundred thousand bits/sec. Meteor trail signals capable of supporting such signaling speeds must have both a high signal level and long endurance and their arrival rate is low. This is of no consequence if the main objective of the link is high throughput. If low waiting times are also a concern then adaptive signaling must be used to take advantage of the more often occurring low signal level trails. An intermediate signaling speed must therefore exist that provides the lowest waiting time for messages of a given length and for a given transmitter power. A too low signaling speed will require too many meteor trail signals before the message has been transferred, and a too high signaling speed will require a high signal level and thus a lower arrival rate trail to transfer the message. Figure 7.3.4 shows the waiting time for a confidence of 0.9 for a 2000 bit message as a function of the signaling rate. The shortest waiting time, approximately 35 seconds, is obtained for signaling speeds between 4 and 8 Kbits/sec and the waiting time increases for both lower and higher signaling speeds. The increase in waiting time is slow however for increasing signaling speeds. The waiting time is only doubled for an increase of signaling speed by a factor eight, from 4 Kbits/sec to 32 Kbits/sec. The waiting time for a 20,000 bits message transferred in packets of 2560 bits is shown in Figure 7.3.5. The waiting time has increased as expected and the signaling speed providing the lowest waiting times is in the range 20 to 50 Kbits/sec. This statistic can also be interpreted as the waiting time for a 2000 bit message transferred in packets of 256 bits, as shown in Figure 7.3.4, but with 10 dB less transmitter power, i.e. 100 W. For this interpretation the signaling

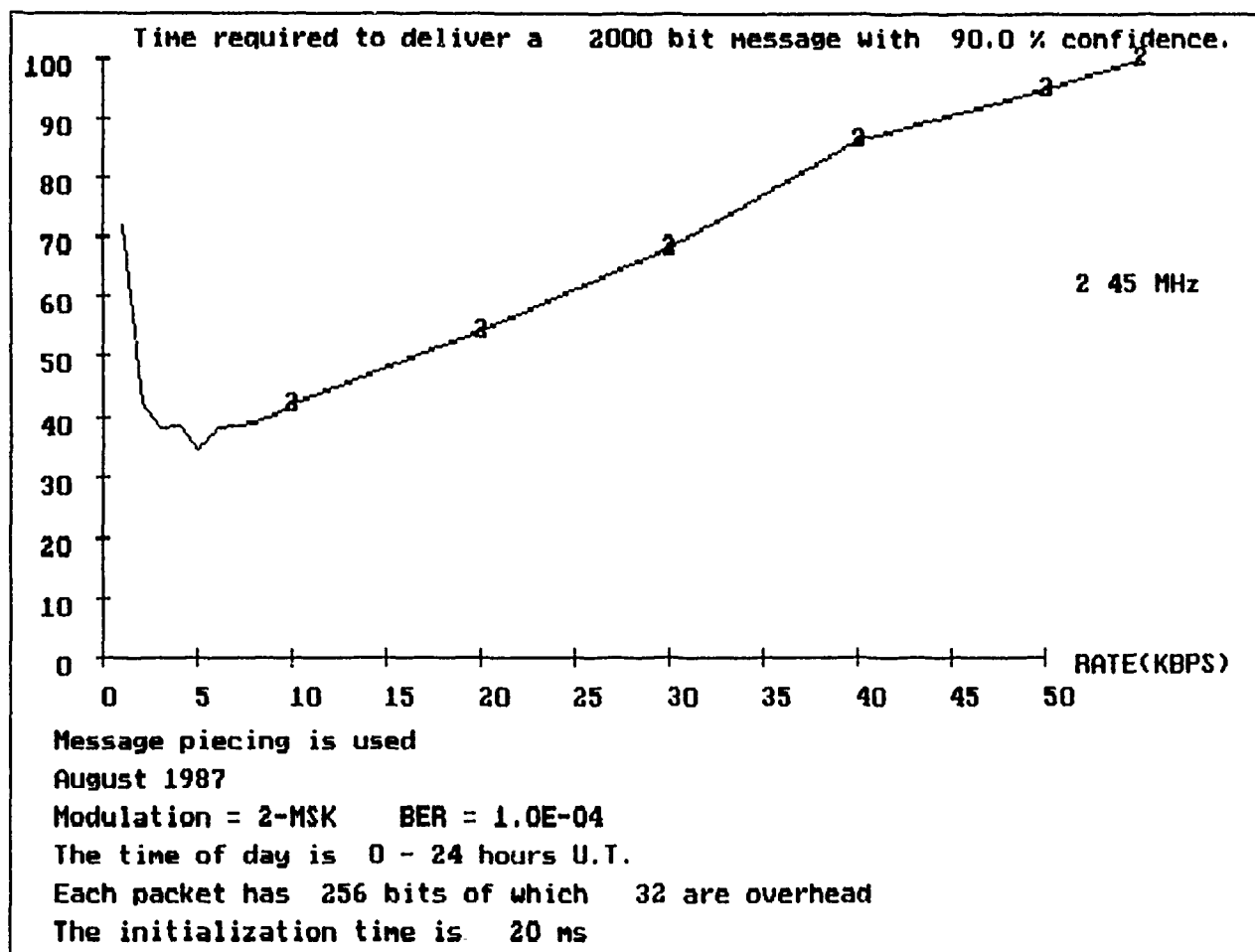


Figure 7.3.4 Waiting time in seconds for a 2000 bit message as a function of signaling rate. Message piecing is used.

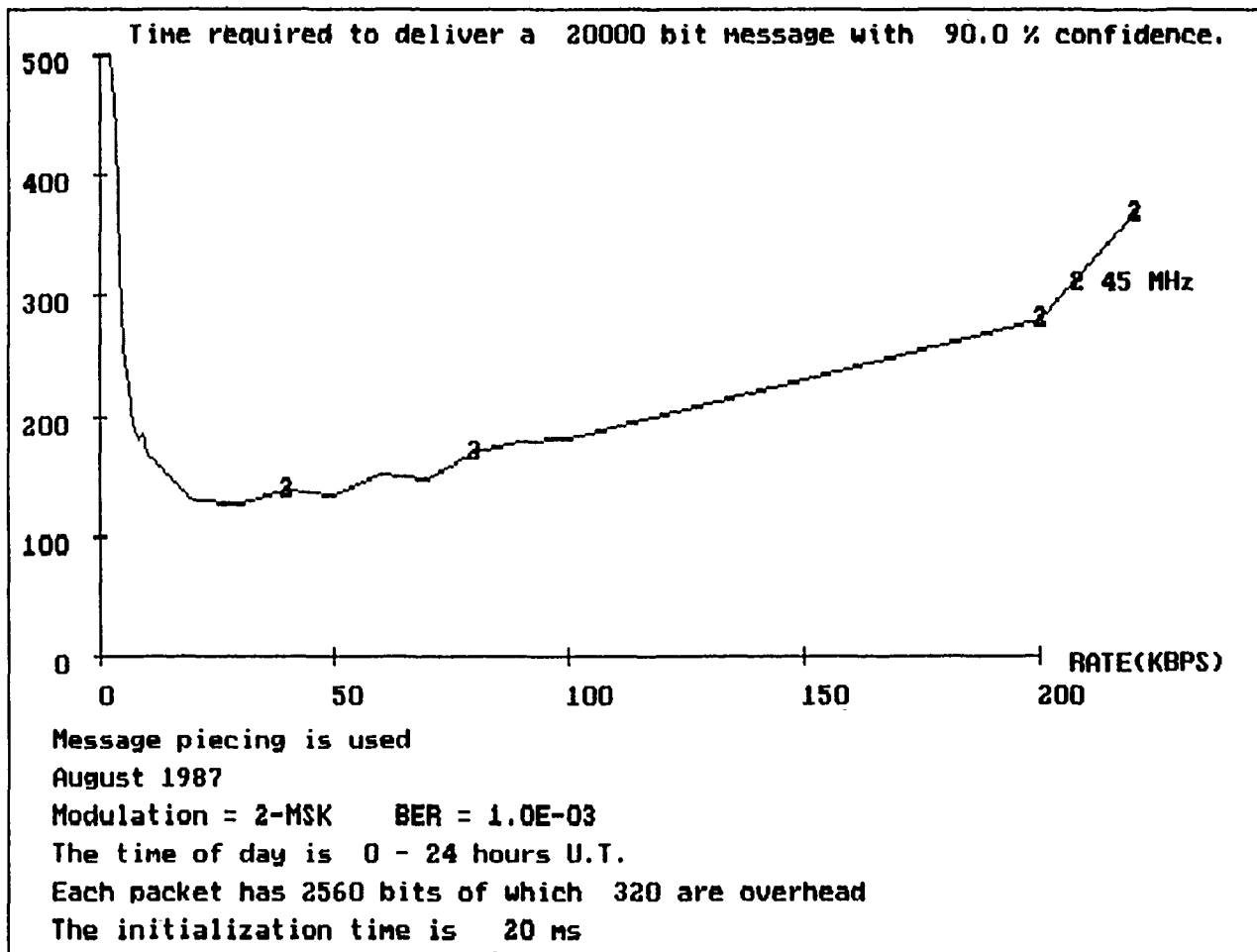


Figure 7.3.5 Waiting time in seconds for a 20,000 bit message as a function of signaling rate. Message piecing is used.

speeds on the X-axis of Figure 7.3.5 must be divided by 10. The optimum signaling speed is then in the range of 2 to 5 Kbits/sec. The lowest waiting time is approximately 120 seconds or three to four times the waiting time provided by the 1000 W case. The increase in waiting time to two minutes is compensated by a tenfold decrease in power consumption by the transmitter. A meteor scatter terminal used for synoptic data transfer with such a transmitter has a power consumption that can rather easily be covered with a combination of storage batteries and solar cells.

The expected variation of the waiting times is indicated in Figure 7.3.6 which presents the waiting time for a 1024 bit message as a function of confidence. The message requires three packets to transfer. The waiting time for half of the messages in a large sample was less than 20 seconds and the waiting time increases with confidence. 90% of the waiting times were less than one minute while 99% were less than two minutes. Thus, a message from even the remotest part of Greenland can be transferred to West Greenland and on to Nuuk or Copenhagen in a few minutes.

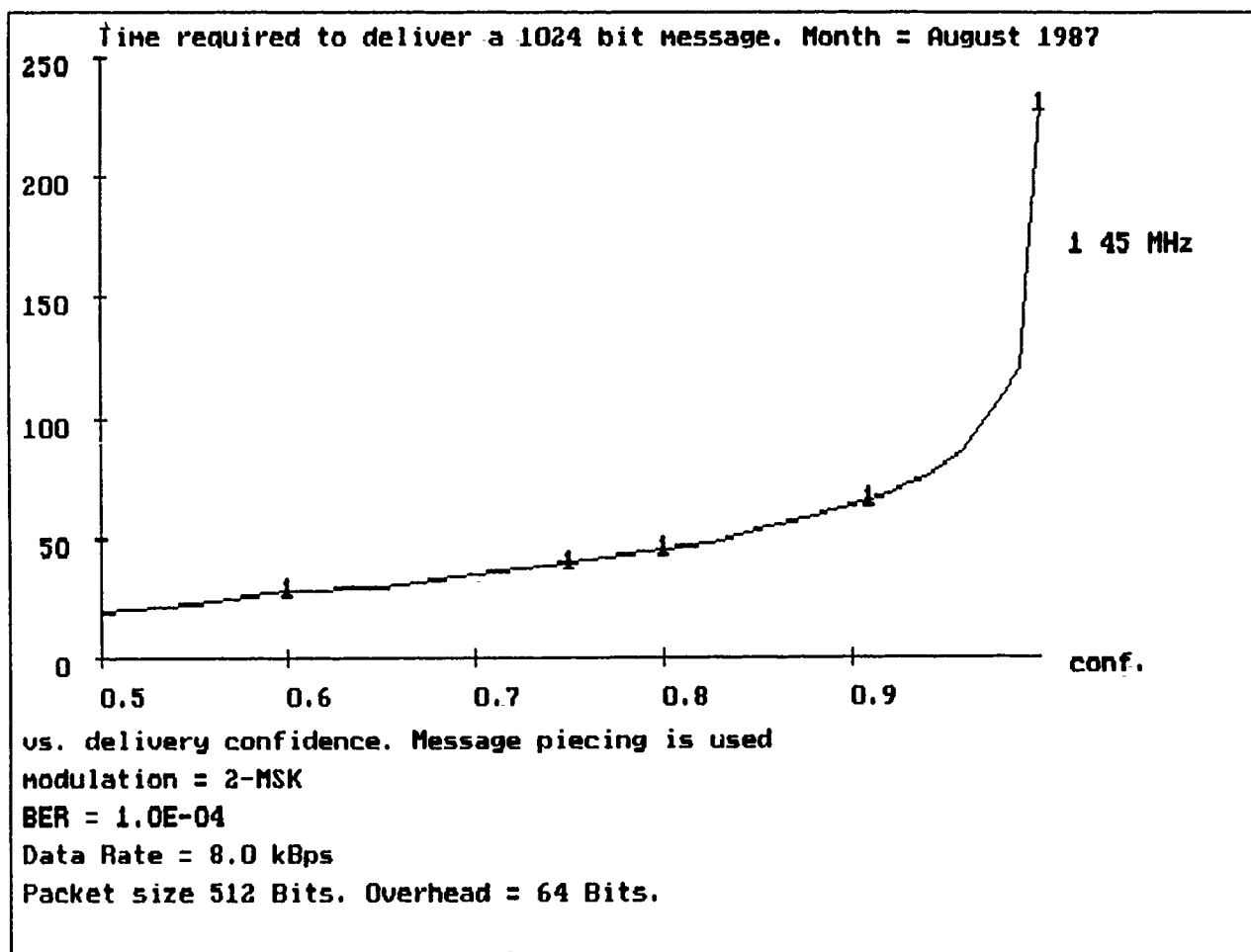


Figure 7.3.6 Waiting Time in Seconds for a 1024 bit Message as a Function of Confidence

8.0 SUMMARY AND RECOMMENDATIONS

A feasibility study has been performed to investigate the possibility of establishing a meteor scatter communication link between station Nord in the extreme Northeast Greenland and the Greenland West coast. The communication link was intended for transfer of large amounts of environmental data from station Nord which does not have access to either satellite or line of sight communication links. The required communication capacity is 100 bits/sec yearround with a target capacity of 300 bits/second to cover future expanded capacity needs.

Two locations on the West coast were selected for the study: Sondrestrom and Thule. Both locations have easy access to the Greenland telecommunication network. A measurement campaign was performed between Sondrestrom and station Nord in April 1987 and it was found that the distance between these locations (1800 km) was too long for a meteor scatter link. Another campaign was performed between Thule and station Nord in August 1987. The distance between these locations is 1170 km. The campaign produced a one week data sample of signals propagated from Thule to station Nord by meteor trail scatter, sporadic E-layer propagation and ionospheric scatter. A frequency of 45 MHz was used for both campaigns.

The acquired data has been analyzed at Air Force Systems Command/Geophysics Laboratory USAF in Boston and propagation statistics as well as communication statistics have been produced. The statistics show that the target communication capacity was available in August 1987 if a meteor scatter communication system operating with 1000 W transmitters and six element Yagi antennas were to be used. The system could use a fixed data rate transmission scheme with an instantaneous data rate

of 64 Kbits/sec. With the use of an adaptive data rate scheme an even larger capacity could be obtained.

Analysis of waiting time for short messages has also been performed to evaluate the usefulness of meteor scatter communication for synoptic data collection in Greenland. The waiting time for 1 to 2000 bit messages was found to be up to two minutes with a confidence of 0.9 using transmitter powers of 100 W. Shorter waiting times were found for transmitter powers of 1000 W.

The August measurement campaign was conducted close to the seasonal maximum meteor scatter activity in early August, and a supplementary investigation should be performed to assure that the target capacity of 300 bits/sec will also be available at the seasonal minimum activity in February. Such investigations can be performed with a computer program, a so called physical meteor scatter model and the investigation does not require further collection system for transfer of geomagnetic data from the inland ice (SRI and NSF). This combined with the continued investigations conducted by AFSC/GL, additional information will be provided on seasonal variations as well as frequency dependence of meteor scatter communication in Greenland.

9.0 BIBLIOGRAPHY

9.1 Introduction to Meteor Scatter

1. McKinley, D. W. R., Meteor Science and Engineering, McGraw-Hill, 1961.
2. Sites, F. J., "Communication via meteor trails," AGARD, 23rd EWPP Symposium, 3-7 October 1971.
3. Oetting, J. D., "An analysis of meteor burst communication for military applications," IEEE Trans. Com., COM-28, No. 9, September 1980.
4. Grossi, M. D., A. Jahved, "Time and frequency spread in meteor burst propagation paths," AGARD, 23rd, EWPP Symposium, 3-7 October 1977.
5. Proc. IRE, December 1957. This volume contains 12 papers on all aspects of meteor scatter communication. All papers are referenced below.

9.2 Meteor Scatter in General

6. Forsyth, P. A., E. L. Vogan, D. R. Hansen and C. O. Hines, "The principles of JANET, a meteor burst communication system," Proc. IRE, December 1957.
7. Campbell, L. L. and C. O. Hines, "Bandwidth considerations in JANET system," Proc. IRE, December 1957.
8. Campbell, L. L., "Storage capacity in burst type communication systems," Proc. IRE, December 1957.

9. Davis, G. W. L., S. J. Gladys, G. R. Lang, L. M. Luke and M. K. Taylor, "The Canadian JANET system," Proc. IRE, December 1957.
10. Montgomery, G. F., "Intermittent communication with a fluctuating signal," Proc. IRE, December 1957.
11. Montgomery, G. F. and G. R. Sugar, "The ability of meteor bursts for intermittent radio communication," Proc. IRE, December 1957.
12. Vincent, W. R., R. T. Wolfram, B. M. Sifford, W. E. Jayne and A. M. Peterson, "A meteor burst system for extended range VHF communication," Proc. IRE, December 1957.
13. Vincent, W. R., R. T. Wolfram, B. M. Sifford, W. E. Jayne and A. M. Peterson, "Analysis of oblique path meteor burst propagation data from the communications viewpoint," Proc. IRE, December 1957.
14. Rach, R. A., "An investigation of storage capacity required for a meteor burst communication system," Proc. IRE, December 1957.
15. Eshleman, V. R., "On the wavelength dependence of the information capacity of meteor burst propagation," Proc. IRE, December 1957.
16. Eshleman, V. R. and R. F. Mlodnosky, "Directional characteristics of meteor propagation derived from radar measurements," Proc. IRE, December 1957.
17. Meeks, J. C. and M. L. James, "On the influence of meteor radiant distribution in meteor scatter communication," Proc. IRE, December 1957.
18. Forsyth, P. A. and E. L. Vogan, "Forward scattering of radiowaves by meteor trails," Can. J. Phys., Vol. 33, 1955.

19. Hines, C. O., "Diurnal variation in the number of shower meteors detected by the forward scattering of radio waves. I. Theory," Can. J. Phys., Vol. 33, 1955.
20. Forsyth, P. A., C. O. Hines and E. L. Vogan, "Diurnal variation in the number of shower meteors detected by the forward scattering of radio waves. II. Experiment," Can. J. Phys., Vol. 33, 1955.
21. Forsyth, P. A. and E. L. Vogan, "The duration of forward scattered signals from meteor trails," Can. J. Phys., Vol. 34, 1956.
22. Pugh, R. E., "The number density of meteor trails observable by the forward scattering of radio waves," Can. J. Phys., Vol. 34, 1956.
23. Hines, C. O. and R. E. Pugh, "The spatial distribution of signal sources in meteoric forward scattering," Can. J. Phys., Vol. 34, 1956.
24. Hines, C. O., "Diurnal variation in the number of shower meteors detected by the forward scattering of radio waves. III. Ellipsoidal theory," Can. J. Phys., Vol. 36, 1958.
25. Forsyth, P. A., "The forward scattered signal from an overdense meteor trail," Can. J. Phys., Vol. 36, 1958.
26. Hines, C. O., "Diurnal variation in forward scattered meteor signals," IATP, Vol. 9, No. 4, 1956.
27. Hines, C. O., "The efficiency of meteor scattering over short and long ranges," Can. DRTE, Rept. 12-2-15, August 1955.
28. Campbell, L. L., "Information loss and delays in two proposed techniques for meteor communication," Can. DRTE, Rept. 12-3-4, November 1953.
29. Vogan, E. L. and P. A. Forsyth, "Privacy in system JANET," Can. DRTE, Rept. 12-3-4, November 1953.

30. Hines, C. O., "Information in JANET systems of fixed and of variable bandwidths," Can. DRTE, Rept. 12-3-14, July 1955.
31. Hansen, D. R. and L. L. Campbell, "A proposed variable information rate JANET system," Can. DRTE, July 1955.
32. Shockley, T. D. and W. B. Jones, "Effects of transmission path parameters on meteor trail propagation," U.S. Navy, NONR-991(02), Tech. Rept. No. 15.
33. Spezio, A. E., "Meteor burst communication systems: Analysis and synthesis," NRL, Washington, DC, December 1978.
34. James, J. C. and M. L. Meeks, "On the relative contribution of various sky regions to meteor trail communication," ONR, NONR-991-02, June 1956, Tech. Rept. No. 1.
35. Nupen, "Bibliography on meteoric radiowave propagation," NBS, Boulder, Tech. Note 94, May 1961.
36. Meeks, M. L. and J. C. James, "Meteor radiant distributions and the radio echoes observed by forward scatter," IATP, Vol. 16, 1959.
37. Meteor Comm. Consultants, "Analysis of meteor burst communications for Navy strategic applications," NOSC, N66001-79-C-0460, February 1980.
38. Eshleman, V. R., "Meteors and radio propagation. Part A. Meteor ionization trails: Their formation and radio echoing properties," RPL Stanford Univ., February 1955.
39. Eshleman, V. R., "Meteor scatter," RPL Stanford Univ., Sci. Rept. 4, August 1958.
40. Heritage, J. L., J. E. Bickel and C. P. Kugel, "Meteor communication in Minimum Essential Emergency Communication Network (MEECN)," DCA, NOSC, Tech. Rept. 138, August 1977.

41. Brown, D. W. and H. P. Williams, "The performance of meteor burst communications at different frequencies," AGARD, CP-244, October 1977.
42. Bartholomé, P. J. and I. M. Vogt, "Comet - a new meteor burst system incorporating ARQ and diversity reception," IEEE, Trans. Com-16, No. 2, April 1968.
43. Sugar, G. R., "Radio propagation by reflection from meteor trails," Proc. IEEE, February 1964.
44. Manning, L. A. and V. R. Eshleman, "Meteors in the ionosphere," Proc. IRE, February 1959.
45. Akram, F., N. M. Sheikh, A. Jahved and M. D. Grossi, "Impulse response of a meteor burst communication channel determined by raytracing," IEEE Trans. Com., April 1977.
46. Santeford, H. S., "Meteor burst communication system. Alaska winter field test program - Test report," Boeing Aerospace Company, Document No. D182-10423-1.
47. Ince, A. N., "Spatial properties of meteor burst propagation," IEEE Trans. Com., Com-28, No. 6, June 1980.

9.3 Ionospheric Absorption

48. Lawrence, R. S., C. G. Little and H. J. A. Chivers, "A survey of ionospheric effects upon earth-space radio propagation," Proc. IEEE, January 1964.
49. Hunsucker, R. D., "Survey of polar and auroral region effects on HF propagation," Radio Sci., Vol. 4, No. 4, April 1969.
50. James, J. C., "The influence of meteor radiant distributions on radio echo rates," ONR NONR, 991(02), Tech. Rept. 3, May 1958.

51. Hunsucker, R. D., "Simultaneous riometer and incoherent scatter radar observations of the auroral D-region," Radio Sci., Vol. 9, No. 2, February 1974.
52. Crysdale, J. H., "Analysis of the performance of the Edmonton-Yellowknife JANET circuit," IRE Trans. Com., March 1960.
53. Maynard, L. A., "Propagation of meteor burst signals during the polar disturbance of November 12-16, 1960," Can. J. Phys., Vol. 39, p. 628, 1961.
54. Cormier, R. J., "Thule riometer absorptions of polar cap absorption events (1962-1972)," AFCRL-TR-73-0060, AD762279, January 1973.
55. Cormier, R. J., "Polar riometer observations," AFCRL-TR-70-0690, AD721183, December 1970.
56. Cormier, R. J., "Riometry as an aid to ionospheric forecasting," AFCRL-TR-70-0689, AD721182, December 1970.
57. Kossey, P. A., J. P. Turtle, R. P. Pagliarulo, W. I. Klemetti and J. E. Rasmussen, "VLF reflection properties of the normal and disturbed polar ionosphere in northern Greenland," Radio Sci., Vol. 18, No. 6, pp. 907-916, November-December 1983.

9.4 Aurora and Scatter

58. Greely, A. W., "Account of auroral displays accompanying the great magnetic storm of Nov. 15-19, 1882, noted at Fort Conger, Grinnel Land. Three years of arctic service," 1884.
59. Garry, G. H., "HF-VHF communications experiment using field aligned ionospheric scatterers," Radio Sci., Vol. 9, No. 11, November 1974.

60. Stathacopulos, A. D. and G. H. Berry, "Geometric considerations in the design of communications circuits using field aligned scatter," Radio Sci., Vol. 9, No. 11, November 1974.
61. Heritage, J. L., S. Weisbrod and W. J. Fay, "Experimental studies of meteor echoes at 200 MHz," IRE Trans. A.P., January 1960.
62. Heritage, J. L., S. Weisbrod and W. J. Fay, "Evidence for a 200 megacycles per second ionospheric forward scatter mode associated with the earth's magnetic field," JGR, Vol. 64, No. 9, September 1959.
63. Philipp, N. D. and E. Y. Glielman, "Power of HE-scatter signals," Geom., Aeron., 1976.
64. Hargreaves, J. K., "Auroral absorption of HF radiowaves in the ionosphere: A review of the first decade of riometry," Proc. IEEE, Vol. 57, No. 8, August 1969.
65. Dyce, R., "VHF auroral and sporadic E propagation from Cedar Rapids, Iowa to Ithaca, New York," IRE Trans. PGAP, April 1955.
66. Booker, H. G., "A theory of scattering by non-isotropic irregularities with application to radar reflections from the aurora," JATP, Vol. 8, p. 204, 1956.
67. Akasofu, S. I., "Physics of magnetospheric substorms," Astrophysics and space science library, Vol. 47, D. Reidl. Publ.
68. Ince, A. N., I. M. Vogt and H. P. Williams, "A review of scatter communications, AGARD, CP-244.
69. Sinno, K., "On the time delay of the appearance of sporadic E following meteor activity," JATP, Vol. 48, p. 35, 1980.
70. Nupen, "Bibliography on auroral radiowave propagation, NBS, Boulder, Tech. Note 128, 1962.
71. Unwin, R. S. and F. B. Knox, "The morphology of the VHF radio aurora at sunspot maximum IV," JATP, Vol. 30, p. 25, 1968.

72. Elkins, T. J., "A model for high frequency radar auroral clutter," RADC-TR-80-122, ADA091049, March 1980.
73. Avery, S. K., A. C. Riddle and B. B. Balsey, "The Poker Flat MST radar as a meteor radar," Radio Sci., Vol. 18, No. 6, November-December 1983.
74. Lewis, E. A., "Numerical search for Sondrestrom-Thule VHF propagation paths via specularly reflecting field-aligned ionization columns," Megapulse, Inc., May 1984.

9.5 System Noise

75. Taylor, R. E., "136 MHz/400 MHz radio-sky maps," Proc. IEEE, April 1973.
76. Cottony, H. V. and J. R. Johler, "Cosmic radio noise intensities in the VHF band," Proc. IRE, September 1952.
77. Brindle, C., D. K. French and J. L. Osborne, "An interpretation of the galactic continuum radiation. II. A three dimensional model for the radioemissivity," Mon. Not. R. Astr. Soc., p. 184, 283, 1978.
78. Cane, H. V., "A 30 MHz map of the whole sky," Aust. J. Phys., 31, p. 561, 1978.
79. Lewis, E. A., CRC Handbook of Atmospheric, p. 276.
80. Hsieh, H. C., "Characteristics of ionospheric thermal radiation," JATP, Vol. 28, p. 738, 1966.
81. Hsieh, H. C., "A theory of ionospheric thermal radiation," JATP, Vol. 28, p. 769, 1966.
82. Hall, M. R. M., "Effects of the troposphere on radio communication, Chap. 4, 1979.

9.6 Communication Theory and Technology

83. Oetting, J. D., "A comparison of modulation techniques for digital radio, IEEE Trans. Com., Com-27, No. 12, December 1979.
84. Amoroso, F., "The bandwidth of digital signals," IEEE Communications Magazine, November 1980.
85. Horstock, N., "The flexible digital receiver," ElektronikCentralen, Denmark, ECR-120, June 1982.
86. Thompson, R. and D. R. Clouting, "Digital angle modulation," Wireless World, December 1976, February 1977.
87. Monsen, P., "Fading channel communications," IEEE Com. Soc. Mag., Vol. 18, No. 1, January 1980.
88. Ostergaard, J. C., "Meteor Burst Receiver Manual, Darcom Electronics, Denmark, February 1984.
89. Weitzen, J. A., W. P. Birkemaier and M. D. Grossi, "A high speed digital modem for the meteor scatter channel," Proceedings of Seventeenth Annual Conference on Information Science and Systems, Johns Hopkins University, March 23-25, 1983.
90. Albright, Lattore, "Some applications of the meteor burst communications mode, The Boeing Company, Seattle, Washington.
91. Nes, H. L., "Propagation characteristics of meteor burst communication systems," SHAPE Technical Centre, Tech. Memo STC-TM-710, July 1983.
92. Nes, H. L., F. A. Eenhorn and W. K. Sekreve, "Test equipment for meteor trail propagation studies," SHAPE Technical Centre, STC-IN-534, May 1983.

93. Brown, D. W., "A physical meteor-burst propagation model and some significant results for communication system design," IEEE Journal on Selected Areas in Communications, Vol. SAC-3, No. 5, September 1985.
94. Weitzen, J. A., W. P. Birkemeier and M. D. Grossi, "An estimate of the capacity of the meteor burst channel," IEEE Trans. Comm., Com-32, No. 8, August 1984.
95. Weitzen, J. A., M. D. Grossi and W. P. Birkemaier, "High resolution multipath measurements of the meteor scatter channel," Radio Sci., Vol. 19, No. 1, p. 375, January-February 1984.
96. Ostergaard, J. C., J. E. Rasmussen, M. J. Sowa, J. M. Quinn and P. A. Kossey, "Characteristics of high latitude meteor scatter propagation parameters over the 45 - 104 MHz band," AGARD, CP-382, 1985.
97. Nes, H., "Meteor burst polarization trials," Electronics Letters, Vol. 21, No. 24, November 1985.
98. Cannon, P. S., A. H. Dickson and M. H. Armstrong, "Meteor scatter communications at high latitudes," AGARD, CP-382, 1985.